

The Roles of Magnetic Field & Oil Composition in Treatment of Heavy Organics in Petroleum Fluids

BY

Mohammed Hamza Khalaf

Submitted in partial fulfillment of the requirements
For the degree of Doctor of Philosophy in Chemical Engineering in the
Graduate College of the University of Illinois at Chicago, 2019
Chicago, Illinois

PhD Dissertation Defense Committee:

Prof. G.Ali Mansoori, Chair and Advisor, Departments of Bio & Chemical Engineering.
Prof. Vivek Sharma, Department of Chemical Engineering.
Prof. Amid Khodadoust, Department of Civil Engineering.
Prof. Said Al-Hallaj, Department of Chemical Engineering.
Prof. Sanjay Behura, Department of Chemical Engineering.

*I dedicate this thesis to
my dad, Hamza, my mom Sabha, my wife, Esraa,
my beloved kids, Ahmed, Rosalyn, and Sultan
for their constant support and unconditional love.
I love you all dearly.*

ACKNOWLEDGMENTS

I would like to express my sincere gratitude and appreciation to the University of Illinois at Chicago (UIC) for having me as a Ph.D. candidate. I am highly excited and honored to have such a wonderful time as a Ph.D. candidate at UIC due to its highly scientific atmosphere, friendly nature and diverse culture.

I would also like to acknowledge a few people who played an important role in the progress and success I have achieved. Firstly, I would like to express my sincere gratitude to my advisor Prof. ***G.Ali Mansoori*** for the continuous support of my Ph.D. study and related research, for his patience, motivation, and immense knowledge. His guidance helped me in all the time of research and writing of this thesis. Besides my advisor, I would like to thank the rest of my thesis committee: ***Dr. Vikas Berry, Dr. Vivek Sharma, Dr. Said Al-Hallaj, Dr. Amid Khodadoust, and Dr. Sanjay Behura***, for their encouragement, valuable time, meaningful suggestions, constructive comments, and critical insights.

I would like to express my special appreciation and thanks to all the faculty and staff of the department of chemical engineering. ***Dr. Vivek Sharma***, you have been a tremendous mentor for me. I would like to thank you for encouraging me to grow as a research scientist. Your advice on both research as well as on my life have been invaluable. ***Dr. Lewis Wedgewood***, you helped me a lot, and I still remember the first few days struggle in the USA, which I could not withstand without your helpful discussions and guidance.

I would like to thank my friends in the chemical engineering department at UIC for all the great times that we have shared. I am particularly thankful to ***Sohaib J. Mohammed***, a racquetball partner, and a good friend, for his infinite patience with my command of the racquet and reaction speed.

ACKNOWLEDGMENTS (continued)

Last but not least, I am grateful to my parents, my family, siblings, friends, and acquaintances, who remembered me in their prayers for the ultimate success. I consider myself nothing without them. They gave me enough moral support, encouragement, and motivation to accomplish my personal goals. My two lifelines, my father, *Hamza*, and my mother, *Sabha* have always supported me in everything so that I only pay attention to the studies and achieving my objective without any obstacle on the way. I would like to thank my wife, *Esraa*, who made my life in the United States very smooth, enjoyable and exciting with her support, mental strength, and love.

In the end, I would like to thank the Higher Committee for Education Development in Iraq (HCED)/Office of the Prime Minister for the financial support. Also, I acknowledge the Advanced Cyberinfrastructure for Education and Research (ACER) group at The University of Illinois at Chicago for providing HPC resources that have contributed to the research results reported within this thesis.

Mohammed Hamza Khalaf

July 2019

CONTRIBUTION OF AUTHORS

Introduction and background about heavy organics in petroleum fluids, research objective, and thesis outline have been discussed in Chapter 1. Chapter 2 represents a literature review about asphaltene and its behavior. Chapter 3 gives a brief introduction to molecular dynamics simulation that is used in this dissertation. Chapter 4 discusses a published work in the Journal of Petroleum Science and Engineering/ Elsevier (full citation added). This work was about the aggregation of asphaltene in different mixtures. In this work, I was the first author, primary and major contributor and my advisor, **Dr. G.Ali Mansoori**, supervised the project, provided deep discussions and revised the manuscript. Chapter 5 discusses a published work in the Journal of Petroleum Science and Engineering/ Elsevier (full citation added). This work was about asphaltene aggregation during nitrogen and air flooding. In this work, I was the first author, primary and major contributor and my advisor, **Dr. G.Ali Mansoori**, supervised the project, provided deep discussions and revised the manuscript. Chapter 6 discusses a published work in the Journal of Petroleum Science and Engineering/ Elsevier (full citation added). This work was about the magnetic treatment of asphaltenic oils. In this work, I was the first author, primary and major contributor, whereas **Dr. Yong** updated and validated the input parameters for this simulation as well as critical discussion about the effects of magnetic field on asphaltene. My advisor, **Dr. G.Ali Mansoori**, supervised the project, provided deep discussions and revised the manuscript. Chapter 7 discusses an unpublished work regarding asphaltene deposition on calcite surfaces. This work was about asphaltene aggregation during nitrogen and air flooding. In this work, I was the first author, primary and major contributor and my advisor, **Dr. G.Ali Mansoori**, supervised the project, provided deep discussions and revised the manuscript.

TABLE OF CONTENTS

<u>CHAPTER</u>	<u>PAGE</u>
1 Introduction	1
1.1 Heavy Organics.....	1
1.2 Heavy Organics Precipitation and Deposition	2
1.3 Research Objectives/Motivation.....	4
1.4 Outline.....	6
2 Literature Review	7
2.1 The History of Asphaltenes.....	7
2.2 Asphaltene Behavior	10
2.3 Remediation of Asphaltene Deposition	16
3 Methodology of Molecular Dynamics Simulation	17
3.1 Introduction.....	17
3.2 Equation of Motion	18
3.3 Interaction Functions and Force Fields.....	20
3.3.1 Force field	20
3.3.2 Intermolecular interactions	21
3.3.3 Intramolecular interactions	22
3.4 Periodic Boundary Condition	23
3.5 Energy Minimization	24
3.6 Thermodynamic Ensembles.....	25
3.7 Temperature and Pressure Couplings.....	25
3.7.1 Velocity-rescaling temperature coupling	26
3.7.2 Parrinello-Rahman pressure coupling.....	26
4 A New Insight into Asphaltenes Aggregation Onset at Molecular Level in Crude Oil (an MD Simulation Study).....	27
4.1 Abstract	27
4.2 Introduction.....	28
4.3 Model Asphaltenes.....	31
4.4 Simulation Details.....	33
4.5 Results and Discussions	34
4.5.1 Radial distribution functions.....	34
4.5.2 Number of aggregates	35
4.5.3 Hydrogen bond (HB) interactions.....	39
4.5.4 Electrostatic (ES) and van der Waals (vdW) interaction energies	40
4.6 Conclusions.....	41
5 Asphaltenes Aggregation During Petroleum Reservoir Air and Nitrogen Flooding..	43
5.1 Abstract	43
5.2 Introduction.....	43
5.3 Molecular Structures	46
5.4 Simulation Methodology	47
5.4.1 Initial configurations	47
5.4.2 Force fields.....	48
5.4.3 Simulation details and algorithm	49
5.5 Results and Discussions	49
5.5.1 Effect of misciblized air and nitrogen on asphaltene aggregation	50
5.5.2 Interaction energies	56

TABLE OF CONTENTS (continued)

<u>CHAPTER</u>	<u>PAGE</u>
5.6	Conclusions..... 59
6	Magnetic Treatment of Petroleum and its Relation with Asphaltene Aggregation
	Onset (an Atomistic Investigation)..... 60
6.1	Abstract..... 60
6.2	Introduction..... 61
6.3	Previous Studies..... 61
6.4	Simulation Methodology 64
6.4.1	Molecular models..... 64
6.4.2	Magnetic field implementation 66
6.4.3	Simulation details..... 68
6.5	Results and Discussions 69
6.5.1	The effect of magnetic field on asphaltene aggregation 69
6.5.1.1	Radial distribution functions..... 69
6.5.1.2	Hydrogen bonds 77
6.5.2	The effect of magnetic field on asphaltene disaggregation..... 78
6.5.2.1	Radial distribution functions..... 78
6.5.2.2	Hydrogen bond..... 83
6.6	Conclusions..... 85
7	Asphaltenes Adsorption on Solid Calcite Surfaces..... 88
7.1	Abstract..... 88
7.2	Introduction..... 88
7.3	Asphaltene Structures 90
7.4	Simulation Method..... 91
7.4.1	Initial configurations..... 91
7.4.2	Force fields..... 92
7.4.3	Simulation details and algorithms..... 93
7.5	Results and Discussions 93
7.5.1	Asphaltene adsorption on solid surfaces..... 94
7.5.2	Interaction energies 99
7.6	Conclusions..... 102
8	Conclusions and Recommendations 104
8.1	Conclusions..... 104
8.2	Recommendations for Future Research 106
	Appendix..... 110
	References..... 113

LIST OF FIGURES

<u>CHAPTER</u>	<u>PAGE</u>
Figure 2-1. Three different model asphaltene reported in the literature.....	9
Figure 2-2. Asphaltene aggregation and flocculation in paraffinic crude oils.	13
Figure 2-3. Asphaltene steric colloidal formation.	14
Figure 2-4. Asphaltene micelle formation.	14
Figure 3-1. A simple MD algorithm	18
Figure 3-2. LJ potential between two approaching atoms.....	22
Figure 3-3. Intramolecular potentials.	23
Figure 4-1. Model asphaltenes used in the present study.	32
Figure 4-2. RDFs for the three model asphaltenes in different n-heptane plus o-xylene mixtures. (a) is A1, (b) is A2, (c) is A3.	36
Figure 4-3. Snapshots of the final configuration from the simulation of A1 asphaltene in different mixtures of n-heptane and o-xylene. a- in pure n-heptane, b- in 80% n-heptane, c- in 40% n-heptane, and d- in pure o-xylene.....	37
Figure 4-4. Snapshots of the final configuration from the simulation of A2 asphaltene in different mixtures of n-heptane and o-xylene. a- in pure n-heptane, b- in 80% n-heptane, c- in 40% n-heptane, and d- in pure o-xylene. Asphaltene molecules only are shown.....	38
Figure 4-5. Snapshots of the final configuration from the simulation of A3 asphaltene in different mixtures of n-heptane and o-xylene. a- in pure n-heptane, b- in 80% n-heptane, c- in 40% n-heptane, and d- in pure o-xylene. Asphaltene molecules only are shown.....	39
Figure 4-6. The average number of HBs of different asphaltenes in different n-heptane plus o-xylene mixtures.	40
Figure 4-7. ES and vdW interaction energies for the three model asphaltenes in different n-heptane concentrations versus simulation time. ES interactions of A1, A2, and A3 are represented by a, b, and c respectively; while vdW interactions of A1, A2, and A3 are represented by d, e, and f respectively.....	41
Figure 5-1. The seven asphaltenes (A1- A7) used in the present study.....	47
Figure 5-2. Cumulative coordination numbers of the 7 used asphaltenes at different concentrations of injected gases. a, c, e, and g are the cumulative numbers at 20, 40, 60, and 80% of air injection. b, d, f, and h are the cumulative numbers at 20, 40, 60, and 80% of nitrogen injection.	51
Figure 5-3. Average cluster size of the 7 asphaltenes at different air concentration where a, b, c, and d represent 20, 40, 60, and 80% of air respectively.	52

LIST OF FIGURES (continued)

<u>CHAPTER</u>	<u>PAGE</u>
Figure 5-4. Average cluster size of the 7 asphaltenes at different nitrogen concentration where a, b, c, and d represent 20, 40, 60, and 80% of nitrogen respectively.	53
Figure 5-5. Snapshots of seven model asphaltenes in 20% misciblized nitrogen. O-xylene and nitrogen molecules were removed for clarity.	55
Figure 5-6. vdW interactions of the 7 asphaltenes at different miscible gas concentrations. ..	56
Figure 5-7. ES interactions of the 7 asphaltenes at different miscible gas concentrations.	57
Figure 5-8. The average numbers of HB interactions at different gas concentrations.	58
Figure 6-1. Model asphaltenes used in this study.	66
Figure 6-2. RDF curves of A2 asphaltene at different magnetic fields in both mediums.	70
Figure 6-3. RDF curves of A3 asphaltene at different magnetic fields in both mediums.	72
Figure 6-4. RDF curves of A4 asphaltene at different magnetic fields in both mediums.	74
Figure 6-5. Snapshots of A2-A4 asphaltenes in paraffin and aromatic mediums at different magnetic fields. Where: I represents A2 in paraffin at 1.5T, II represents A2 in aromatic at 1.5T, III represents A3 in paraffin at 1.0T, IV represents A3 in aromatic at 1.0T, V represents A4 in paraffin at 0.5T, and VI represents A4 in aromatic at 0.5T.	76
Figure 6-6. The average number of hydrogen bonds of asphaltenes in both mediums.	78
Figure 6-7. RDF curves of A1-A4 asphaltenes at different magnetic fields.	79
Figure 6-8. Snapshots of different asphaltenes at different magnetic fields. Where: I represents A1 at 0 T, II represents A2 at 1 T, III represents A3 at 2 T, and IV represents A4 at 0 T.	83
Figure 7-1. Structure of asphaltene (A) and the four hypothetically modified structures M1-M4 used in this study.	91
Figure 7-2. Density profile of A asphaltene in the presence (black line) and absence (red line) of injected air, on smooth (a) and rough (b) surfaces.	95
Figure 7-3. Snapshots of the final configurations of onset of adsorption of Asphaltene (A) in the absence (left-side figures) and presence (right-side figures) of injected air, on smooth (top figures) and rough (bottom figures) surfaces.	95
Figure 7-4. Density profile of M1 asphaltene in the presence (black line) and absence (red line) of injected air, on smooth (a) and rough (b) surfaces.	97
Figure 7-5. Density profile of M2 asphaltene in the presence (black line) and absence (red line) of injected air, on smooth (a) and rough (b) surfaces.	97

LIST OF FIGURES (continued)

<u>CHAPTER</u>	<u>PAGE</u>
Figure 7-6. Density profile of M3 asphaltene in the presence (black line) and absence (red line) of injected air, on smooth (a) and rough (b) surfaces.	98
Figure 7-7. Density profile of M4 asphaltene in the presence (black line) and absence (red line) of injected air, on smooth (a) and rough (b) surfaces.	98
Figure 7-8. Density profiles of xylene, heptane, and air in z-direction away from the surfaces.	99
Figure 7-9. Intermolecular interactions between molecules and smooth and rough surfaces. (A) vdW interactions (B) Electrostatic interactions.	100

LIST OF TABLES

<u>TABLE</u>	<u>PAGE</u>
Table 2-1. Asphaltene and resin concentrations (wt%) of different crude oils	15
Table 4-1. Specifications of model asphaltenes reported in Figure 4-1	32
Table 4-2. The fractions of asphaltene molecules in various associations.	36
Table 5-1. Partial atomic charges and Lennard-Jones parameters for Nitrogen and Oxygen.	48
Table 7-1. Total interactions (kJ/mol) between selected atoms of asphaltene A and smooth and rough calcite. The chosen atoms are shown on the structure.	101
Table 7-2. Total interactions (kJ/mol) between M1 hypothetically selected segments and smooth and rough calcite. The chosen atoms are shown on the structure.	101
Table 7-3. Total interactions (kJ/mol) between M2 hypothetically selected segments and smooth and rough calcite. The chosen atoms are shown on the structure.	101
Table 7-4. Total interactions (kJ/mol) between M3 hypothetically selected segments and smooth and rough calcite. The chosen atoms are shown on the structure.	102
Table 7-5. Total interactions (kJ/mol) between M4 hypothetically selected segments and smooth and rough calcite. The chosen atoms are shown on the structure.	102

LIST OF ABBREVIATIONS

CMC	Critical Micelle Concentration
EOR	Enhanced Oil Recovery
ES	Electrostatic
HB	Hydrogen Bond
LJ	Lennard-Jones
MD	Molecular Dynamics
MMP	Minimum Miscibility Pressure
NMR	Nuclear Magnetic Resonance
NPT	Isobaric-Isothermal Ensemble
NVE	Microcanonical Ensemble
NVT	Canonical Ensemble
OPLS-AA	Optimized Potentials for Liquid Simulations All Atom
PBC	Periodic Boundary Condition
PME	Particle Mesh Ewald
RDF	Radial Distribution Function
SANS	Small Angle Neutron Scattering
SARA	Saturates, Aromatics, Resins, and Asphaltenes
SAXS	Small Angle X-ray Scattering
vdW	van der Waals
VMD	Visual Molecular Dynamics

SUMMARY

Increasing worldwide demand for energy and depletion of the conventional oil sources has created demand, economic feasibility and new technological challenges for tapping tremendous unconventional oil sources including heavy, extra-heavy oils, bitumen and oil sands. However, using these resources is associated with several challenges such as aggregation and deposition of heavy organics and low mobility arising from their high viscosities. Most of the industrial problems and challenges are associated with heavy organics deposition and especially asphaltene. Thus, this dissertation summarizes the asphaltene problems; the asphaltene behavior in the petroleum industry, highlighting asphaltene aggregation and precipitation during composition change; asphaltene deposition on solid surfaces; and the effect of magnetic fields on asphaltene aggregation. This dissertation reports on the successful fulfillment of the research objectives as follows:

(1) Asphaltene aggregation and precipitation is a function of the medium where asphaltene is soluble in aromatics and insoluble in paraffins. Composition change is one of the important parameters that cause asphaltene flocculation and precipitation. However, not all asphaltenes aggregate and flocculate due to their structures. In this work, molecular dynamics (MD) simulation was employed to investigate aggregation and flocculation of different asphaltene structures dissolved in different mixtures of normal heptane and ortho xylene. The roles of interaction energies on the onset of asphaltenes aggregation due to the changes in the composition (aromaticity) were investigated. The results showed that asphaltene behavior was affected by the aromaticity of the medium and asphaltene architecture, thus each structure behaved differently from one another. At high paraffine content, it was shown that asphaltene preferred face-to-face stacking, where the planes of the aromatic ring systems were aligned in parallel between two asphaltene molecules due to the high interactions

SUMMARY (continued)

between these aromatic cores. In addition, it was observed that flexible asphaltenes had low aggregation affinity comparing to the rigid asphaltene even with its high hydrogen bond interactions. From the results it could be concluded that the major factor in asphaltene aggregation is the architecture of each asphaltene molecule, where the number and length of the side chains, the number and distribution of heteroatoms, and the size and number of the aromatic cores are connected in representing asphaltene behavior.

(2) Asphaltene aggregation and precipitation is one of the concerns during enhanced oil recovery (EOR) that may happen inside reservoir porous media which could cause formation damage. There are several reports about supercritical nitrogen injection. However, this process may be costly if huge quantities of nitrogen are required. Accordingly, the economically promising method is an injection of supercritical air which contains about 79% nitrogen. In this work, asphaltene aggregation during miscible nitrogen/air flooding at reservoir conditions was investigated using MD simulation. The effect of injected misciblized gas concentrations and the role of interaction energies on different asphaltene structures were investigated. The results showed that the asphaltene aggregation process was highly affected by the content of injected fluids due to the solubility effects. Also, the aggregation was a function of asphaltene structure where structures with long aliphatic chains and archipelago architecture showed low association affinity than other flat asphaltenes. In the comparison of the use of misciblized nitrogen and air, there were no appreciable differences on asphaltene aggregation. The results of interaction energies showed that van der Waals interactions were affected by the concentration of the injected fluid.

(3) Recent experimental studies have shown that magnetic treatments reduce oil rheological properties and reduce heavy organic deposition. Most of these studies have focused on wax

SUMMARY (continued)

crystallization and there is little information about the effect of magnetic fields on asphaltene aggregation. In this work, asphaltene aggregation, under the influence of the magnetic field, was investigated using MD simulation. Local molecular structures, simulation trajectory, and hydrogen bond interactions were also investigated. The simulation results indicated that asphaltene aggregation in different mediums was influenced by the magnetic field and it was a function of its intensity. In a paraffinic solvent, the magnetic field could reduce the onset of asphaltene aggregation in the range of 20–35% and 25–70% in aromatic medium. Hydrogen bonds were also affected by magnetic treatments and these alterations were due to changes in the distances and the orientation of asphaltene molecules. It could be concluded that the effect of magnetic treatment on the onset of asphaltene aggregation was dependent on the intensity of the applied magnetic field, the medium, and the architecture of asphaltene.

(4) Asphaltene deposition could cause severe blockages in the reservoirs, wells, pipelines, and production and processing facilities. It is an insidious phenomenon and affected by different parameters such as changes in pressure, temperature, or composition, nature and distribution of reservoir fluids, the mineralogy of the rocks, ...etc. It was reported that asphaltene molecular structure such as the presence of different heteroatoms and its polarity play roles in asphaltene adsorption to the solid surfaces. In this study, molecular dynamics simulations were conducted to investigate the onset of asphaltene adsorption on smooth and rough calcite surfaces. The results showed an immobile and high dense layer of xylene rapidly adsorbed on the calcite while asphaltenes showed different adsorption affinities. The calculations and trajectory visualization showed that the morphology of the solid surface had a key role in the asphaltene adsorption whereas the adsorption of asphaltene was higher on the rough surface than that on the smooth surface. It was observed that asphaltene molecules

SUMMARY (continued)

accumulated as one aggregate on the protrudes of the rough calcite and randomly distributed and adsorbed on the smooth surface where the aromatic cores were parallel to the surface. Also, it was shown that asphaltene aggregation in the bulk was enhanced by air injection. Intermolecular energies showed higher interaction energies between asphaltene-rough calcite than asphaltene-smooth calcite. The interactions of asphaltene atoms with calcite showed that heteroatoms have an immense contribution to the adsorption process. Interaction energies of asphaltene heteroatoms showed that oxygen and nitrogen had either attraction or repulsion to the calcite surface. While sulfur had a high attraction to the calcite, and it may work as an adsorption site that could be enhanced by other heteroatoms.

1 Introduction

1.1 Heavy Organics

Crude oil is a complex mixture of different hydrocarbons in a wide range of molecular weights. It also includes other polydisperse organic compounds such as resins, asphaltenes, and organometallic compounds. Their structures are composed of carbon, hydrogen, metals, nitrogen, oxygen, and sulfur. In addition, there is a presence of inorganic oxides; salts; and metals (Khalaf and Mansoori, 2018, 2019). One of the ways to characterize heavy-end organic constituents of crude oils is to separate them through column chromatography into four groups: saturates, aromatics, resins, and asphaltenes known as SARA (Escobedo and Mansoori, 2010; Kim et al., 1990).

Saturates are also known alkanes which consist of normal-alkanes, iso-alkanes that are known as paraffins and cyclo-alkanes, which are known as naphthenes. The first four kinds of paraffins are gases under normal conditions. As the molecular weight increases, the boiling point and melting point increase as well. However, the volatility decreases by increasing the carbon number. Paraffins with $+C_{18}$ are solid under normal conditions and known as waxes. They are completely dissolved in petroleum mixtures at normal conditions (Bagdat and Masoud, 2015; Johnsen et al., 2011).

Aromatics are unsaturated hydrocarbons and characterized by one or more planar rings of atoms that are connected by double bonds. Benzene is the best-known aromatic hydrocarbon and counted as the base of different aromatic compounds.

Asphaltenes are the polar and heavier fraction of the crude oils. They are insoluble in paraffins and are soluble in aromatic and polar hydrocarbons like xylene (Khalaf and Mansoori, 2018). The molecular structure and detailed molecular behavior of asphaltene molecules are not fully known yet. The asphaltene fraction of petroleum fluids may also

contain some metals such as iron, nickel, and vanadium (and/or their oxides) (Khalaf and Mansoori, 2019). Asphaltenes present in petroleum fluids are polydispersed and contain a broad molecular weight distribution similar to polymers (Kawanaka et al., 1991; Pacheco-Sánchez and Mansoori, 1997).

The precursors of asphaltenes are resins which are soluble in a crude oil mixture. Resins are known to have much lower molecular weights than asphaltenes in addition to their low polarity and aromaticity (Mansoori, 2009). They also have a high tendency to be connected with large asphaltene aggregates (Mansoori, 2009; Mousavi-Dehghani et al., 2004).

1.2 Heavy Organics Precipitation and Deposition

Increasing worldwide demand for energy and depletion of the conventional oil sources has created demand, economic feasibility, and new technological challenges for tapping tremendous unconventional oil sources including heavy, extra-heavy oils, bitumen and oil sands. Simultaneously, by using these resources, the inevitable problem becomes the deposition of heavy organics (Luo and Gu, 2007). Most of the reservoirs, wells, pipelines, and production and processing facilities blockages are due to the precipitation and deposition of heavy organics. It is important to illustrate the variation between precipitation and deposition. Precipitation is the formation of a solid phase that comes out of the liquid phase as a function of thermodynamic variables (Ru and Alta'ee, 2015). However, deposition is the formation of a scale of precipitated solids on solid surfaces as a function of hydrodynamics, heat and mass transfer, solid-surface interactions (Hammami and Ratulowski, 2007). One of the serious problems in the oil industry is the deposition of heavy organics (Kawanaka et al., 1991). It causes complete clogging of pipes; serious damages of lines and/or production and processing equipment; and increasing the cost of production, transportation, and refining processes (Vazquez and Mansoori, 2000; Grijalva-Monteverde et al., 2005; Escobedo and

Mansoori, 2010). For example, Prions field in the North Aegean Sea had some wells were shut down within a few days of production due to heavy organic deposition (Adialalis, 1982). In Venezuela, stimulating treatments using acid resulted in complete plugging of the well due to heavy organic slug (Lichaa, 1977). The Ventura Avenue field in California experienced heavy organic deposition during acidizing and CO₂ injection which resulted in the re-drilling of many wells (Leontaritis and Mansoori, 1988). Tecominoacan and Jujo oil fields in Mexico had heavy organic deposition that caused complete blockage in some of the wells which required crucial aromatic wash to remove deposits. In the oil filed of Gulf of Mexico there was heavy organic deposition in under-sea pipelines causing high production rates to decrease which was associated with a high economic loss (Escobedo and Mansoori, 1992).

Petroleum heavy organics are classified as paraffine/wax, resins, asphaltenes, diamondoids, mercaptans, and organometallic compounds (Pacheco-Sánchez and Mansoori, 1997). The deposition of these compounds happen due to various reasons that depend on the molecular nature of these materials. For example, mercaptans and organometallic deposit due to solubility effects. Diamondoids and paraffine/wax deposit due to temperature changes (lowering oil temperature). Resins are usually associated with asphaltenes and they are not known to deposit alone (Mansoori, 2010). Asphaltenes deposit due to various reasons, the major parameters that controlling asphaltene precipitation and deposition are: (1) Nature and distribution of reservoir fluids, (2) Injection of fluids (composition changes), (3) Temperature changes, (4) Pressure changes, (5) The mineralogy and properties of the rocks, (6) Flow regimes, (7) Wall effect and electrokinetic phenomena, (8) Asphaltene/resin ratio, (9) and The brine amount and composition (Mansoori, 2010; Branco et al., 2001; Mirzayi et al., 2008).

Asphaltene deposition could occur in primary, secondary, and tertiary oil recovery and may occur in three steps (Mansoori, 2001). The first step is the formation of very small

particles that become suspended in the petroleum fluid. The second step is the flocculation of these particles. The third step is the deposition of these large particles due to their large size, or sticking of these particles onto solid surfaces and building a solid carbon layer on the internal walls of oil facilities (Abouie et al., 2015).

1.3 Research Objectives/Motivation

The crude oil production provides more than 80 million barrels a day (Energy Information Administration, 2019). This is a high energy demand all over the world which encourages the use of unconventional oil sources. However, using these resources is associated with several challenges such as aggregation and deposition of heavy organics and low mobility arising from their high viscosities. Most of the industrial problems and challenges are associated with heavy organic deposition, and especially asphaltene.

Asphaltene aggregation and deposition is a very insidious phenomenon. The laboratory studies suggested that the solution of asphaltene precipitation and deposition requires detailed analyses of asphaltene properties and its structure to understand its behavior in hydrocarbon solvents. The connection between asphaltene molecular structure and the asphaltene aggregation in different solvents is not well understood. Thus, to understand, predict, and develop a microscopic model of asphaltene there needs to be a lot of investigation on a molecular level. Thus, the main goal of the current study is to demonstrate and highlight the asphaltene problems and asphaltene behavior in the petroleum industry. To build a whole picture of asphaltene behavior at different length scales, one needs to understand and find a structure-function relationship. To achieve that, the work is divided into two folds. The first part includes studying the asphaltene aggregation and asphaltene behavior at different conditions and mediums. The second part involves investigating the effect of external forces (magnetic field) on the asphaltene aggregation and disaggregation as

well as observing the behavior of the other heavy organics in petroleum fluids. In both folds, molecular dynamics (MD) simulation technique was used to probe the microscopic behavior of asphaltenes.

The aim of using MD simulation in the current research is to fill an important gap in the understanding of asphaltene aggregation behavior, the nature of the association of asphaltenes in mixed (paraffinic and aromatic) solvents and/or during enhanced oil recovery (EOR) processes. The important parameter that leads to asphaltene flocculation and precipitation are the composition changes due to vaporization, blending with other oils, and/or EOR. The current study investigates the effects of asphaltene chemical structure, the composition changes on the asphaltene behavior, and aggregation processes during the blending or EOR. Studies proved that gas injection enhances asphaltene aggregation and promotes phase separation, which finally leads to asphaltene deposition; the problem being more severe for heavy oils. Transport of asphaltene aggregates within reservoir fluids inside the pores may block some of the pores leading to formation damage. Accordingly, asphaltene aggregation and deposition on calcite surface during air flooding is investigated. Understanding the interactions between asphaltenes, injected gases, and mineral surfaces is important to clarify asphaltene deposition affinity and reduce the possibility of asphaltene precipitation during EOR.

Moreover, MD simulation is used to investigate the effect of the external magnetic field on asphaltene aggregation/disaggregation. Few scientific evidences are available in the literature about the role of the magnetic field on asphaltenes' behavior. Some of the studies claimed that polar species (e.g., asphaltenes) were affected by magnetic fields, while others focused on paraffines. Due to the presence of different heteroatoms in asphaltene structures and their asymmetrical charge distribution, asphaltenes are affected by magnetic fields. It is believed that magnetic treatments change asphaltenes' intermolecular interactions which lead

to forming new associative structures (Loskutova et al., 2008). Therefore, asphaltene molecules may aggregate or disaggregate due to the effect of the applied magnetic field.

1.4 Outline

The dissertation is organized in the following style:

Chapter 2 introduces the basic knowledge about asphaltenes such as definitions, behavior properties, and remediation of asphaltene deposition. Chapter 3 presents a brief description of molecular dynamics simulation, whereas it explaining the used algorithms, interaction functions, and thermodynamic ensembles. Chapter 4 contains a study focused on the effects of the asphaltene chemical structures, the composition changes on the asphaltene behavior, and aggregation processes. This was published in the Journal of Petroleum Science and Engineering as “A new insight into asphaltenes aggregation onset at a molecular level in crude oil (an MD simulation study)”. Chapter 5 contains a study focused on the effects of air injection and asphaltene chemical structure on asphaltene aggregation processes. This was published in the Journal of Petroleum Science and Engineering as “Asphaltenes aggregation during petroleum reservoir air and nitrogen flooding”. Chapter 6 presents a brief description of the magnetic treatments of petroleum fluids. It contains a study focused on the effects of magnetic field, asphaltene chemical structures, and the medium on asphaltene aggregation processes. This was published in the Journal of Petroleum Science and Engineering as “Magnetic treatment of petroleum and its relation with asphaltene aggregation onset (an atomistic investigation)”. Chapter 7 contains a study focused on the effects of air injection and asphaltene chemical structure on the adsorption of asphaltene on calcite surfaces. “Molecular Dynamics Simulation of Asphaltenes Adsorption on Calcite surfaces”. Chapter 8 summaries the major findings of the dissertation and discusses future related research

2 Literature Review

2.1 The History of Asphaltenes

The term asphaltene was proposed by Boussingault in 1837 when he defined the constituent of France's bitumen that was turpentine soluble and alcohol insoluble (Boussingault, M., 1837). According to Nellensteyn, asphaltene is the petroleum fraction that is insoluble in low boiling point, paraffines but soluble in tetrachloride (Nellensteyn, 1924). This was a jump in the separation method that led to the use of heptane and pentane for asphaltene separation. Nellensteyn also suggested that asphaltene was a pure high molecular weight hydrocarbon. In 1931, Marcusson assumed that asphaltene was not a pure hydrocarbon petroleum fraction, but contained a small amount of sulfur, nitrogen, and oxygen (Marcusson, 1931). This assumption was followed from modification by Hillman and Barnett, (1937) who suggested that asphaltene composed of a chain structure and was formed by aromatic and saturated rings connected by short chains. In 1961, Yen with others, found that short-range order existed in solid asphaltene. They assumed that the diffraction patterns were due to the stacking of aromatic rings (Yen et al., 1961). To date, Yen's model is confirmed by different measurements and shown to be valid for asphaltene.

From the structural point of view, asphaltene is a multipolymer component that contains different building blocks. The molecular structures of asphaltenes are not yet fully known. Throughout the references, asphaltene fraction could contain more than 10^5 different molecular structures (Rogel and Carbognani, 2003). However, asphaltenes that are known are composed of polycyclic clusters, alkyl groups, nitrogen, oxygen, and sulfur (Khalaf and Mansoori, 2018). Because of their associating affinity, asphaltenes have a broad range of molecular weights, varying from hundreds to thousands. Recently, researchers suggested that the molecular weight of asphaltene monomer is in the range of 500-1000 Da with an average of about 750 Da (See for example Boek et al., 2009), and a molecular size varying between

1.2–2.4 nm (Ganeeva et al., 2011). Researchers classified asphaltene according to their separation into two groups, heavy and light asphaltenes. Asphaltenes that are separated by adding a minimum amount of n-alkanes are called heavy, polar, and insoluble. However, asphaltenes that are separated by adding a maximum amount of n-alkanes are called light, nonpolar, and soluble (Mansoori et al. 1988; Tojima et al., 1998).

Recent studies suggest that asphaltene molecular architecture could be found in two main structures (Murgich, 2003). The first is called island asphaltene which is composed of a large central aromatic core, and in some cases, is called rigid asphaltene. The second is called archipelago asphaltene which is found in several places all over the world. Archipelago asphaltene has separated aromatic cores connected by alkyl chains. The size of aromatic cores and length of alkyl chains help archipelago asphaltene to be more flexible than island asphaltene. Some studies show that island asphaltene forms strong and thermally stable aggregates (~ 400 °C, where bonds being in cracking). These aggregates are stabilized by adsorption of archipelago asphaltene where this adsorption is thermally stable up to 200 °C. These colloids adsorb free radicals, resins, metals, ...etc. (Storm et al., 1996; Liao et al., 2006). In the literature, there are many different proposed asphaltenes for different reservoirs. Figure 2-1 shows three different model asphaltenes proposed by different researchers for different oils. Models A1 and A2 represent island asphaltene, and model A3 represents archipelago asphaltene (Takanohashi et al., 2003; Pacheco-Sánchez et al., 2004).

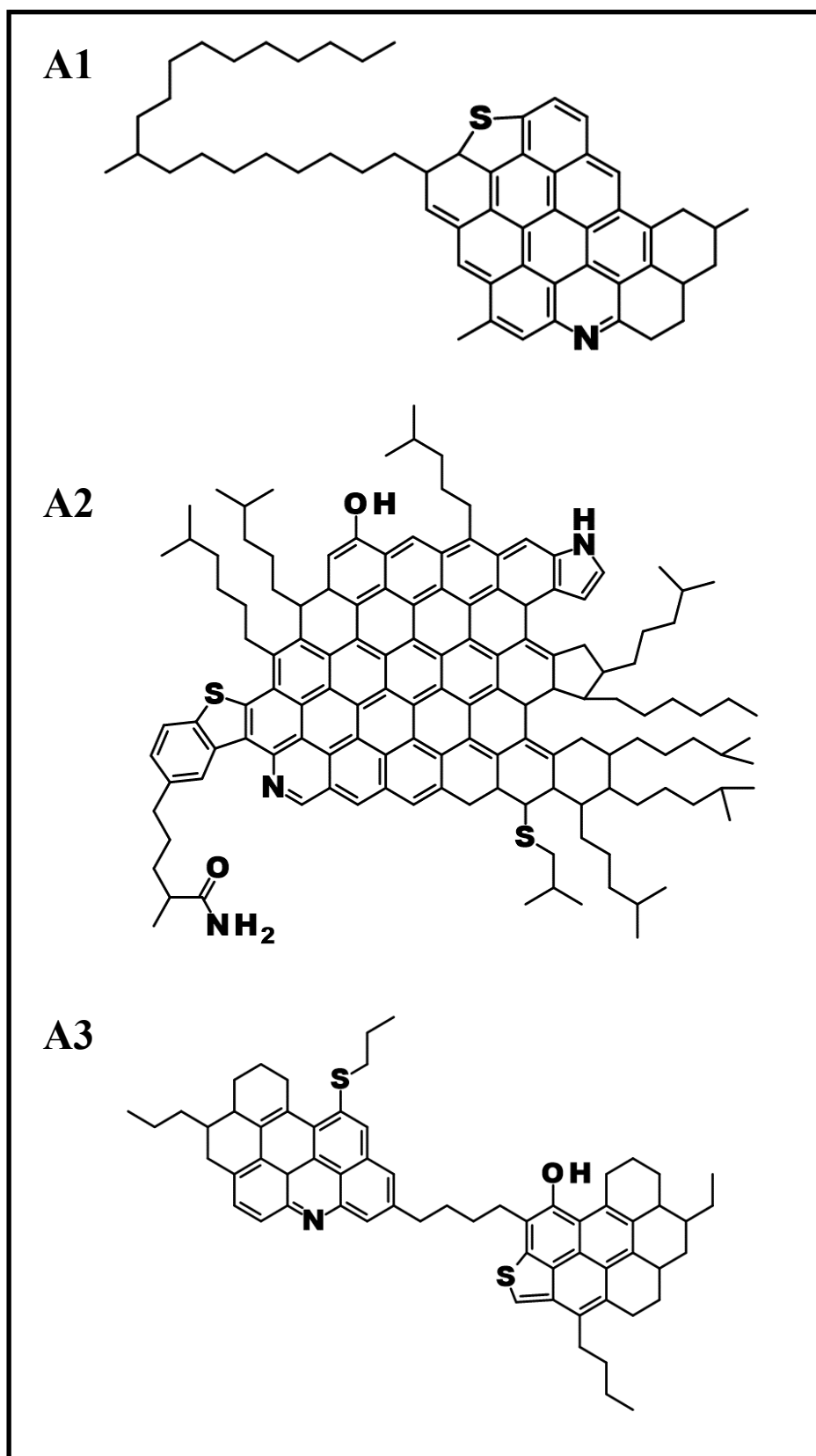


Figure 2-1. Three different model asphaltene reported in the literature.

2.2 Asphaltene Behavior

Asphaltenes are a heavy fraction of crude oils with density ranges from 1.1 to 1.2 gm/ml, H/C ratio between 1 to 1.2, and a wide range of solubility parameters 19-24 Mpa^{0.5} (Hirschberg et al., 1984). Besides the density and polarity, asphaltene has high effects on the crude oil rheological properties which are a function of the asphaltene concentration (Barré et al., 2008). Oils that have high asphaltene content have higher viscosities which are costly in production, transportation, and refining (Ghanavati et al., 2013).

The existence of asphaltenes in the crude oil results in many consequences. For example, it has been reported that asphaltene influence wax crystallization. It could act as a site of nucleation for wax and diamondoids crystallization (Mansoori, 2010). It may work as a surfactant by introducing its aliphatic chains into the wax crystal structures which leads to a lower crystallization (Ganeeva et al., 2011). The rate of wax deposition is profoundly affected by the degree of dispersed asphaltene (Lei et al., 2016). This was proved by the presence of asphaltene in paraffine deposit. The analysis of Hassi-Messaoud paraffin deposit showed 6% alkylated asphaltene that has more heteroatoms in comparison with asphaltene in the system (Daaou et al., 2008). Also, asphaltene is a high polar compound, and due to that, it could act as a glue and mortar during the heavy organic deposition process resulting in a high barrier to the flow (Pacheco-Sánchez and Mansoori, 1997). Asphaltene is responsible for the dark color of most crude oils. Dissolving asphaltene in benzene at very low concentration gives a red color, after 3 ppm the color becomes yellow (Kawanaka et al., 1991).

Asphaltene aggregates could form a nanometer scale particle which imposes a significant impact on both the upstream and downstream processes. They may cause fouling, foaming, erosion, corrosion, etc. (Pacheco-Sánchez and Mansoori, 1997). The difficulty of dealing with heavy organic deposits is directly related to the amount and nature of asphaltene presence in the system (Branco et al., 2001). As mentioned before, asphaltene has high sticky

properties, and has a high affinity for solid surfaces. Due to that, asphaltene clusters deposit on solid surfaces and could partially or totally plug the conduit (Branco et al., 2001).

The main variable that controls the asphaltene aggregates formation is the molecular structures of the asphaltenes. The wide range of polar groups and molecular weight distribution caused asphaltenes to be partially dissolved and partially in colloidal and/or micellar state. The dispersion degree depends on the chemical composition of the crude oil system (Kawanaka et al., 1991; Pacheco-Sánchez and Mansoori, 1997; Branco et al., 2001). However, other studies have shown that asphaltene solubility is mainly related to the fusion mode of the aromatic rings rather than aromaticity, molecular weight, and the presence of heteroatoms (Ganeeva et al., 2011). Studies reported that asphaltene is in a dissolved state when its concentration is less than 2 mg/L (Akhmetov et al., 2002). Researchers reported that when the asphaltene concentration range is 50 – 200 mg/L, the size of asphaltene nanoaggregates could be 10 nm. Increasing the concentration to more than 2 g/L leads to clusters formation with a fractal dimension that is composed of 8-10 nanoaggregates (Lisitza et al., 2009). In the letter of size, Anisimov et al., (1995) reported that the size of asphaltene particles could reach 1 μm and aggregated particles could be 4 – 5 μm . One may classify asphaltene aggregates into three categories: Stable asphaltenes when the size is $< 0.1 \mu\text{m}$; colloidal asphaltene when the size is $0.1 - 1 \mu\text{m}$; and flocculated asphaltene when the size is $> 1 \mu\text{m}$. While asphaltenes that stabilized by resin are electrically charged and have a diameter of 3 – 4 nm (Escobedo and Mansoori, 1995a). Durand et al., (2009) reported that asphaltenes form nano and micro-aggregates when its concentration is about 3%. Asphaltene aggregates could be in different shapes. Small angle x-ray (SAXS) and neutron scattering (SANS) showed that asphaltene aggregates could be elongated cylindrically, rod-like, disk-like, or elongated ellipsoids, while the rheological properties interpreted it to disk-like (Ganeeva et al., 2011).

These studies indicate that small asphaltene particles could be dissolved in the crude oil system, whereas relatively large particles could aggregate and flocculate due to the solubility and high paraffin content. Because of the large size of flocculated asphaltene and the sticky properties of asphaltene, these clusters cause irreversible asphaltene deposition. Murgich, (2003) reported that organic molecules that have favorable contact area (core) form aggregates between them instead of other molecules. This will produce a core of aggregated large molecules with smaller outer molecules. The outer layers of asphaltene aggregates are mainly alkyl side chains; thus, adding more molecules becomes difficult due to the steric repulsion. It is worth to mention that asphaltene aggregates need to go through structure deformation of the aromatic cores and side chains to produce stable stackings. Thus, the formation of large stable aggregates is less favorable due to the steric repulsion of the chains. This was approved by Murgich et al., (1996) where they found that alkyl chains slightly deformed from free molecules to give better aromatic-aromatic interactions. Also, Rogel, (1995) found that aggregated asphaltenes under vacuum conditions were in energetically favored structures. This means asphaltene has the potential to be in the aggregated state rather than the dispersed state. Pacheco-Sánchez et al., (2003) placed two identical asphaltenes in parallel to study the interaction energies as a function of separation distance. They found that attraction was very high at close distances 4 – 5 Å and with high repulsion when the distance reached 3 Å. Also, they reported the geometries of asphaltene stackings. They claimed that face-to-face stacking was due to π - π interactions; T-shape and offset stackings were due to π - σ and σ - σ interactions respectively. Asphaltene aggregation and flocculation in paraffinic crudes are described in Figure 2-2 which represents the aggregation of asphaltene starting from a molecular level.

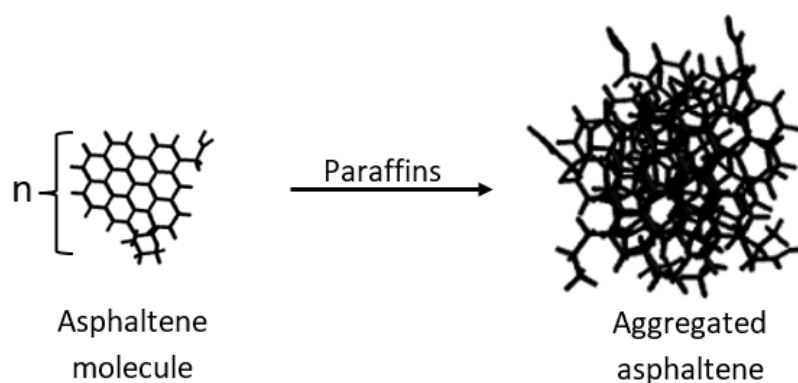


Figure 2-2. Asphaltene aggregation and flocculation in paraffinic crude oils.

In the presence of a sufficient amount of resin in the mixture, asphaltene could form steric colloids where resin works as a peptizing agent. When adding asphaltene molecules to asphaltene aggregates, it becomes unfavorable due to the energy barriers, resin molecules start stacking. At the right conditions, resin covers the surface of asphaltene aggregates and extends their aliphatic chains into the crude oil (aliphatic-phase) which makes a protection layer that prevents other colloids from approaching each other. In this case, resin neutralizes the polar charge, thereby making the micelle more soluble in the crude oil. Lichaa (1977) suggested that there is a critical resin concentration in the crude oil mixture. Below this concentration, asphaltene aggregates may flocculate and precipitate, while above that concentration, they may not flocculate or precipitate. If the resin can not fit and blocks the vacancy sites on asphaltene aggregates, asphaltene flocculation will happen. For stable colloidal asphaltene, other factors may contribute and enhance the precipitation and deposition of asphaltene colloids. These factors are heating, agitating, pressurizing, and/or changes in composition (Branco et al., 2001). Figure 2-3 shows asphaltene steric colloids' formation. Generally, asphaltene and resin molecules have 3D structures; thus, asphaltene steric colloids are in complex shapes.

In the case of the excess amount of aromatic solvents, several studies were done to investigate the asphaltene in the micellar form where asphaltenes can self-associate similar to surfactants (Pacheco-Sánchez and Mansoori, 1997). Most of these studies focused on the critical micelle concentration of asphaltene in aromatic solvents. Similar to surfactants, the surface tension measurements were utilized to detect the asphaltene critical micelle concentration (CMC). Sheu (1996) showed that an asphaltene below CMC is in a molecular state and when it is above CMC is in the micellar form. CMC of asphaltene is about 0.3 mg asphaltene/gm solvent (Priyanto et al. 2001a) while others reported asphaltene CMC is about 0.05 wt%. There are several studies focused on the shape of these micelles in the aromatic solvents. Some of these studies suggested that asphaltene forms are disk-like, sphere-like, and/or cylindrical-like.

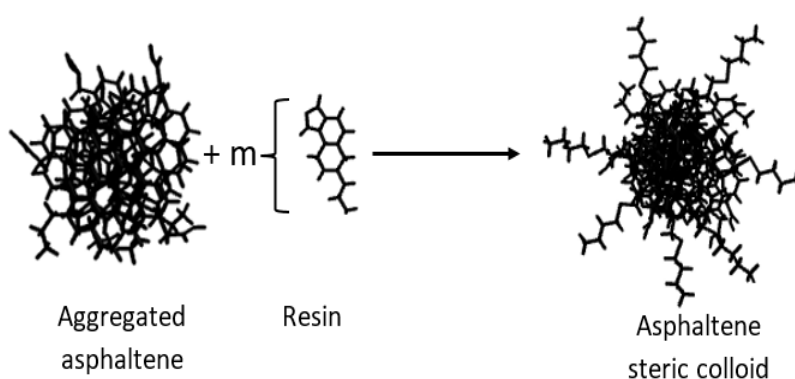


Figure 2-3. Asphaltene steric colloidal formation.

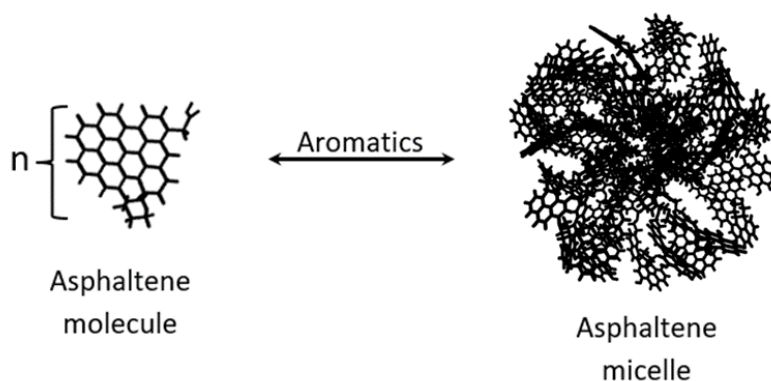


Figure 2-4. Asphaltene micelle formation.

Asphaltene precipitation and deposition are usually found in light crude oils even when the heavy crude has more asphaltene. This is because light crude oils are rich with light (low boiling point) components that asphaltenes are insoluble in. Asphaltene deposition around different locations showed that its problems are not related to its concentration. All over the world, asphaltene content ranges from traces to ~20 %, see Table 2-1. In Venezuela, Boscan crude oil has 17 wt% asphaltene and does not have any deposition problems. While Mata-Acema crude oil that has 0.4 wt% asphaltene suffers from asphaltene deposition (Leontaritis and Mansoori, 1988). Table 2-1 shows asphaltene and resin concentration of different fields over the world.

Table 2-1. Asphaltene and resin content (wt%) of different crude oils (Mansoori, 2010).

Crude oil	Resin	Asphaltene	Asphaltene/Resin
Canada, Athabasca	14	15	1.07
Canada, Alberta	8.5	5.3	0.62
Canada, Cold Lake	25	13	0.52
USA, MS, Baxterville	9.9	17.2	1.93
USA, LA, Brookhaven	4.6	1.65	0.36
Mexico, Panucon	26	12.5	0.48
Mexico, Tecoaminocan	8.8	1.5	0.17
Mexico, Isthmus	8.1	1.3	0.16
Brazil, Campos, Atabasca	21.55	2.8	0.13
Venezuela, Boscan	29.4	17.2	0.58
Russia, Balachany	6	0.5	0.08
Russia, Kaluga	20	0.5	0.025
India, Mangala crude	20-30	<0.5	<0.02
Iraq, Kirkuk	15.5	1.3	0.08
Algeria, Hassi Messaoud	3.3	0.15	0.05
France, Lagrave	7.5	4	0.53

2.3 Remediation of Asphaltene Deposition

A Proper understanding of asphaltene behavior during petroleum processes can help and reduce the heavy organics aggregation and deposition problems. Heavy organic deposition happens in flow lines, productions facilities, and/or downstream. It has high economic impacts where the remediation causes substantial loss to the oil production, or the damage in the wells and equipment. Modifications and changes in the operation process could help eliminate and reduce heavy organic deposition better than chemical additives and/or mechanical means. The presence of asphaltene in the heavy organic deposits makes the deposit hard to deal with. There are several remediation methods reported in the literature which include: (1) Production alternation techniques such as shear reduction, elimination of incompatible materials, reduction of the pressure-drop, and neutralization the electrostatic forces; (2) Chemical treatments such as dispersants, antifouling, coagulants (their roles are similar to resins), adding polar solvents, etc.; (3) Mechanical treatments such as pigging, mechanical vibration, manual stripping, etc.; (4) Thermal treatments such as in-suite composition, steam or hot water injection, circulating hot solvents, etc.; (5) and Applying external forces such as electric field, magnetic field, ultrasound, microwave techniques, etc., (Mansoori, 2010; Pacheco-Sánchez and Mansoori, 1997).

3 Methodology of Molecular Dynamics Simulation

3.1 Introduction

Computer Simulation is a powerful research tool used in science today. For complex systems, computer simulations became a useful tool to understand and investigate these systems. In the recent development of computers, large and complex systems can be deeply explained through computer simulations. Now, computer simulation is a connection between the microscopic length scale and the macroscopic properties of targeted systems. In some cases, experiments are impossible, too dangerous, and/or expensive examples include fighting, explosions, high-pressure experiments. Thus, computer simulation is a handy tool to complete these investigations. They are also bridges between the experimental and theory by testing the theoretical models and comparing them with experimental results. In the experiment, systems are subjected to measurements, and the results are in numeric forms. A theoretical model is a set of mathematical equations, and it is valid when it can describe the systems' behavior.

The use of computational techniques in chemistry is known as computational chemistry, which includes quantum mechanics of molecules and the dynamics of large molecular systems. One of the computational chemistry simulations is molecular dynamics (MD) simulation. It describes the movements of interacting particles (atoms or molecules) for a period of time. Molecular dynamics simulation is a technique where the time evolution of a set of interacting atoms is followed by integrating their equations of motion (Newton's equation of motion).

Computations involve following the motion of a large number of interacting particles (Abraham, et al., 2014). They involve a long series of time-steps, at each of which Newton's equation is solved to calculate the new positions and velocities from the previous positions and velocities and the forces (Van Der Spoel et al., 2005). This process is quite simple, but

there are many of them at each time-step. Since the simulation is at the atomic level and for accuracy, the time-step must be very small which is usually a femtosecond (10^{-15} seconds). The total computation may results in $\sim 10^{-8}$ seconds which could take a few days of computer time (Abraham, et al., 2014). Figure 3-1 shows a simple MD algorithm.

Understanding the MD simulation results requires carefully visualization of the results carefully, which contain millions of numbers that represent the history of the velocity, position, and forces. The visualization of the molecular movements can give a quite description of the process and the behavior of the specific molecules under corresponding conditions.

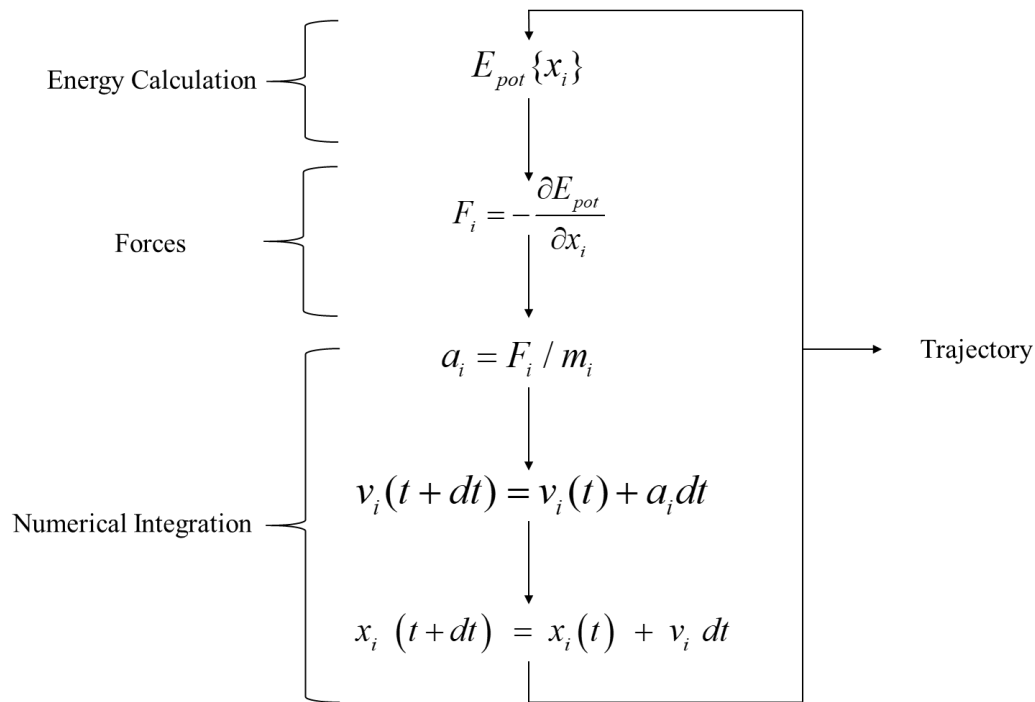


Figure 3-1. A simple MD algorithm

3.2 Equation of Motion

It is mentioned before that force on each particle is a function of the position of the particle. By definition of Newton's second law, the force could be changed if the position of other

particle are changed. MD simulations are based on solving Newton's equation of motion for a system composed of N interacting atoms as follows:

$$m_i \frac{\partial^2 \mathbf{r}_i}{\partial t^2} = \mathbf{F}_i \quad (2-1)$$

where m_i , \mathbf{r}_i and \mathbf{F}_i are the mass of atom i , position vector of atom i and the force acted on atom i . Beside the force computing, the potential energy is also computed which is the negative derivative of the potential function $U(\mathbf{r}_1, \mathbf{r}_2, \dots, \mathbf{r}_N)$:

$$\mathbf{F}_i = - \frac{\partial U}{\partial \mathbf{r}_i} \quad (2-2)$$

This equation is solved simultaneously for all atoms in small time steps, and the coordinates are written on an output file at regular intervals. Computing the forces and potentials as functions of the position generates the trajectory over a time period.

In MD simulations, different integrating algorithms are used to integrate the equation of motion. The famous algorithms are *verlet*, *velocity verlet*, and *leap-frog* integrators. In this work, the leap-frog algorithm is used which is the default integrator in GROMACS package (Van Der Spoel et al., 2005). It uses position at time t and velocity at time $t - \frac{1}{2}\Delta t$. The position and velocity are then updated using the force that is calculated from the position and time. The sum of interactions with other particles give the total force on each particle at a particular time. The leap-frog integrator is given by these equations:

$$\mathbf{r}(t + \Delta t) = \mathbf{r}(t) + \Delta t \mathbf{v}(t + \frac{1}{2}\Delta t) \quad (2-3)$$

$$\mathbf{v}(t + \frac{1}{2}\Delta t) = \mathbf{v}(t - \frac{1}{2}\Delta t) + \frac{\Delta t}{m} \mathbf{F}(t) \quad (2-4)$$

Molecular dynamics is a statistical mechanics method. Thus, configurations are distributed according to some statistical distribution function. According to statistical

physics, physical quantities are represented by averages over configurations (Abraham, et al., 2014). When the system reaches equilibrium, many macroscopic properties can be extracted by averaging the trajectories (Van Der Spoel et al., 2005). The property $\langle X \rangle$ can be calculated as following:

$$\langle X \rangle = \frac{1}{t} \int_0^t X(t) dt \quad (2-5)$$

3.3 Interaction Functions and Force Fields

In MD simulations, both intermolecular (non-bonded) and intramolecular (bonded) interactions are employed to calculate the potential, U . The equation to calculate the force acting on a particle to solve equation (2-2) is as follows:

$$U = U_{intermolecular} + U_{intramolecular} \quad (2-6)$$

Where $U_{intermolecular}$ is the potential that arises from the interaction of two distinct atoms and $U_{intramolecular}$ is the potential in the same molecule that comes from the interaction between the atoms connected by bond, angle and dihedral.

3.3.1 Force field

Force fields are a set of mathematical expressions that describe the dependence of system energy on the coordinates of its particles. It consists of a set of parameters of interatomic energy in an analytical form. Force field parameters are the bond length, angle, dihedral, Lennard-Jones parameters, and the atomic charges. These parameters are usually obtained either from a proper quantum mechanical calculation, or by fitting to experimental data such as X-ray and NMR results. Several force fields are used in MD simulations to describe

specific molecules such as AMBER, CHARMM, OPLS, etc (Van Der Spoel et al., 2005). The parameters of the force fields are available in most of the open source simulation packages. Also, several online servers provide all the parameters for targeted systems. One of the web servers that generates all OPLSAA parameters is *LigParGen* which is managed by professor Jorgensen's group at Yale University (Dodda et al., 2017).

3.3.2 Intermolecular interactions

The intermolecular interactions were calculated from van der Waals (vdW) interaction, which is represented by Lennard-Jones (LJ), and the electrostatic interaction, represented by Coulomb (Abraham, et al., 2014) as the following:

$$U_{intermolecular} = U_{LJ} + U_C \quad (2-7)$$

where U_{LJ} and U_C are Lennard-Jones and Coulomb potential, respectively.

Lennard-Jones potential between atoms i and j is given by:

$$U_{LJ}(r_{ij}) = 4\epsilon_{ij} \left[\left(\frac{\sigma_{ij}}{r_{ij}} \right)^{12} - \left(\frac{\sigma_{ij}}{r_{ij}} \right)^6 \right] \quad (2-8)$$

Where ϵ_{ij} and σ_{ij} are LJ potential parameters and r_{ij} is the distance between the atoms.

Coulomb interaction between two charged atoms is given by:

$$U_c(r_{ij}) = \frac{1}{4\pi\epsilon_0} \frac{q_i q_j}{\epsilon_r r_{ij}} \quad (2-9)$$

where q_i and q_j are the charges on atom i and j, respectively, and ϵ_r is the dielectric constant.

Figure 3-2 shows the LJ potential of two atoms as a function of the separation distance.

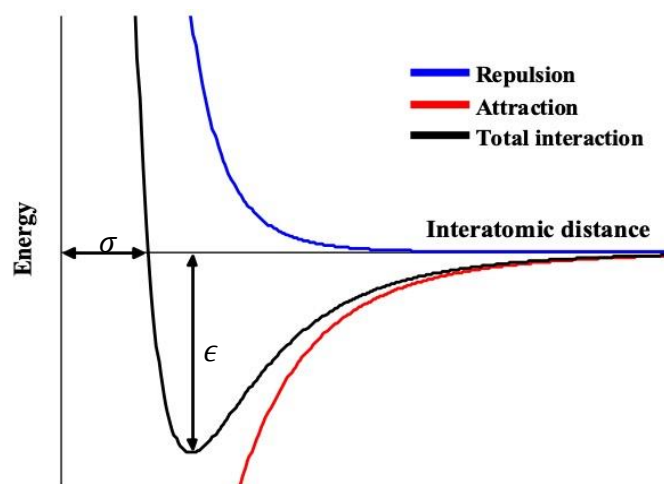


Figure 3-2. LJ potential between two approaching atoms.

3.3.3 Intramolecular interactions

The intramolecular potentials were calculated for two-body (bond stretching, b), three-body (angle, a), and four-body (dihedral, d) interactions as follows:

$$U_{intramolecular} = U_b + U_a + U_d \quad (2-10)$$

where U_b , U_a , U_d are the potential comes from bond stretching, bond angle, and dihedral angle, respectively.

Bond stretching potential describes the chemical bond between two covalently bonded atoms and it is a function of the interatomic distance. There are different forms of bond stretching potential. The default function in OPLS-AA in GROMACS is Harmonic potential; it is given and illustrated in Figure 3-3.

Angle bending potential describes the bending (vibration) of three (i,j,k) atoms and it is a function of the angle between them. The default form of angle potential in the OPLSAA force field is Harmonic potential; it is given and illustrated in Figure 3-3.

The dihedral angle potentials (sometimes referred to 4-body torsion potentials) describe the interaction arising from torsional forces in the molecules. They come from torsion of the angle between four atoms (i, j, k, l). The default form of dihedral potential in GROMACS for OPLS-AA force field is Ryckert-Bellemams potential; it is given and illustrated in Figure 3-3.

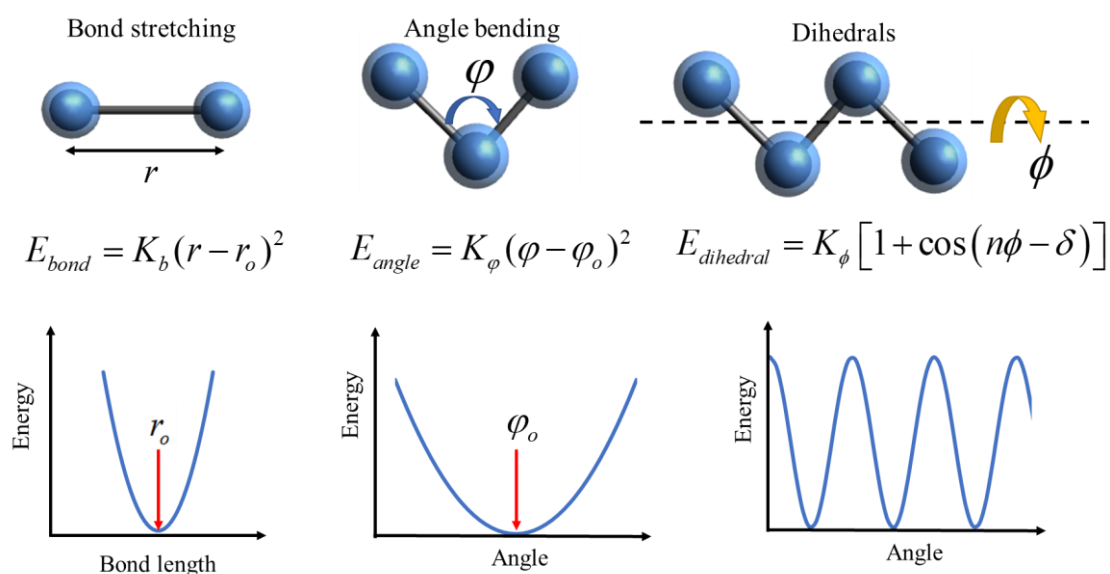


Figure 3-3. Intramolecular potentials.

3.4 Periodic Boundary Condition

In molecular simulations, the number of simulated particles is negligible in comparison with the macroscopic system. To overcome this, the periodic boundary condition (PBC) is used. This means putting the atoms of the targeted system in a small box (usually nm size) which is replicated to the infinity in the three dimensions. PBC is very useful in MD simulations which allows the calculation of bulk thermodynamic properties in a small size box (Abraham, et al., 2014).

For the system of N interacting particles, each particle in the box interacts not only with other particles, but also with their images. Since the potentials are a finite (short) range, a cut-off distance is used where the atoms interact with the nearest atoms or their images. To avoid more than one image in the cut-off distance, the cut-off must exceed half of the short box vector. The cut-off and the simulation box size are very important, especially when dealing with macromolecules (e.g. polymers or asphaltene). If this is the case, a solvent molecule (e.g. water) could interact with both sides of the macromolecule. Thus, the box vectors should be at least two times the cut-off plus the length of the macromolecule (Adams, et al., 1979).

3.5 Energy Minimization

The forces between the molecules in the initial system are extremely high; therefore an energy minimization is essential before performing the simulation. There are three famous energy minimization methods used in MD simulations which are the steepest descent, conjugate gradients, or lbfgs (limited-memory Broyden-Fletcher-Goldfarb-Shanno) (Abraham, et al., 2014). Steepest descent method was employed in our simulations for the energy minimization step. In this method, the initial forces and potential are calculated (Abraham, et al., 2014). The new positions are calculated as follows:

$$\mathbf{r}_{n+1} = \mathbf{r}_n + \frac{\mathbf{F}_n}{\max(|\mathbf{F}_n|)} h_n \quad (2-11)$$

where h_n is the maximum displacement and \mathbf{F}_n is the force. The new position is accepted or rejected as follows:

If $U_{n+1} < U_n$, the new position is accepted and $h_{n+1} = 1.2h_n$.

If $U_{n+1} > U_n$, the new position is rejected and $h_{n+1} = 0.2h_n$.

The algorithm stops when the maximum of the absolute values of the force components is smaller than a specified value.

3.6 Thermodynamic Ensembles

The choice of simulation parameters (algorithm, ensemble, temperature or pressure) is based on simulation efficiency reproducibility of experimental data, thermodynamic, and transport properties. In MD simulation, there are several thermodynamics ensembles depending on the collection of microscopic states that are similar to macroscopic states. The macroscopic state of a system is typically described by a group of parameters such as temperature, T , pressure, P , number of interacting particles, N , volume, V , energy, E , and the chemical potential, μ . The ensembles that are used in MD simulations are as follows: (1) Microcanonical Ensemble (NVE) which is characterized by a fixed number of particles, N , a fixed volume, V , and fixed energy, E . (for isolated systems); (2) Canonical Ensemble (NVT) which is characterized by fixed number of particles, N , fixed volume, V , and fixed temperature, T ; (3) and Isobaric-Isothermal Ensemble (NPT): which is characterized by fixed number of particles, N , fixed pressure, P , and fixed temperature, T .

3.7 Temperature and Pressure Couplings

The system configurations that come from integrating the equation of motion help in estimating the standard and dynamic properties of the system. MD simulations are similar to actual experiments where they need the system to be prepared; the temperature and pressure are controlled. Thus, to control the temperature and the pressure of a system, there are several temperatures and pressure couplings is used which are related to the desired ensemble. In this

dissertation, velocity-rescaling temperature coupling, and Parrinello-Rahman pressure coupling are employed (Van Der Spoel et al., 2005).

3.7.1 Velocity-rescaling temperature coupling

Velocity-rescaling mimics strong temperature coupling and produces a correct canonical ensemble. It ensures a correct kinetic energy distribution by modifying the velocity (Abraham, et al., 2014).

$$T(t) = \frac{1}{K_B N_f} \sum m_i v_i^2(t) \quad (2-12)$$

$$T_{new} - T(t) = (\lambda^2 - 1)T(t) \quad (2-13)$$

$$\lambda = \sqrt{\frac{T_o}{T(t)}} \quad (2-14)$$

K_B is Boltzmann's constant, N_f is the number of degrees of freedom.

3.7.2 Parrinello-Rahman pressure coupling

This coupling is used for constant pressure simulations when the pressure (or volume) fluctuations are important, especially for small systems. The box vectors obey the equation of motion and are represented by matrix \mathbf{b} (Abraham, et al., 2014).

$$\frac{d^2 \mathbf{b}}{dt^2} = u \mathbf{W}^{-1} \mathbf{b}'^{-1} (\mathbf{P} - \mathbf{P}_{ref}) \quad (2-15)$$

$$(\mathbf{W}^{-1})_{ij} = \frac{4\pi^2 \beta_{ij}}{3\tau_P^2 L} \quad (2-16)$$

β_{ij} is the approximate thermal compressibility which determines the strength of coupling and how the box deforms. τ_P is the pressure time constant, and L is the largest box matrix element.

4 A New Insight into Asphaltenes Aggregation Onset at Molecular Level in Crude Oil (an MD Simulation Study)

REPRINTED WITH PERMISSION FROM MOHAMMED H. KHALAF AND G.ALI MANSOORI, A NEW INSIGHT INTO ASPHALTENES AGGREGATION ONSET AT MOLECULAR LEVEL IN CRUDE OIL (AN MD SIMULATION STUDY), JOURNAL OF PETROLEUM SCIENCE AND ENGINEERING 162 (2018) 244-250. COPYRIGHT 2018 ELSEVIER.

4.1 Abstract

The findings reported here are to understand the nature of asphaltenes aggregation behavior at the molecular level in crude oil. Previous studies have been rich with the statistical and macroscopic aspects of heavy organics behavior in petroleum fluids. Molecular dynamics simulations of three different model asphaltene molecules in a "modeled crude oil" composed of n-heptane and o-xylene were conducted. The roles of van der Waals (vdW), hydrogen bond (HB), and electrostatic (ES) interaction energies on asphaltenes aggregation were investigated. Trends in aggregations, radial distribution functions (RDFs), vdW, HB, and ES interactions were produced and analyzed. Our studies indicated that asphaltenes with different molecular structures behaved differently from one another. At high paraffinic conditions, the preferred stacking of asphaltene molecules was face-to-face. The presence of HBs enhanced the stability of the aggregate. The number of HBs varied in each model of asphaltene, depending on their detailed structures. The ES interactions between asphaltenes were either attraction or repulsion depending on the molecular structure. Overall, the major factor was the architecture of each asphaltene molecule, such as the number and length of chains, the number and position of heteroatoms, and the number and size of the aromatic cores where they are linked together to represent asphaltene behavior.

4.2 Introduction

Asphaltene constituents are the polar and heavy part of the SARA analysis. While they are insoluble in paraffins, they are soluble in aromatic and polar hydrocarbons like toluene, xylenes, etc. Asphaltenes are known to have a high tendency to be associated together and form aggregates that eventually may deposit, causing fouling in porous media of the reservoir and flow lines.

Numerous molecular dynamics (MD) simulation studies regarding asphaltene aggregations already exist. Here are examples of a few of these studies: Takanohashi et al., (1994, 1998) used molecular mechanics and MD simulations to investigate the association of coal-derived asphaltene-like molecules relation with coal rank. They claimed that non-bonded interactions depended on the coal rank, where vdW interactions increase when the coal rank increased. Also, they used benzene, methanol, and pyridine as solvents to study the association of coal-derived molecules. They found that dissociation of molecules occurred in pyridine, but not in benzene or methanol. They reported that pyridine could provide both HBs and aromatic-aromatic interactions, while other compounds could only provide one kind of interaction which was not enough for dissociation. Rogel (1995) used MD simulation to study the aggregation process and the calculations of solubility parameters of two model asphaltenes. The simulation results showed a decrease in solubility parameters as the aggregation state increased. Also, interaction energies were higher in heptane than in toluene. Later, Rogel (2000) studied the association of asphaltene and resin and found that the main force in the association process was vdW. Then, claimed that the contribution of HBs in the association process was low and there were few structural changes in the association. Also, Rogel reported that asphaltenes with a low H/C ratio, high aromaticity, high aromatic condensation, and high molecular weight have a greater tendency to associate. These results agreed with experiments, where deposited asphaltene was found to have low H/C, high

aromaticity, and high molecular weight. To study asphaltene aggregation morphology, Pacheco-Sánchez et al., (2004a) used molecular simulation geometry optimization for three different model asphaltenes. They found that asphaltenes aggregate in different morphologies (face-to-face, T-shape, and offset stacking). Later, Pacheco-Sánchez et al., (2004) used MD simulation to study the effect of pressure on asphaltene immersed in n-heptane and toluene. They found that dissociation of asphaltene aggregates immediately occurred in toluene as a function of the pressure. They reported that the dominant stacking was offset with a separation distance that matched with what was reported in the literature. Carauta et al., (2005) used molecular mechanics and quantum mechanics to find the mean distance between the asphaltene molecules which was about 4.1 Å and the shortest distance was about 3.6 Å, thus agreeing with the Yen's model. Vicente et al., (2006) used Monte Carlo and MD simulation methods to estimate the Hildebrand solubility parameter of a model asphaltene. Their results closely matched experimental results. Alvarez-Ramirez et al., (2006) used molecular and quantum mechanics to calculate the binding energy of asphaltene-asphaltene, asphaltene-resin, and resin-resin compounds in a vacuum through different orientations (face-to-face, T-shape, edge-to-edge, and random). They found that face-to-face configuration had the deepest potential, which was the same as reported in the literature. Zhang and Greendfield (2007) used an MD simulation to analyze a model asphalt (i.e., A mixture of asphaltene represented by a model of asphaltene, a resin represented by 1,7-Dimethylnaphthalene, and a maltene represented by n-C₂₂). They found that the orientations of the nearest asphaltene molecules were affected by the molecular structure of asphaltene as well as the temperature. At low temperatures, asphaltenes with high aromaticity and short aliphatic chains tended to remain almost parallel, whereas at high temperatures, they were more likely to be in a T-shape orientation. For asphaltenes with low aromaticity and long aliphatic chains, they tended to be in either a T-shape or parallel at high temperatures. Boek

et al., (2009) developed a computer algorithm to generate asphaltene molecular structures depending on experimental data (molecular weight, elemental analysis and NMR spectroscopy). Later, they used an MD simulation to study the asphaltene aggregation process of the model asphaltenes constructed by their algorithm in n-heptane and toluene. They found that asphaltenes were associated in parallel and T-shapes (Headen et al., 2009). Yaseen and Mansoori (2017) used MD simulation to study the interactions between asphaltenes and solvents. They reported that inter- action energies increased with the pressure and decreased with increasing the temperature. Finally, De León et al., (2015) used an MD simulation to calculate asphaltene solubility parameters and studied the asphaltene aggregation of four asphaltenes. Their findings showed that asphaltene molecules had a lower energy in the aggregation state than in the monomer state. They also reported vdW energy was due to an aromatic core, and electrostatic energy was due to the presence of heteroatoms where they equally contributed in asphaltene aggregation.

Because of asphaltene solubility, the onset of its aggregation process is affected by the crude oil composition. Previous simulation studies of asphaltenes were performed in pure aromatic and pure paraffinic solvents. However, there is a need to understand and evaluate the onset of aggregation of asphaltene in media with varied aromaticity, mixed solvents its molecular nature, and its interaction energies that are responsible for the behavior of asphaltene.

The aim of the present study is to fill an important gap in the understanding of asphaltene aggregation behavior, which is the nature of the association of asphaltenes in crude oil at the molecular level. To understand the asphaltene aggregation onset in crude oil, mixtures of normal-heptane and ortho-xylene as "modeled crude oil" were used. By varying composition of n-heptane and o-xylene (in the concentration range of 0 –100 wt% in 20% increment), aromaticity of the "modeled crude oil" was varied. Ortho- xylene and n-heptane

were chosen because they represent good solvent and bad solvent for asphaltene, respectively. A 7 wt% asphaltene concentration (10 asphaltene molecules) was used to represent the asphaltene concentration found in many crude oils. As demonstrated, this study reveals a great deal about the nature and the detailed roles of vdW, ES, and HBs on the onset of asphaltene aggregations.

4.3 Model Asphaltenes

Asphaltene appears in crude oils with different structures, depending on the nature of petroleum and how it was formed. Due to their associating nature, asphaltene molecules in petroleum span a wide range of molecular weights, varying from a few hundred to thousands. Recent studies suggested that the monomer molecular weight of asphaltene is in the range of 500-1000, with an average of about 750 (Boek et al., 2009). Regarding structure, asphaltene monomers with a single aromatic region are called continentals. Alternatively, asphaltene monomers that have a number of aromatic regions connected by bridging groups are called archipelagoes. The main challenge during the simulation is the choice of proper model asphaltenes to represent the real asphaltene molecules. In this study, three different model asphaltenes, as proposed by Boke et al., (2009) were chosen. Figure 4-1 shows model asphaltenes labeled as A1, A2, and A3, where A1 and A3 represent continental (island) asphaltenes, while A2 represents an archipelago asphaltene. Their specifications are presented in Table 4-1.

The intermolecular interactions that are responsible for asphaltene association are van der Waals (vdW), electrostatic charge transfer, and hydrogen bonding (Takanohashi et al., 1998). Thus, an investigation of each kind of interaction is necessary. For these reasons and to have a good representation of asphaltenes, three structures were chosen. These asphaltenes

have different aromatic rings, different heteroatoms, and different numbers and lengths of aliphatic chains.

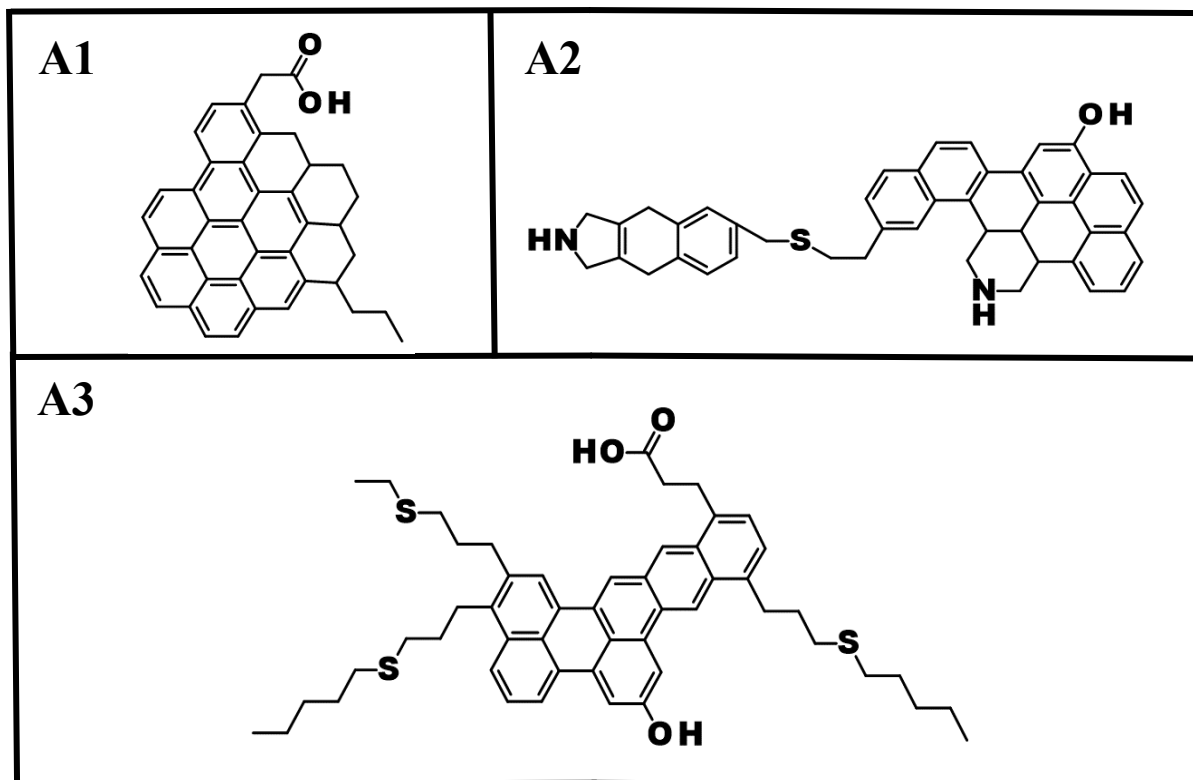


Figure 4-1. Model asphaltenes used in the present study.

Table 4-1. Specifications of model asphaltenes reported in Figure 4-1

Property	A1	A2	A3
Chemical formula	$C_{40}H_{30}O_2$	$C_{44}H_{40}N_2OS$	$C_{51}H_{60}O_3S_3$
Molecular weight	542.665	644.866	817.215
Aromaticity	0.7	0.68	0.55
No. of aromatic rings	8	7	7
No. of side chains	2	1	4

4.4 Simulation Details

The MD simulation studies used in this work were conducted by using a GROMACS 5.1.2 simulation package (Van Der Spoel et al., 2005). In every simulation, an Optimized Potentials for Liquid Simulations All Atom (OPLS-AA) force field was used to describe the intra-intermolecular interactions. The total energy in this force field was then calculated based on the sums of both bonded (bending, stretching, and torsion) and nonbonded (vdW, represented by Lennard-Jones, and electrostatic, represented by coulomb) energies. OPLS-AA is shown to work well for organic liquids in reproducing experimental data and has been successfully used for asphaltene aggregation simulations (Boek et al., 2009; Yaseen and Mansoori, 2017).

Energy minimizations were conducted to eliminate any high-energy structures. These were followed by 100 ps NVT and 500 ps NPT simulations to bring the system to the equilibrium temperature and pressure. In each simulation, periodic boundary conditions were applied to represent the bulk in a small box, using two-femtosecond time steps. A Particle Mesh Ewald (PME) method was applied to the coulomb intermolecular forces. In all nonbonded interactions, the cutoff is set to 1 nm. The simulations were done at a constant temperature and pressure (300 K and 1 bar). The LINCS algorithm was utilized to constrain all bond lengths in the simulation. V-rescale thermostat and Parrinello-Rahman pressure coupling were used to keep the temperature and pressure constant. Throughout the simulation (50 ns), the atomic positions were recorded every 10 ps so that the position of molecules could be tracked. In the simulations, a 7 wt % asphaltene concentration (10 asphaltene molecules) was used to represent the asphaltene concentration found in many crude oils. The concentration of the solvents was varied from o-xylene only to n-heptane in 20% increments.

4.5 Results and Discussions

Ten molecules of each of the three kinds of asphaltenes A1- A3 (Figure 4-1) were used in each simulation. The data obtained from the simulations were analyzed to check how the three model asphaltenes behaved in different solvent mixtures. Radial distribution functions (RDFs), trajectory movies, hydrogen bonds (HBs) and interaction energies were investigated to understand the behavior of the asphaltene molecules. The data reported here are for 0, 40, 80, and 100 wt% n-heptane concentrations.

4.5.1 Radial distribution functions

Radial distribution function (RDF) is employed to identify the aggregation of the asphaltenes. Figure 4-2 (a) shows the RDFs of A1 asphaltenes calculated from the molecules' center of mass in different n-heptane plus o-xylene mixtures. At 100% n-heptane, the figure shows peaks at 0.5, 0.78, 0.88, and 1 nm. The first highest peak represents the association of A1 molecules in face-to-face stacking, and the second peak represents their T-shape stacking. Reported in the literature, the shortest distance between solid asphaltene is about 0.37 nm. From the simulation trajectories and the distance between the molecules, the face-to-face stacking was about 0.5 nm, and the T-shape stacking was more than 0.6 nm. It agreed with the distances reported by Headen et al., (2009). In the case of 80% n-heptane, RDF calculations showed the same behavior as in 100% n-heptane with slightly lower peaks. This indicates that there was less asphaltene association than in 100% n-heptane. In the case of 40% n-heptane, calculations showed only two peaks (at ~0.5 and ~0.75 nm). This indicates less aggregation where stacking occurred in face-to-face and T-shaped formations. When the solvent was 100% o-xylene, there was only one small peak at 0.5 nm in comparison with high n-heptane concentrations (4 times lower than 100% n-heptane).

Figure 4-2 (b) shows the RDFs of A2 asphaltenes in different n-heptane and o-xylene mixtures. At 100% n-heptane, the A2 RDF curve shows two high peaks: one at 0.5 nm which

represents face-to-face stacking; and the other at 0.62 nm, which represents T-shape or offset stacking. At 80% n-heptane, the curve shows two peaks: one at 0.56 nm, representing face-to-face stacking, and the other at 0.68 nm, representing T-shape or offset stacking. In the case of 40% n-heptane, the curve has a similar trend to the tendencies found in 100% n-heptane, but with a lower association probability. At 0.56 nm, the stacking is face-to-face and at 0.61 nm the stacking is T-shape or offset. When the solvent is pure o-xylene, A2 shows zero association.

As shown in Figure 4-2(c), in all n-heptane plus o-xylene mixtures, RDF curves show almost the same behavior throughout; the only differences being the peak heights and the distances of the nearest molecules. At 100%, 80%, and 0% n-heptane, the stacking seemed to be face-to-face; at 40% n-heptane, this model seemed to prefer T-shaped or offset stacking. That might explain why the height of the peak at 0% n-heptane appears higher than that of 40% n-heptane.

4.5.2 Number of aggregates

Table 4-2. The fractions of asphaltene molecules in various associations. It reports the number of aggregates for three model asphaltenes as a function of the n-heptane concentration. According to this table, generally, A1 has a higher aggregation tendency than A2 and A3. In addition to the contribution of HB attraction and the small side chain steric repulsion, A1 has a large aromatic core that leads to higher aromatic-aromatic interactions than A2 and A3. A2 and A3 did not tend to form large aggregates even when the solvent was pure n-heptane.

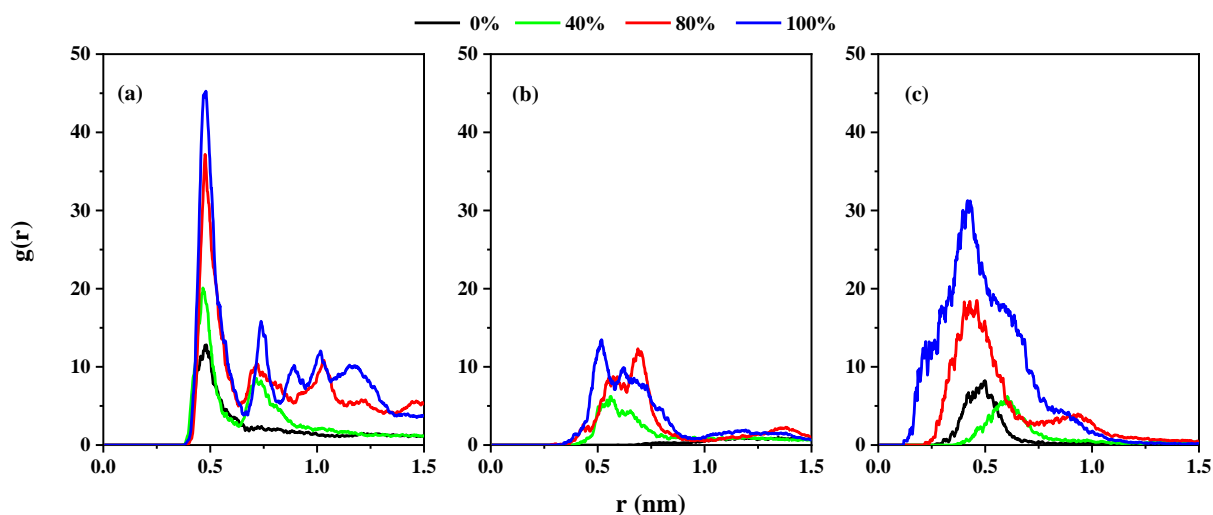


Figure 4-2. RDFs for the three model asphaltenes in different n-heptane plus o-xylene mixtures. (a) is A1, (b) is A2, (c) is A3.

Table 4-2. The fractions of asphaltene molecules in various associations.

Model Heptane %	A1				A2				A3			
	0	40	80	100	0	40	80	100	0	40	80	100
Monomers	0.3	0.2	-	-	1	0.2	0.1	0.3	0.8	0.2	0.1	0.1
Dimers	0.2	0.2	-	-	-	0.8	0.6	0.4	0.2	0.8	0.6	-
Trimers	-	-	-	-	-	-	0.3	0.3	-	-	0.3	0.9
Pentamers	0.5	-	-	-	-	-	-	-	-	-	-	-
Hexamers	-	0.6	-	-	-	-	-	-	-	-	-	-
Decamer	-	-	1	1	-	-	-	-	-	-	-	-

Figure 4-3, Figure 4-4, and Figure 4-5 report snapshots of the final simulation configurations from the simulation of the three model asphaltenes in different mixtures, starting from pure n-heptane to pure o-xylene. According to Figure 4-3 (a-d), A1 had face-to-face formation as the dominate stacking. Figure 4-4 (a-d) indicates that A2 did not associate

in pure o-xylene and gave limited association in pure n-heptane. Figure 4-5 (a-d) indicates that A3 had limited association in all cases studied.

While A1 and A2 have almost the same aromaticity, A1 associated more than A2. A3 had lower aromaticity than A2, but A3 showed higher association than A2. These indicate that aromaticity alone may not have been the controlling role on the association, contrary to what has been reported that the driving forces for asphaltene association are mainly aromatic-aromatic interactions (Boek et al., 2009; Rogel, 2000; Takanohashi et al., 1994). The simulations indicated other factors that play a role in the aggregation such as the number and location of the side chains, number, and locations of heteroatoms that contribute in hydrogen bond interactions, as well as the geometry of the aromatic core.

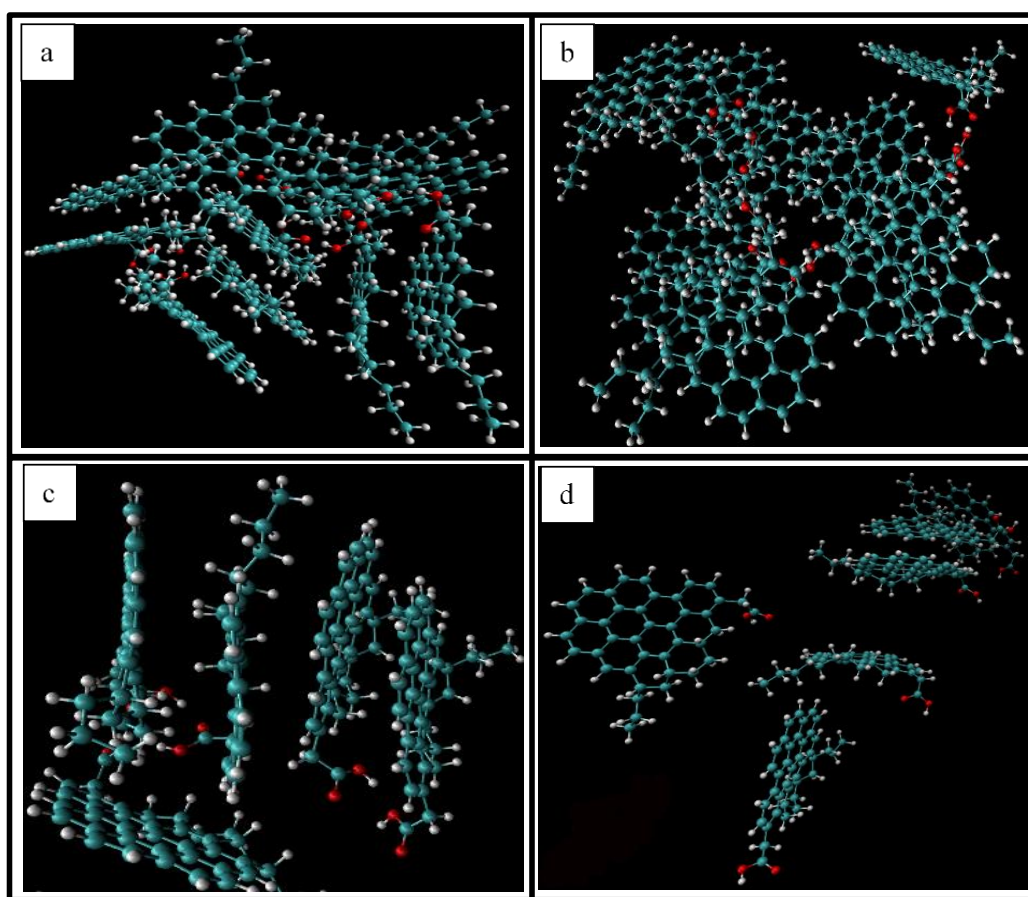


Figure 4-3. Snapshots of the final configuration from the simulation of A1 asphaltene in different mixtures of n-heptane and o-xylene. a- in pure n-heptane, b- in 80% n-heptane, c- in 40% n-heptane, and d- in pure o-xylene.

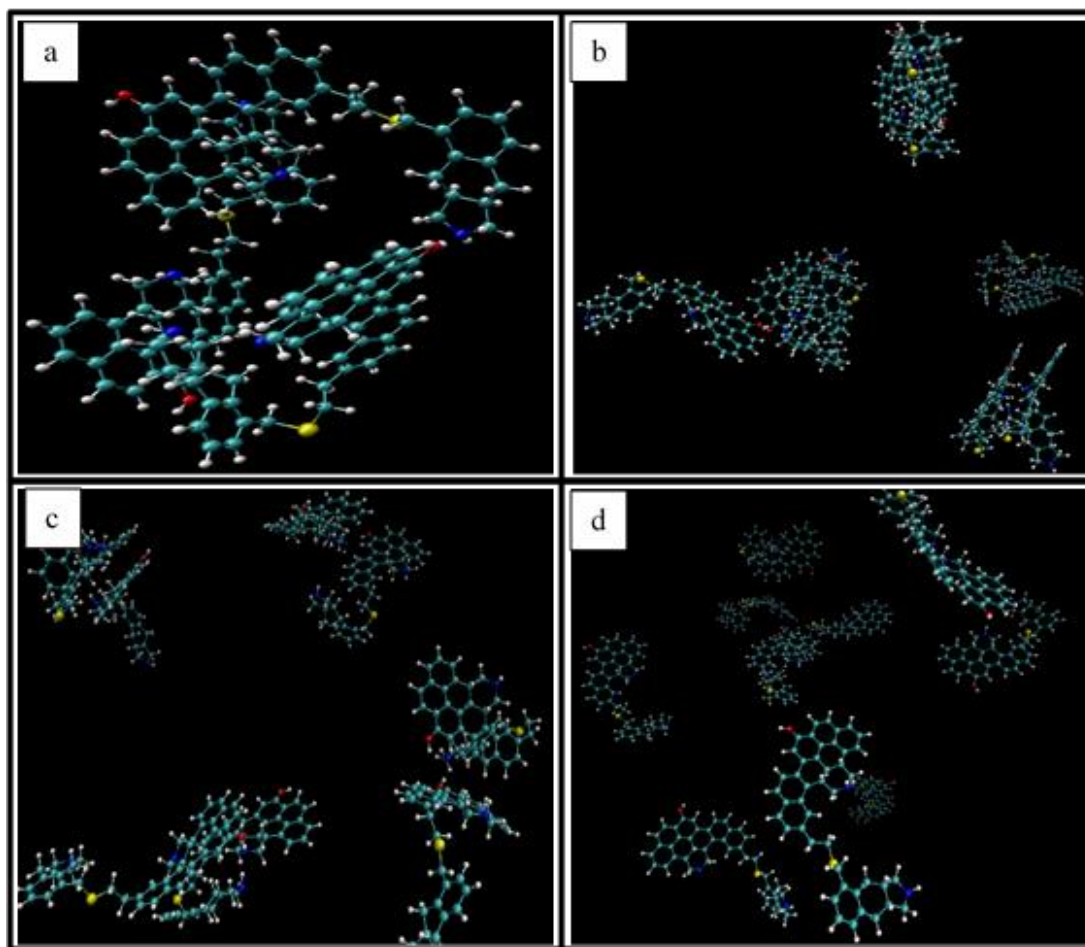


Figure 4-4. Snapshots of the final configuration from the simulation of A2 asphaltene in different mixtures of n-heptane and o-xylene. a- in pure n-heptane, b- in 80% n-heptane, c- in 40% n-heptane, and d- in pure o-xylene. Asphaltene molecules only are shown.

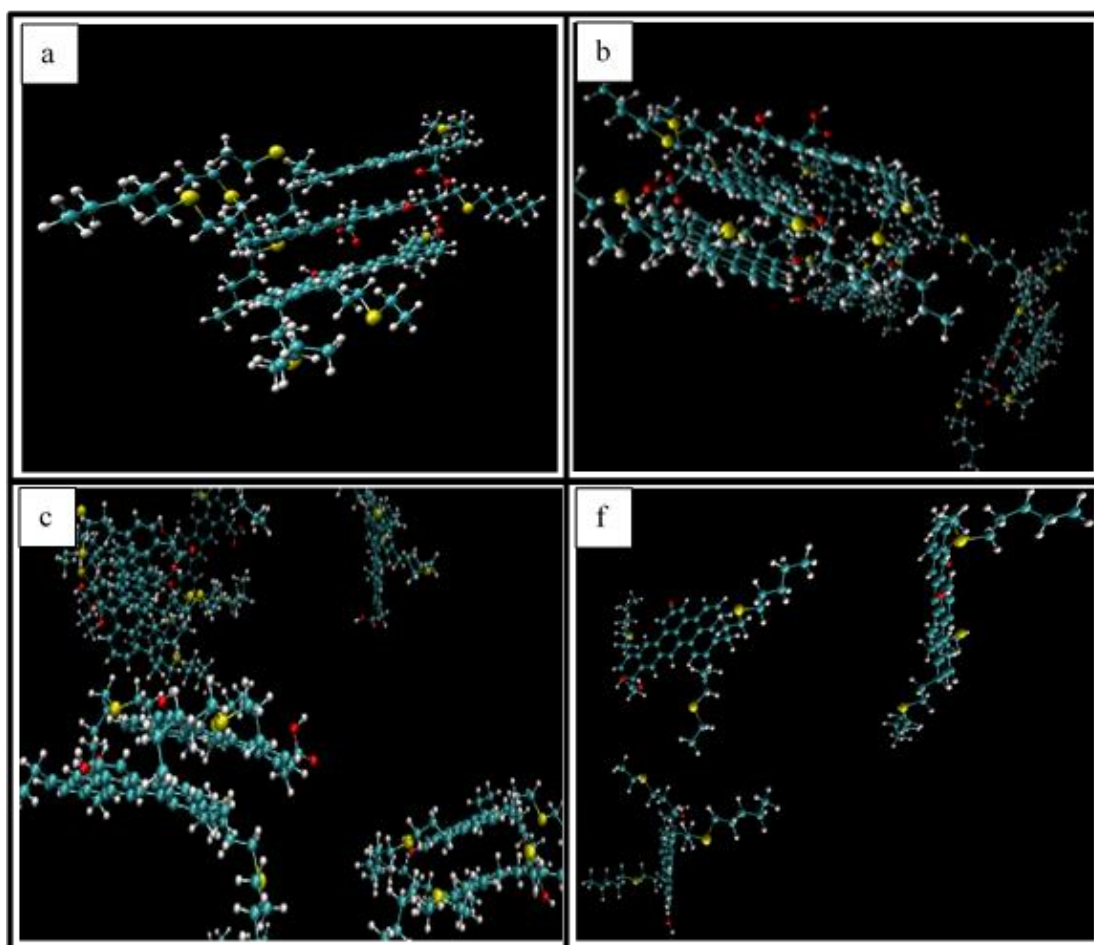


Figure 4-5. Snapshots of the final configuration from the simulation of A3 asphaltene in different mixtures of n-heptane and o-xylene. a- in pure n-heptane, b- in 80% n-heptane, c- in 40% n-heptane, and d- in pure o-xylene. Asphaltene molecules only are shown.

4.5.3 Hydrogen bond (HB) interactions

Hydrogen bond is an attractive interaction between a hydrogen atom that is bonded to a highly electronegative atom (oxygen, nitrogen or fluorine) and another highly electronegative atom. In this study, the HBs are mainly between asphaltenes only. The solvents (o-xylene and n-heptane) do not have sites for HBs interactions. The number of HBs in every simulation were calculated. The maximum numbers of HBs were 11 in the case of A1 at 100% n-heptane; 17 in the case of A2 at 80% n-heptane; and 11 in the case of A3 at 100% n-heptane. The average number of HBs at different n-heptane plus o-xylene mixtures for the three models is shown in Figure 4-6. According to Figure 6, A2 model has a higher number of HBs

than those of A1 and A3. This seems to be due to the higher number of heteroatoms that produce HBs between the ten A2s. Also, A2 has an archipelago structure, giving it a better chance to have more HBs (as a result of the main aromatic cores interacting with the secondary aromatic cores). Also, the two OH and one NH segments of A2 are distributed on its three sides, increasing the possibility of having more HBs.

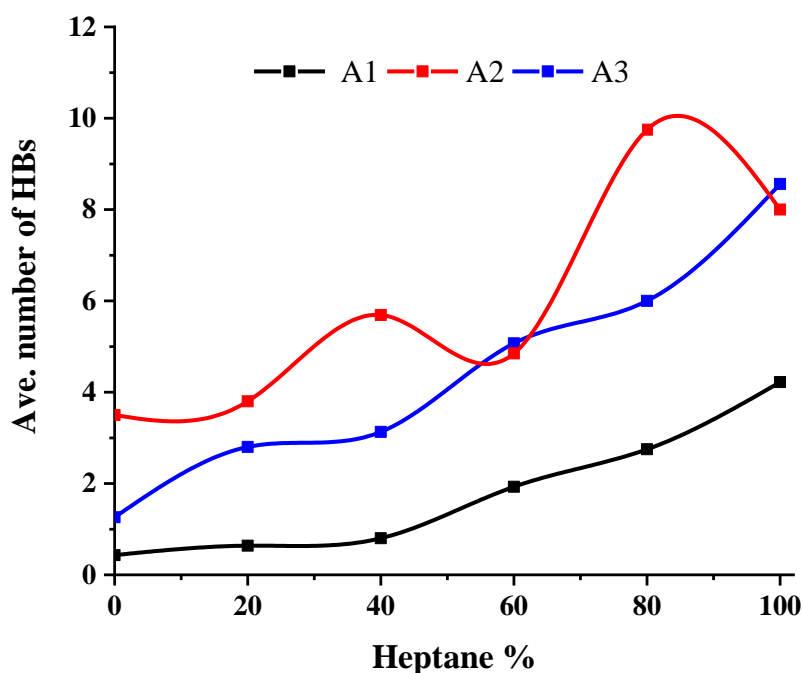


Figure 4-6. The average number of HBs of different asphaltenes in different n-heptane plus o-xylene mixtures.

4.5.4 Electrostatic (ES) and van der Waals (vdW) interaction energies

The ES and vdW interaction energies for the three model asphaltenes during the simulations in different solvent mixtures are reported in Figure 4-7. According to the figure, increasing n-heptane concentration led to a decrease in ES repulsion between asphaltene molecules. This is due to the reduction of ES interactions between o-xylene and asphaltenes, which eventually leads to an increase in the asphaltene-asphaltene interactions. The ES interactions were different for different asphaltenes. Where ES interactions of A1 and A3 were repulsion, while for A2 were an attraction. The ES attractions in A2 were due to the heteroatoms bonded

to the aromatic core. Similarly, vdW interactions increased with n-heptane concentration due to the reduction in asphaltene-o-xylene interaction. Furthermore, the association of A2 and A3 were limited in comparison with A1, despite high attraction. The low association can be attributed to their structures.

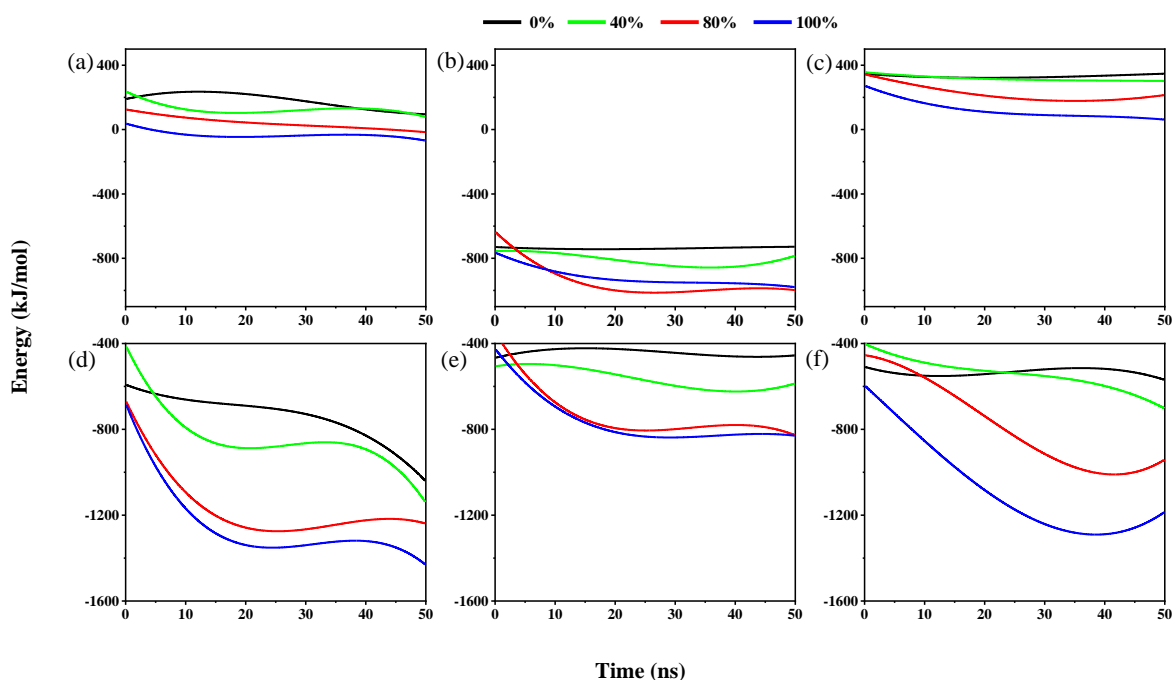


Figure 4-7. ES and vdW interaction energies for the three model asphaltenes in different n-heptane concentrations versus simulation time. ES interactions of A1, A2, and A3 are represented by a, b, and c respectively; while vdW interactions of A1, A2, and A3 are represented by d, e, and f respectively.

4.6 Conclusions

A molecular dynamics simulation of three different model asphaltenes in different mixed solvents of n-heptane and o-xylene were conducted. The roles of van der Waals, hydrogen bond, and electrostatic interaction energies on the interaction between asphaltenes were investigated. At a high n-heptane concentration, the preferred stacking of asphaltene molecules was face-to-face because of high aromatic interactions between the aromatic cores. The presence of hydrogen bond interactions enhanced the stability of the aggregate, even in pure o-xylene. The electrostatic interactions were either attraction due to the presence of the

heteroatoms in the aromatic core, or repulsion due to aliphatic chains that do not contribute to hydrogen bond interactions. Overall, the important thing is the architecture of the asphaltene molecules (such as the number and length of the chains), the number and position of the heteroatoms, and the number and size of the aromatic cores where they all contribute to representing the asphaltene behavior. The above findings of the role of the mixtures of paraffinic (n-heptane) and aromatic (o-xylene) solvents on three unique asphaltene models may help to understand the behavior of asphaltenes in complex petroleum fluids better.

5 Asphaltenes Aggregation During Petroleum Reservoir Air and Nitrogen Flooding

REPRINTED WITH PERMISSION FROM MOHAMMED H. KHALAF AND G.ALI MANSOORI, A NEW INSIGHT INTO ASPHALTENES AGGREGATION ONSET AT MOLECULAR LEVEL IN CRUDE OIL (AN MD SIMULATION STUDY), JOURNAL OF PETROLEUM SCIENCE AND ENGINEERING 173 (2019) 1121-1129. COPYRIGHT 2019 ELSEVIER.

5.1 Abstract

Aggregation onsets of seven different asphaltenes dissolved in model oils due to the effects of misciblized compressed air or nitrogen injections were studied through molecular dynamics simulation. Natures of aggregations, cumulative coordination numbers, and interaction energies were investigated. Onsets of aggregation were highly affected by injected gas concentration. In more cases, little differences were observed between using air and pure nitrogen. However, asphaltene aggregation onset was highly affected by its molecular architecture. Asphaltenes with long aliphatic chains and archipelago structure showed low aggregation affinities.

5.2 Introduction

In producing petroleum from underground reservoirs, there are primary, secondary and tertiary oil recovery techniques. In primary oil recovery, the location of the producing well is carefully chosen, as petroleum would flow out as a result of the reservoir gas-cap pressure. To maintain the gas-cap amount and pressure it is recommended to reinject the separated-gas from the produced petroleum. For various reasons that are not achieved, in order to maintain the gas-cap amount and pressure one may inject air/nitrogen in the reservoir. There is the

question whether the asphaltene content of the oil will aggregate, grow in size and plug the porous media and production facilities as a result of the gas-cap's air/nitrogen dissolution in the oil (Dehghani et al., 2007).

The secondary oil recovery process (Water-Injection) is used after the gas-cap pressure is reduced to such low levels where it cannot be maintained to force the oil out of the reservoir. Forced water-injection forces the oil out of the reservoir. Upon completion of primary and secondary recovery stages, a substantial fraction of the oil (60-70%) remains in the reservoir, primarily in the form of being adsorbed in the porous media of the reservoir formation. That is when the tertiary or enhanced oil recovery (EOR) process would be used to get the oil out of the reservoir (Mansoori and Jiang, 1985; Kawanaka et al., 1988). One of these EOR methods is done by injecting dense (supercritical) gases (e.g., natural gas, separated gas, flue gas/carbon dioxide, air/nitrogen). Supercritical fluids (sc-fluids) have densities near that of a liquid and low viscosity, since they are gases. Also, an sc-fluid has solvent potential, the same as hydrocarbon solvents so that it could dissolve even solids (Park et al., 1987). Therefore, sc-fluids are used in EOR to reduce the viscosity and improve the mobility of the oil due to its swelling by being miscibilized with the injected sc-fluids toward the wells. The sc-fluids and the bulk (crude oil) are considered miscible when there is no interface between them and the pressure at this point is known as minimum miscibility pressure (MMP) (Benmekki and Mansoori, 1988). To ensure that sc-fluids are dissolved in the bulk, the injected pressure should be higher than MMP. Natural gas has become less favorable for gas injection because it is highly sought as a clean transportation fuel and residential and commercial use for heating. Carbon dioxide is another good option, but it has several drawbacks which include its lack of purity, unavailability in large volumes, causing unnecessary oil/water emulsions, and the corrosion it may cause in the well-surface facilities (Mohammed and Mansoori, 2018b; Mungan, 2003).

One of the economically promising methods of EOR for underground petroleum reservoirs is an injection of high pressure (supercritical) air. Literature is rich in discussing nitrogen injection. However, purification of nitrogen for huge underground reservoirs is economically prohibitive. Accordingly, the use of pure nitrogen and air are compared (which contains ~79% nitrogen) in this report. This process is particularly attractive for off-shore reservoirs and other remote locations where separated-gas, natural gas, and other more proper gases, which would miscibilize with oil at lower pressure, are not available and/or economically not attractive (Mungan, 2003).

In the process of compressed air or nitrogen injection, when miscibility is reached, there is always the question whether the asphaltene content of the oil will aggregate, grow in size and plug the porous media and production facilities as a result of its interaction with compressed air or nitrogen (Jamaluddin et al., 2002). This is a problem which requires much research to understand the conditions under which asphaltenes may start to aggregate due to compressed air or nitrogen flooding and the factors which may contribute to its aggregation.

The instability of asphaltene during compressed gas flooding is attributed to the changes in the solubility of asphaltene and heavy fractions, where the injected fluids modify the composition and conditions of the reservoir fluids. Experimental investigations showed that nitrogen injection influences the aggregation and deposition of asphaltenes, and the problem is more severe for heavy oils. Most of the investigations focused on asphaltene aggregation during hydrocarbon gas and CO₂ injection (Mohammed and Mansoori, 2018a, 2018b) and there was little or no MD simulation of asphaltene aggregation during air or nitrogen flooding. Thus, understanding the behavior of asphaltene during the high-pressure gas flooding is required to reduce the possibility of asphaltene precipitation during such EOR.

One of the promising methods to study the onset of asphaltene aggregation during EOR is the use of molecular dynamics (MD) simulation. MD simulation of the sc-fluids injection and

its interaction with the live oil (oil in the reservoir) is computationally challenging at the present time due to the tremendous number of components in the oil and requirement of huge computational resources. For these reasons, asphaltenes dissolved in ortho-xylene (their best hydrocarbon solvent) and then pressurized it with compressed air or nitrogen to study the onset of asphaltenes aggregation.

This study aims to use the MD simulation technique to investigate the onset of asphaltene aggregation during air or nitrogen flooding, since ortho-xylene is being used to represent the oil phase, of which asphaltenes are completely miscible. The intention to examine the impact of sc-fluids concentration on the process and find the difference between the use of compressed air and pure nitrogen.

5.3 Molecular Structures

This study is conducted to understand the effect of the molecular structure of the asphaltenes and the presence of different heteroatoms on the aggregation during air and nitrogen injection. In the present study, seven different well-known asphaltenes were chosen. Figure 5-1 shows seven different asphaltenes named A1-A7. A1-A3 are reported in Boek et al., (2009), A4 and A5 are reported in Pacheco-Sánchez et al., (2004), A6 is reported in Zhang and Greendfield, (2007) and A7 is reported in Takanohashi et al., (2003). The asphaltenes in this study were extracted from Athabasca (A1-A3), Venezuelan (A4), Mayan (A5), Kuwait (A6), and Khafji (A7).

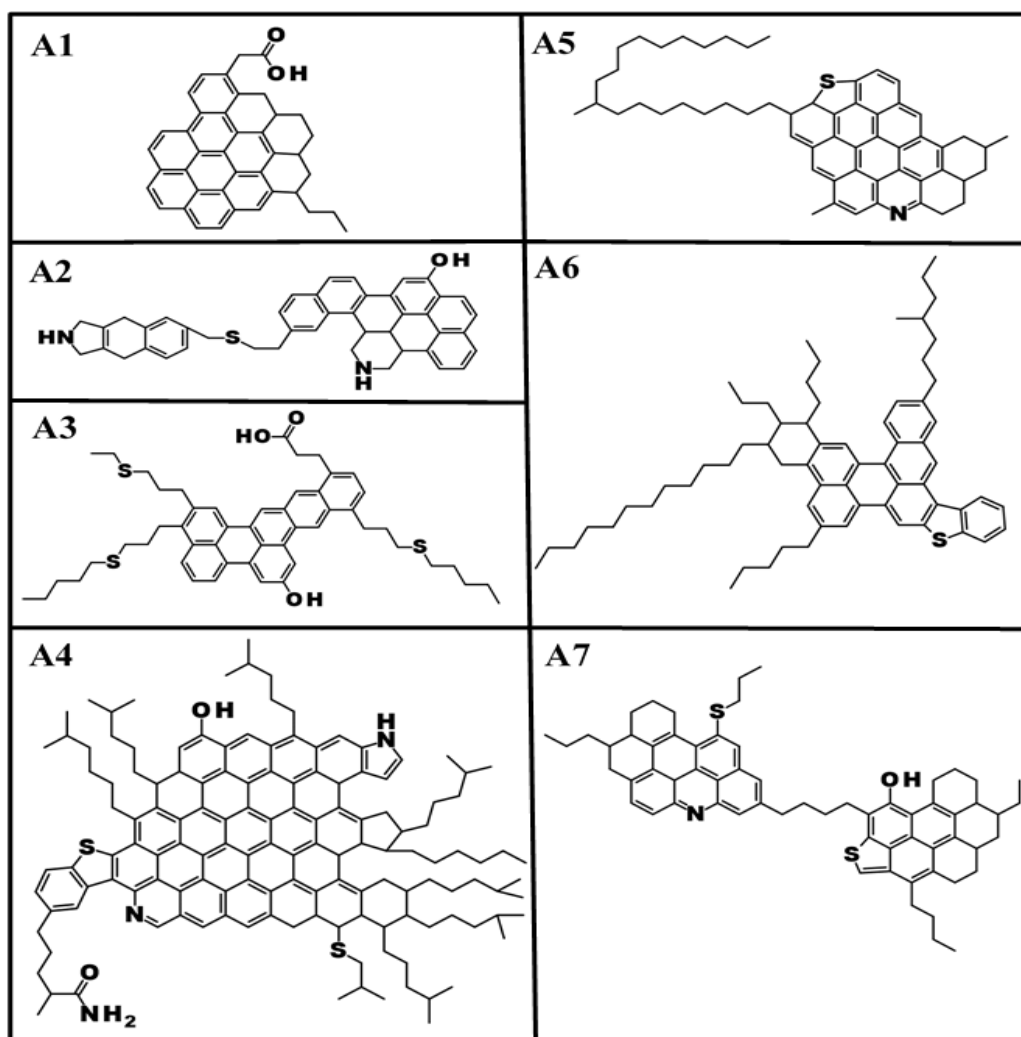


Figure 5-1. The seven asphaltenes (A1- A7) used in the present study.

5.4 Simulation Methodology

5.4.1 Initial configurations

Twenty-four molecules of each asphaltene model were used in this study. Asphaltene molecules were randomly distributed in the simulation box to study the onset of asphaltene aggregation. In each simulation, the dimensions of the simulation box were varied depending on the asphaltene and compressed gas concentration. To a better representation of asphaltene in real systems, these asphaltenes were placed in o-xylene at a constant concentration (7 wt%). Four different concentrations, 20, 40, 60, and 80 wt% of compressed air or nitrogen,

were added to the system to better visualize the effect of compressed air or nitrogen on the onsets of asphaltenes aggregation. The ingredients of air are based on 79% nitrogen and 21% oxygen only (neglecting the effects of small concentrations of other gases). The minimum miscibility of nitrogen in crude oil system is about 360 bar, thus in all the simulations, 400 bar of injection pressure was chosen. Simulations temperature of 350 K was chosen based on the reservoir's conditions (Dehghani et al., 2007).

5.4.2 Force fields

Lennard-Jones parameters and partial atomic charges of nitrogen and oxygen were used as described in Vujić and Lyubartsev (2016) and reported in Table 5-1. For other molecules (asphaltenes and o-xylene), OPLS-AA force field had been employed. The total energy was calculated based on the summation of bonded (bending, stretching, and torsion) and nonbonded (van der Waals represented by Lennard-Jones and electrostatic represented by coulomb) energies. In addition, OPLS-AA works well in calculating and producing hydrogen bonds between all possible donors and acceptors interactions. OPLS-AA is shown to work well for organic liquids in reproducing experimental data and therefore used successfully for asphaltene aggregation simulations (Khalaf and Mansoori, 2018; Yaseen and Mansoori, 2017).

Table 5-1. Partial atomic charges and Lennard-Jones parameters for Nitrogen and Oxygen.

Atom	Charges	ε (kJ/mol)	σ (nm)
N	-0.482	0.3026	0.332
M-N ^a	0.964	0	0
O	-0.112	0.4217	0.305
M-O ^b	0.224	0	0

a: massless charge point in nitrogen.

b: massless charge point in oxygen.

5.4.3 Simulation details and algorithm

A series of classical MD simulations were carried out using GROMACS 5.1.2 simulation package. After preparing the simulation box in the desired concentrations, energy minimizations were conducted using “steepest descent” method to eliminate any high-energy structures. Energy minimization was followed by 100 ps NVT and 500 ps NPT ensemble simulations to bring the system to equilibrium temperature and pressure. In all the simulations, the leapfrog algorithm was used to integrate the equation of motion. The periodic boundary conditions were applied to represent the bulk in a small box and two-femtosecond time steps were applied. The Particle Mesh Ewald (PME) method was applied to calculate long-range Coulomb interaction forces. In all nonbonded interactions, the cutoff was set to 1 nm. The simulations were performed at constant temperature and pressure (350 K and 400 bar). To constrain the bond lengths in the simulations, the LINCS algorithm was utilized. To keep the temperature and pressure constant, V-rescale thermostat and Parrinello-Rahman pressure coupling were used. Throughout the simulation (50 ns of NPT), the atomic positions were recorded every 10 ps, which allowed the tracking of the position of the molecules.

5.5 Results and Discussions

In EOR processes, compressed air or nitrogen is injected in different quantities depending on the reservoir conditions. To simulate real systems, different air and nitrogen concentrations were used to investigate the impact of injected fluids on asphaltene aggregation. Twenty-four asphaltene molecules of each structure were used in the simulation box with periodic conditions. The effect of injected fluids concentrations on the asphaltene aggregation process at 350 K and 400 bar were analyzed through: (i). Cumulative coordination number, N ,

(Equation 1), (ii). the van der Waals (vdW) interaction energies, (iii). The electrostatic interaction energies (ES), and (iv). The hydrogen bond (HB) interaction energies.

5.5.1 Effect of misciblized air and nitrogen on asphaltene aggregation

The effect of injected sc-fluids concentration on asphaltene aggregation was analyzed through the use of asphaltene cumulative coordination number $N(r)$, defined by the following equation (Headen and Boek, 2011).

$$N(r) = \int_0^r \rho g(r) 4\pi r^2 dr \quad (5-1)$$

$N(r)$ represents the number of asphaltene molecules in a sphere of radius r . Where ρ is the local density of asphaltene molecules and $g(r)$ is the asphaltene radial distribution function.

Figure 5-2 shows the $N(r)$ of asphaltene molecules (A1-A7) at four different misciblized nitrogen and air concentrations (20, 40, 60, and 80 wt%). In both compressed gasses, the onset of all seven asphaltene aggregation remains almost the same when the injected gases concentration is below 60%. At 20% misciblized gases concentration, dissolved A1 becomes unstable and shows a high aggregation affinity in comparison with other asphaltenes.

Increasing the concentration of misciblized gases to 40 wt% enhanced the aggregation of all 7 asphaltenes. A1 showed higher aggregation onset than other asphaltenes. Aggregation onsets of A2-A7 were slightly increased from 20% concentration. This clarifies that A2-A7 have lower aggregation affinity than A1 due to their molecular structure and size. According to the results of misciblized gas flooding, injection of 40% misciblized gas is applicable for A2-A7 asphaltenes and is not preferred for A1 asphaltene.

Stability of asphaltenes was highly affected when the injected sc-fluids concentration reached 60%. Similarly to the previous case, A1 showed higher aggregation onset, and other asphaltenes started alternating. A5-A7 asphaltenes showed big changes in their aggregation onset and their aggregation affinities were higher than A2-A4 asphaltenes.

When the misciblized gas was 80%, the aggregation onset was high: A1 and A6 showed higher aggregation onsets, while the others stayed in between. A2 and A3 did not show high aggregation affinity, due to their molecular structures. A2 asphaltene has an archipelago structure which gives it the ability to interact with itself through its aromatic and hydrogen bonds. A3 has long aliphatic chains in comparison with its aromatic core size, where they participate in steric repulsion.

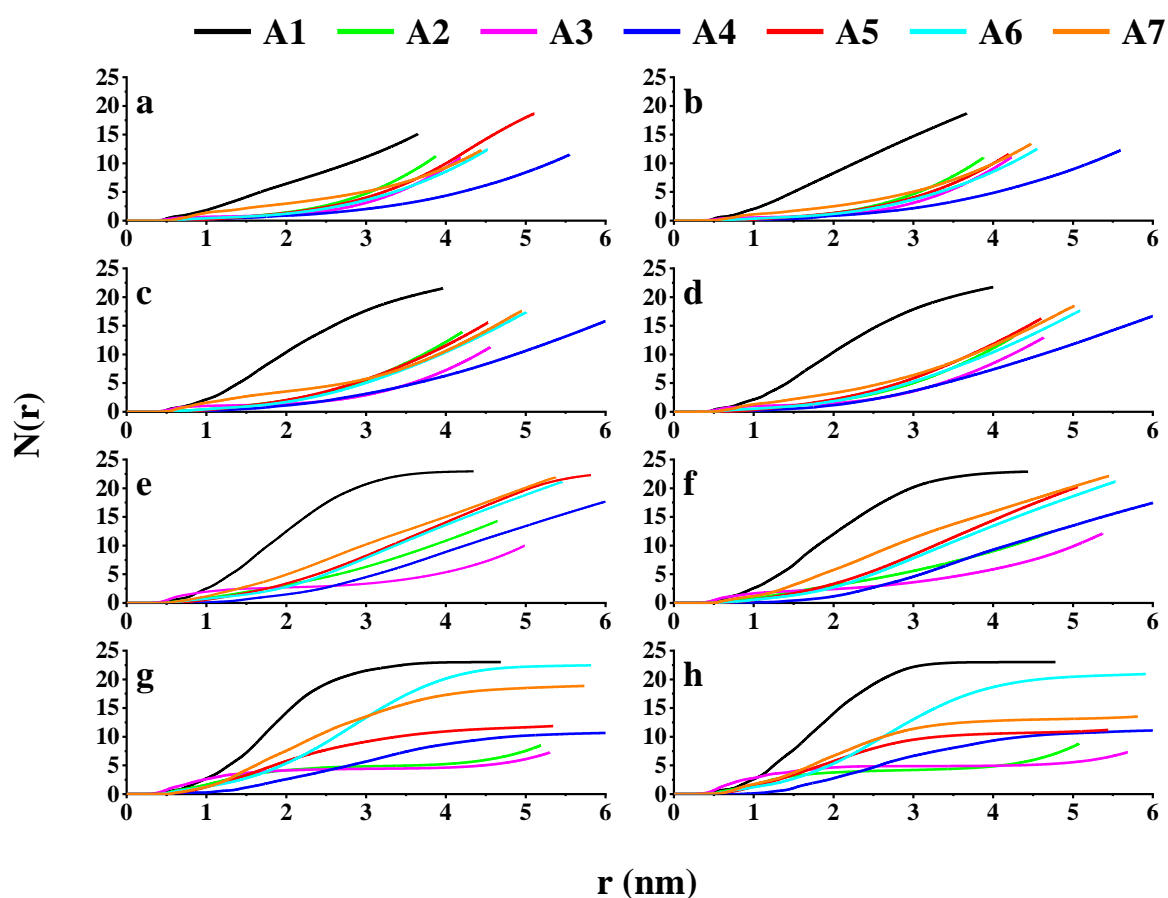


Figure 5-2. Cumulative coordination numbers of the 7 used asphaltenes at different concentrations of injected gases. a, c, e, and g are the cumulative numbers at 20, 40, 60, and 80% of air injection. b, d, f, and h are the cumulative numbers at 20, 40, 60, and 80% of nitrogen injection.

In addition to cumulative coordination number, the average size of aggregates (average number of asphaltene molecules in the aggregates) was analyzed and reported in Figure 5-3 and Figure 5-4. The reported results are in both compressed gases for the last 10 ns of the

simulations. At 20% of compressed gases, A1 was unstable and reached clustering point (more than 8 molecules in the aggregate). A2-A7 were in nanoaggregate ranges (less than 8 molecules in the aggregate). Increasing the concentration of injected gases to 40% enhanced the affinity of aggregation of other asphaltenes, such as A4. When the concentration became 60%, the asphaltenes were unstable except for A2 and A3 due to their structures. A2 and A3 showed stable behavior in all the cases, and even at 80% injected gases.

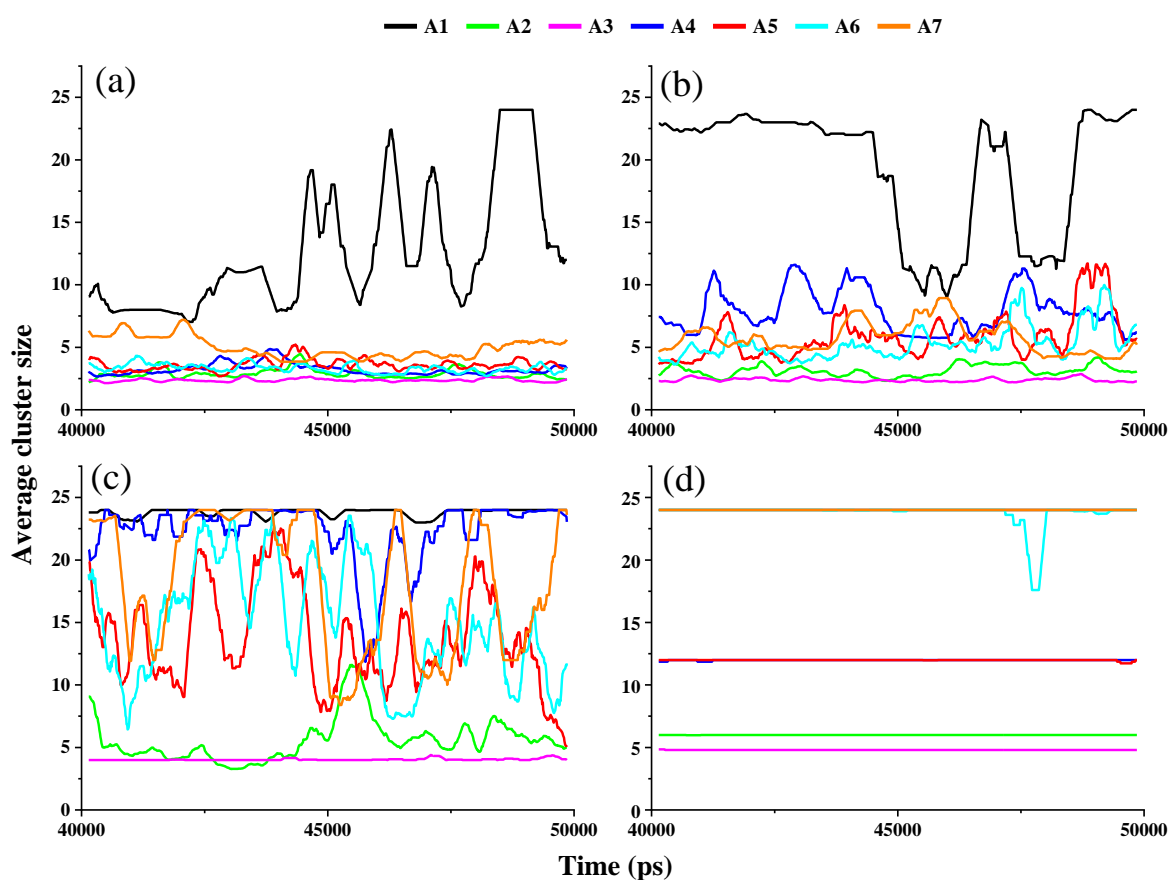


Figure 5-3. Average cluster size of the 7 asphaltenes at different air concentration where a, b, c, and d represent 20, 40, 60, and 80% of air respectively.

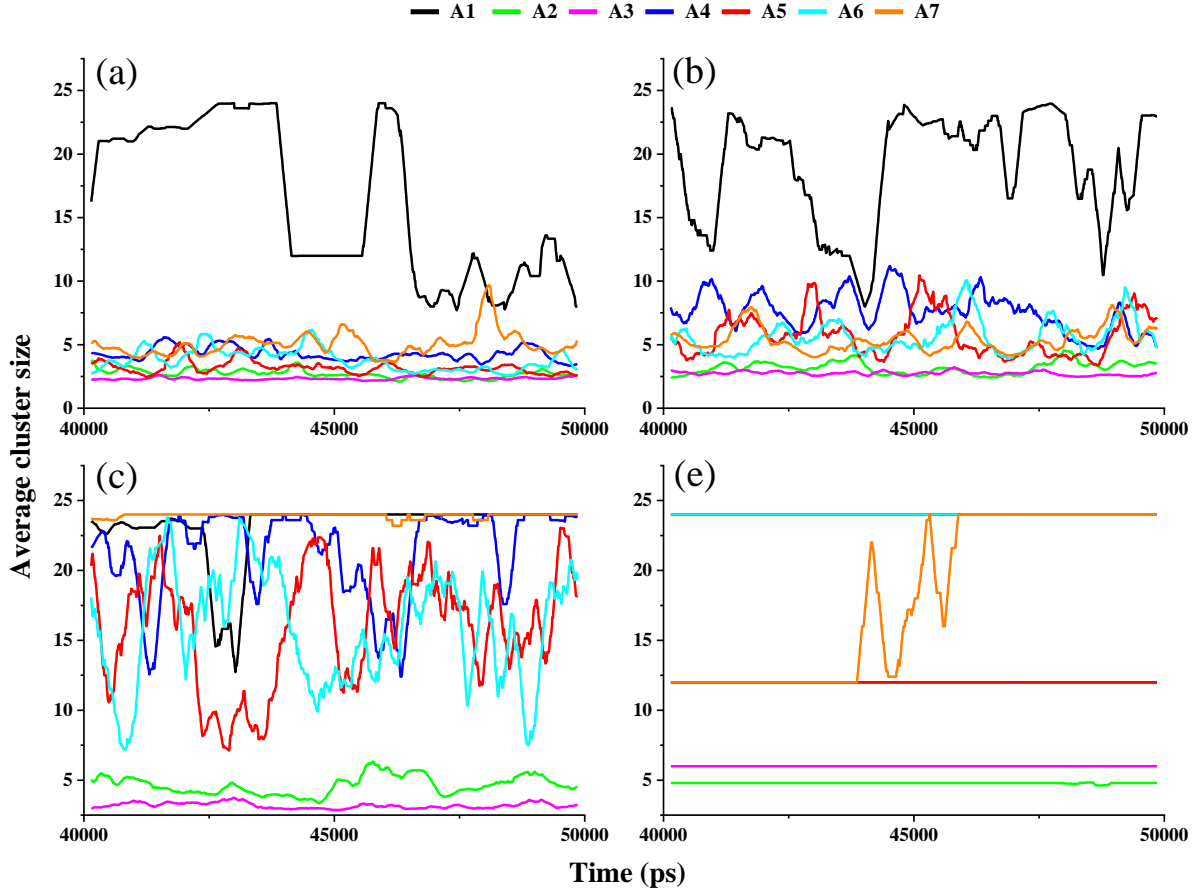


Figure 5-4. Average cluster size of the 7 asphaltenes at different nitrogen concentration where a, b, c, and d represent 20, 40, 60, and 80% of nitrogen respectively.

The results show that the general trends of the onsets are the same in both injected compressed gases. This means there are no differences between the use of compressed air or compressed nitrogen. Out of all the concentrations, trajectory visualization and $N(r)$ calculations showed that A1 affinity to aggregate was higher than other asphaltenes. When the injected high-pressure gas was 40%, A1 showed very high aggregation onsets. For A2-A7, the aggregation onset increased with the increase of the misciblized gas concentration. A4 had almost constant behavior, where the onset of aggregation was slightly affected by increasing the concentration. For A1 and A4-A7, when the concentration of misciblized gas was high (80%), the aggregation was severe and happened immediately. This is because misciblized gas changes the solubility of A4-A7 asphaltenes in the system which finally lead

to phase separation. We can conclude that an asphaltene with a chemical structure similar to A1 will have a higher tendency to aggregate than the other asphaltenes at low and moderate nitrogen and air concentrations. Figure 5-5 shows snapshots of seven model asphaltene placed in 20% misciblized nitrogen. According to the snapshots, A1 had the highest aggregation affinity. The detailed analysis of trajectories, which are not reported here, and the calculated results, conclude that the aggregation affinities of the seven model asphaltenes with respect to each other are as follows:

$$A1 > A7 > A6 > A4 > A5 > A2 > A3$$

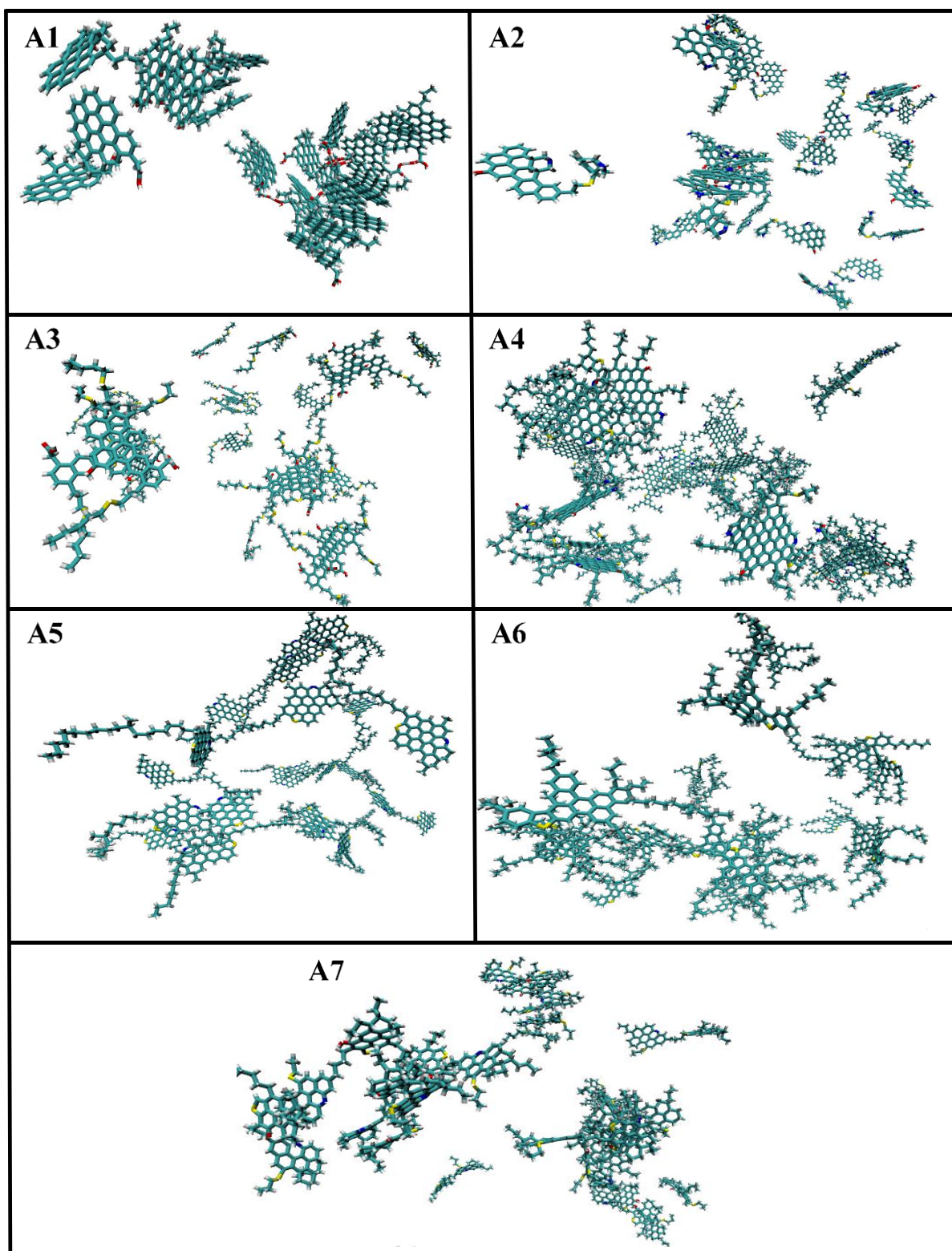


Figure 5-5. Snapshots of seven model asphaltenes in 20% misciblized nitrogen. O-xylene and nitrogen molecules were removed for clarity.

5.5.2 Interaction energies

Reported in the literature, the driving force for asphaltene aggregation is the core-core attraction which is represented by vdW energies. In our previous study (Khalaf and Mansoori, 2018), we showed that the energies were affected by the medium and asphaltene's molecular structure. To understand the effect of compressed gases on electrostatic (ES), van der Waals (vdW), and the average number of hydrogen bonds (HB) interaction energies, we report the interaction energies between asphaltenes at different compressed gas concentrations. The results are reported in Figure 5-6 and Figure 5-7 for the last 10 ns of simulations.

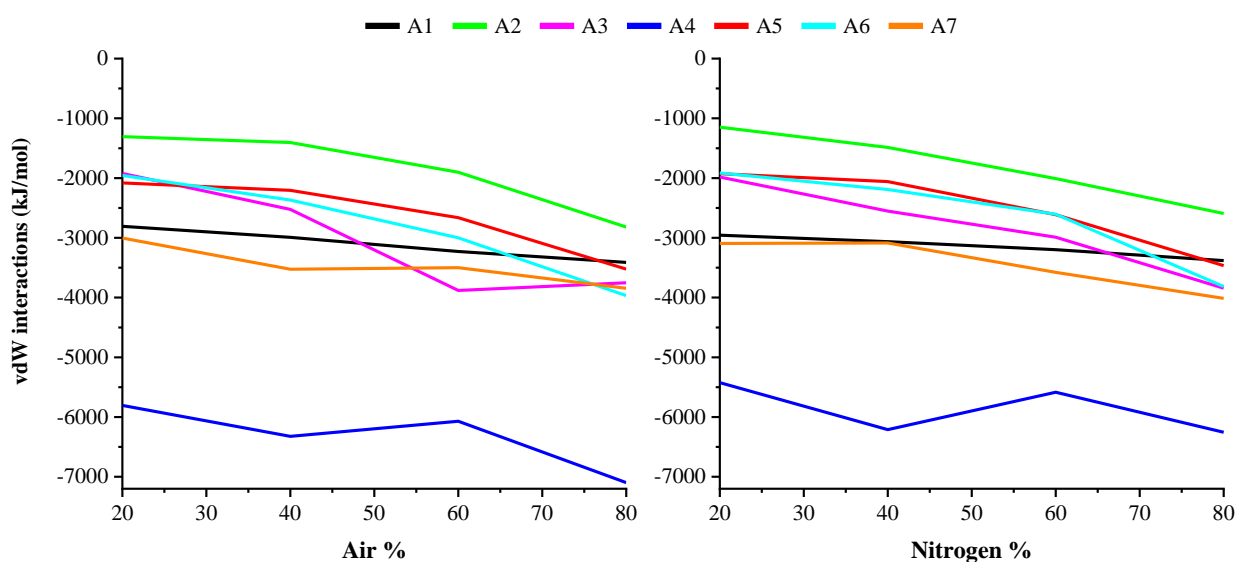


Figure 5-6. vdW interactions of the 7 asphaltenes at different miscible gas concentrations.

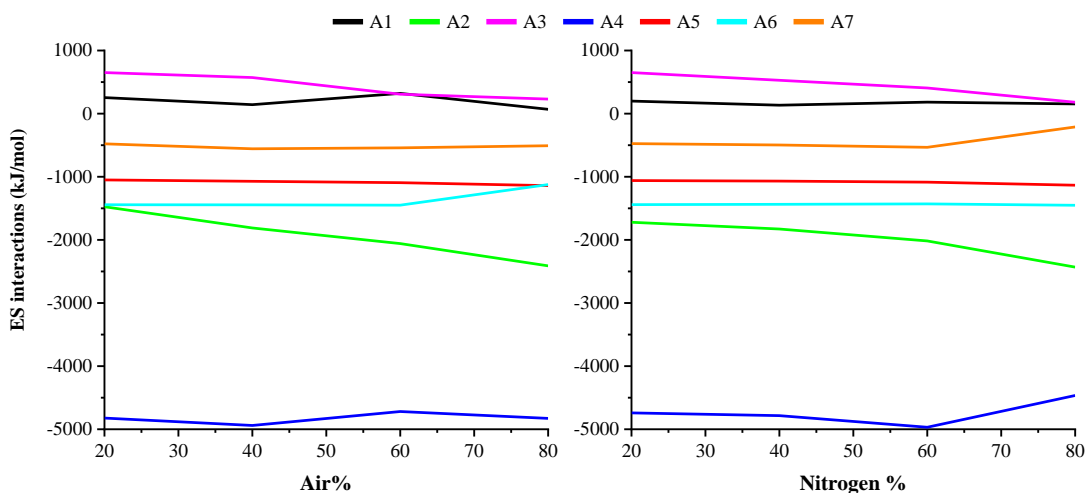


Figure 5-7. ES interactions of the 7 asphaltenes at different miscible gas concentrations.

In both compressed gases, the results showed that increasing misciblized gas concentration leads to increase in the vdW interactions (increase the attraction energy) between the asphaltene molecules in all the 7 cases, see Figure 5-6. This is due to the reduction in the aromatic-aromatic interactions between asphaltene and o-xylene. For example, in both gases, the vdW attractions of A2 and A3 doubled when the concentration of compressed gases increased from 20% to 80%. Basically, vdW interactions are related to the size and geometry of the aromatic core of asphaltenes. Thus, the aggregation affinity of A1 was the highest in comparison with the other 6 asphaltenes. On the other hand, ES interactions are affected by the presence of heteroatoms connected to the aromatic core, which contribute to the reduction of π electron clouds. Due to that, the ES interactions of A2, A4, A5, A6 and A7 were attraction, while A1 and A3 were repulsion, see Figure 5-7. From the interactions results and the aggregations trends, the ES interactions have low effects on the aggregation process in comparison with the effects of vdW interactions. The interaction energies are almost the same in compressed nitrogen and compressed air. Of course, this is because of the injected air has 79% nitrogen which dominates on the interactions.

The average numbers of HBs between asphaltenes with increasing the concentrations of misciblized gases are reported in Figure 5-8. According to this figure, the average number of HBs between A2 molecules was higher than other asphaltenes. A1, A2, A3 were almost the same in misciblized nitrogen and air. In the case of A4, there was a difference between misciblized nitrogen and air flooding. A5 has only an acceptor position with no donor position and A6 has no sites for HBs, thus they do not have the potential to participate in HB interactions. In addition, HBs may affect the shape of aggregated asphaltene (Yaseen and Mansoori, 2018). Overall, there were slight differences in the average number of HBs of some asphaltenes. However, even with these differences, the general trends of aggregation of these asphaltenes in misciblized air and nitrogen were the same. Due to this, we can conclude that HBs had small effects on the aggregation process in comparison with vdW interactions.

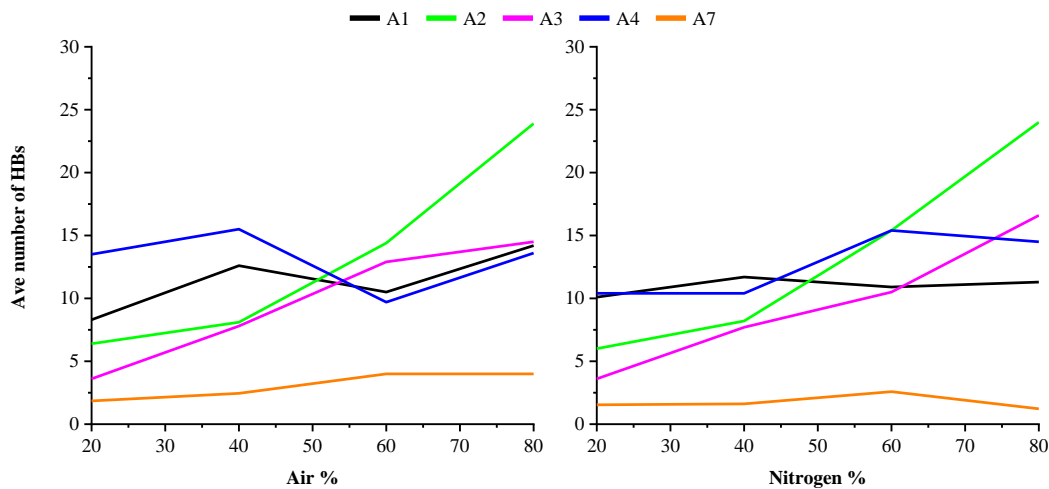


Figure 5-8. The average numbers of HB interactions at different gas concentrations.

According to the results, the general trend of aggregation affinity was almost the same in both nitrogen and air flooding when the concentration was below 60%. The simulation results suggested that injection of air is applicable at low concentrations. Air injection is economically preferred and is applicable everywhere due to its availability and purity.

5.6 Conclusions

Molecular dynamics simulations of different asphaltenes in different concentrations of misciblized nitrogen and air were conducted. The effect of injected misciblized gas concentrations and the role of interaction energies were investigated. The asphaltene aggregation process is highly affected by the concentration of injected gases due to the solubility effects. Asphaltenes with long aliphatic chains and archipelago architecture showed low association affinity than other flat asphaltenes. Overall, there are no appreciable differences between the use of misciblized nitrogen and air on asphaltene aggregation during enhanced oil recovery. Additionally, the architecture of asphaltene plays an important role in the aggregation process.

6 Magnetic Treatment of Petroleum and its Relation with Asphaltene Aggregation Onset (an Atomistic Investigation)

REPRINTED WITH PERMISSION FROM MOHAMMED H. KHALAF, G.ALI MANSOORI, AND C. W. YONG, A NEW INSIGHT INTO ASPHALTENES AGGREGATION ONSET AT MOLECULAR LEVEL IN CRUDE OIL (AN MD SIMULATION STUDY), JOURNAL OF PETROLEUM SCIENCE AND ENGINEERING 176 (2019) 926-933. COPYRIGHT 2019 ELSEVIER.

6.1 Abstract

Magnetic treatment is often used in certain oil industries for alterations in petroleum rheological properties. In this report, we introduce the scientific basis for the role of magnetic treatment on the onset of asphaltenes aggregation from petroleum fluids. Molecular dynamics simulations are used to study the effect of magnetic fields that are applied to three different model asphaltenes (A1-A3) in paraffinic and aromatic oil media. Radial distribution functions, hydrogen bond interactions, and the simulation trajectories are produced and analyzed. Our simulation results show that the onset of asphaltene aggregation in petroleum fluids is affected by the magnetic field and it is a function of its strength. In a paraffinic medium, magnetic field reduced aggregation of the model asphaltenes studied in the range of 20-35%. Where the magnetic field of 1.5T caused a high disruption of A1 aggregation and changed the dominated stacking. However, the highest disruption of A2 and A3 asphaltenes was at 1.0T. In an aromatic medium, magnetic field reduced the association of the model asphaltenes studied in the range of 25-70%. Where 0.5T diminished the association of A2 and A3 asphaltenes while 1.0T was able to do that for A1 asphaltene. The stacking modes and distances between asphaltene molecules were also affected by magnetic field. For example, in paraffinic medium, 0.5T enhanced the aggregation of A1 and A2 asphaltenes with multiple-layer stacking where some of the peaks appeared farther than the reported

cutoff of asphaltene stacking. Hydrogen bond results showed that magnetic fields did changes on the average number of hydrogen bonds. These changes were due to changes in the orientation and the distances between asphaltene molecules. The difference in asphaltene response to the magnetic treatment was due to the differences in their structures. Overall, the effect of magnetic field on the onset of asphaltene aggregation is dependent on the magnetic field strength, asphaltene architecture, and the medium.

6.2 Introduction

Heavy, extract heavy crude oils and oil sands are known to have high viscosity and a high chance of heavy organics deposition. There are several processes to fight heavy organic deposition. Such as (1) Pigging of the pipelines. (2) Exothermic chemical reactions which generate heat causing softening and melting of heavy organics. (3) Paraffin and asphaltene deposition inhibitors which are used to fight such depositions in oil fields, pipelines, etc. (4) There is also literature in which they claim a magnetic field could inhibit heavy organic deposition and could make a viscosity reduction (Marques and Rocha, 1997; Tao and Xu, 2006; Gonçalves et al., 2011). Magnetic fields have become of major interest in certain parts of the petroleum production technology. It is claimed that crude oils under magnetic treatment get improvements in their viscosity, volatility, electrical conductivity, etc (Morozov et al., 1978).

6.3 Previous Studies

There are several industrial reports available about modifying crude oil rheological properties and eliminate heavy organics deposition when crude oils are exposed to a magnetic field. For example, Marques et al. (1997) studied the paraffin crystallization under magnetic

treatments. They concluded that pure paraffin in hydrocarbon solutions showed susceptibility to a magnetic field and there was a fair relation between magnetic field strength, exposure time, and the oil rheological properties. Also, they did a field test on producing wells of high and mild paraffinic oils and found a high reduction in oil viscosity and heavy organics deposition rate. Gonçalves et al. (2011) claimed a 39% viscosity reduction in one of six oil samples. Their analysis on that sample showed the viscosity reduction was due to the presence of paramagnetic species, a high aromatic/aliphatic ratio, and a high water content. Also, they reported that paraffin could not be responsible for the viscosity reduction under the effect of a magnetic field. Morozov et al. (1978) studied the effect of magnetic field on the physical properties (volatility, dielectric constant, electrical conductivity, optical density, and electrical charging tendency) of a kerosene sample. Their results showed that the magnetic field influenced the physical properties of kerosene. They claimed that aromatic materials were sensitive to a magnetic field. Loskutova and co-workers (Loskutova and Yudina, 2003; Loskutova et al., 2008) studied changes in crude oil rheological properties due to magnetic fields. They concluded such changes were due to the presence of free radicals and vanadium complexes that concentrated in the resinous-asphaltic fraction as well as the ratio between neutral and acidic resins. The orientation of free radicals and vanadium complexes due to a magnetic field lead to structural transformations and changes in oil rheological properties. They explained the high activity of acidic resin by its polarity in comparison to the neutral resin. Lesin et al. (2010) investigated the magnetic properties of the wax deposit sample from an oil producing well. They concluded that wax deposit sample had superparamagnetic properties due to the presence of iron oxide nanoparticles, Also, reported the presence of sulfur, oxygen, nickel, vanadium and other atoms in asphaltene-resin colloids caused higher magnetic susceptibility. Tung et al. (2001) studied the influence of magnetic field on paraffinic oil viscosity and deposition rate. They found that oils with high

asphaltene-resin content were highly affected due to their polarity. Also, found that magnetically treated oils behaved as Newtonian fluids and there were reductions in wax crystals size and wax deposition rate.

In addition to experimental investigations, there are several simulations about the effect of magnetic fields. Kulkarni and Wani (2013) discussed the alignment of wax magnetic dipoles with external magnetic field leading to disturbing the crystal agglomeration process. They argued that wax magnetic dipoles generated a repulsion force between them, preventing their aggregation and deposition. Moosavi and Gholizadeh (2014) used MD simulation to investigate the effect of a constant magnetic field on solvent properties. They found that the magnetic field influences the number of hydrogen bonds, solvent structure, diffusion coefficient, viscosity, and surface tension. They reported that the magnetic field increased the force of hydrogen bonds. They claimed that solvent molecules were distributed along the magnetic field direction. In another study, Chang and Weng (2006) investigated the effect of magnetic field and liquid water using MD simulation. They reported that the number of hydrogen bonds increased slightly as the strength of the magnetic field increased while diffusion coefficient decreased. Recently, Chen et al. (2018) investigated the effect of magnetic field on waxy crude oil using MD simulation. Their results showed that the magnetic field had different effects on waxy crude oil. The density decreased and increased with increasing magnetic field strength; diffusion coefficient increased at the low magnetic field and decreased at high magnetic field; viscosity reduction appeared in a specific range of magnetic fields; aggregation and molecular morphology were affected by magnetic field.

In most of the studies, there is a discrepancy among experimental results of the influence of magnetic fields on crude oils. It can be seen that some of the studies mentioned that magnetic fields have effects only on polar species (asphaltenes) while others focused on paraffines. Even in paraffinic oils, there is a discrepancy between the results. Some of them

found that magnetic field reduced wax crystallization. However, others reported that magnetic field enhanced wax crystallization. It is shown that most of the studies were about wax, and there is little scientific information about the role of magnetic treatment of petroleum on asphaltenes. Some of the studies reported that the magnetic field has effects on polar species (Loskutova and Yudina, 2003; Marques et al., 1997; Tung et al., 2001).

In crude oils, the polar and charged particles are asphaltenes or other particles associated with asphaltene aggregates (Leontaritis and Mansoori, 1992; Ganeeva et al., 2011). Thus, we believe asphaltene molecules present in oils are influenced by magnetic fields due to their asymmetrical charge distribution and polarity. To our knowledge, there is no MD simulation about the effects of magnetic field on asphaltene aggregation or deposition. The only available MD simulation is about waxy oil and they did not include asphaltene in the system (Chen et al., 2018). Therefore, we were motivated to undertake the present study. Molecular dynamics (MD) simulation technique is used to investigate the onset of asphaltenes aggregation with and without the effect of an external magnetic field in well-defined media. We examine the impact of the magnetic field strength and the medium on the onset of asphaltene aggregation/disaggregation at the molecular level.

6.4 Simulation Methodology

6.4.1 Molecular models

To study the effect of asphaltene molecular structure on asphaltene behavior under magnetic treatment, three different asphaltene structures were chosen. They are named A1, A2, and A3 and are shown in Figure 6-1. A1, A2, and A4 are island asphaltenes while A3 is an archipelago asphaltene. These three asphaltene models, as were used in some other studies, they exhibited different behaviors (Khalaf and Mansoori, 2018, 2019; Yaseen and Mansoori, 2017).

It is known that asphaltenes are soluble in aromatics and insoluble in paraffins. Thus, o-xylene and n-heptane are used. It is believed the studies performed here for the onset of asphaltene aggregation is also valid in the case when the same kinds of asphaltenes are present in real crude oil. Of course, the nature of aggregations beyond onset point will be a strong function of the medium.

For all the molecules in the system (asphaltenes, n-heptane, and o-xylene), the OPLS-AA force field was used. OPLS-AA was shown to work well for organic liquids in reproducing experimental data and was used successfully for asphaltene aggregation simulations (Khalaf and Mansoori, 2018; Mohammed and Gadikota, 2019; Mohammed and Mansoori, 2018b, 2018c; Yaseen and Mansoori, 2017).

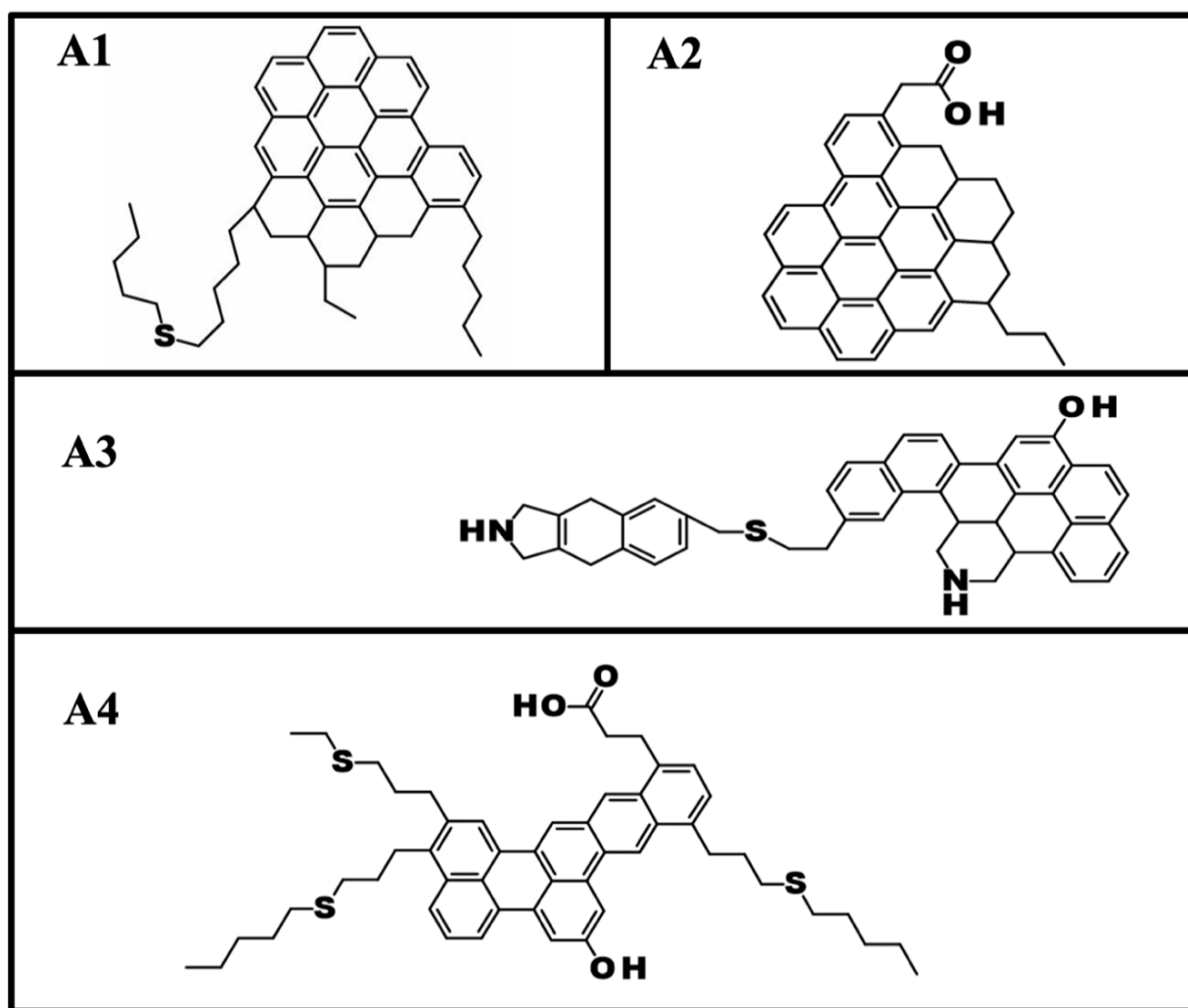


Figure 6-1. Model asphaltenes used in this study.

6.4.2 Magnetic field implementation

It is well known that magnetic field, as well as electric field, exert a force on charged species, known as Lorentz force (Valle et al., 2017; Griffiths, 1999). The expression for the Lorentz force that is exerted by a magnetic field on a moving electric charge is given by:

$$\vec{F} = q\vec{E} + q\vec{v} \times \vec{B} \quad (6-1)$$

where F is the Lorentz force, q is the charge of the particle, E is the electric field, v is the velocity, and B is the magnetic field. This force is perpendicular to the velocity and the magnetic field. When the angle between magnetic field lines and the particle velocity are perpendicular, the particle will experience helical motion.

The asymmetrical charge distributions in materials are the reasons for a magnetic field effect on the re-distribution of such materials. This may change their interactions, resulting in manipulating, aggregation, and disaggregation. Lorentz force may cause various effects on the configurational and transport properties of affected species.

In this study, all MD simulations were conducted using DL_POLY_4 simulation package (Todorov and Smith, 2016). In addition to the molecular force field, DL_POLY_4 allows the use of external forces (such as electric, magnetic, gravitational, etc.). The total energy in DL_POLY_4 package is calculated based on (Todorov and Smith, 2016):

$$U = \sum U_{bonded} + \sum U_{nonbonded} + \sum U_{external} \quad (6-2)$$

$U_{external}$ represents different external energies that DL_POLY_4 can apply them to the system, such as magnetic interactions. Magnetic force will introduce additional acceleration to the acceleration that is caused by molecular forces.

$$\vec{F}_B = q(\vec{V} \times \vec{B}) = \vec{a}_B m_i \quad (6-3)$$

$$\vec{a} = \frac{q}{m}(\vec{V} \times \vec{B}) + \vec{a}_c \quad (6-4)$$

Where \vec{a}_c is the original acceleration due to molecular forces (in the absence of magnetic field). The change in the molecular forces due to magnetic forces will cause several effects on the structural and transport properties of the investigated system.

MD simulation is based on integrating the equation of motion of interacted particles. If these particles carry an electric charge, applying a magnetic field to the system generates a magnetic force which is known as Lorentz force (Chen et al., 2018; Moosavi and Gholizadeh, 2014).

6.4.3 Simulation details

After preparing the simulation box in the desired concentrations, energy minimizations were conducted to eliminate any high-energy structures. Energy minimization followed by 50 ps NVE and 100 ps NPT ensemble simulations, to bring the system to equilibrium temperature and pressure. In all the simulations, periodic boundary conditions were applied in all directions to represent the bulk in a small box, two-femtosecond time steps were applied. The Particle Mesh Ewald (PME) method was applied to calculate long-range Coulomb interaction forces. In all nonbonded interactions, the cutoff was set to 1 nm. The simulations were performed at constant temperature and pressure (300 K and 1 bar). All hydrogen-containing bonds were constrained using the SHAKE algorithm. To keep the temperature and pressure constant, Nose-hoover NPT coupling was used. Throughout the simulation (20 ns of NPT), the atomic positions were recorded every 10 ps, which allowed the tracking of the position of the molecules.

A 7 wt% asphaltene concentration (10 asphaltene molecules) was used to represent the asphaltene concentration found in many crude oils. In each simulation, asphaltene molecules were placed in o-xylene or n-heptane at normal conditions (300 K and 1 bar) with and without magnetic field. Magnetic fields were applied along the z-direction. Four different magnetic field strengths (0.0, 0.5, 1.0, and 1.5), measured in Tesla (T), were applied to the

system. Topology parameters of the system and input files were generated using DL_FIELD (Yong, 2016). All the collected data were analyzed using DL_ANALYSER (Yong and Todorov, 2017). The molecular configurations and trajectories were visualized by VMD package (Humphrey et al., 1996).

6.5 Results and Discussions

6.5.1 The effect of magnetic field on asphaltene aggregation

Ten molecules of each of the three kinds of asphaltenes (A2, A3, A4) reported in Figure 6-1 were used in each simulation. Radial distribution functions (RDFs), and hydrogen bond (HB) interactions, and trajectories were investigated to understand the effect of magnetic fields on various asphaltene's behavior.

Radial distribution function is an indication of local molecular structure arrangement and it is a good measure of the onset of asphaltene aggregation. A series of regular peak is a good indication of the extent of molecular aggregation. On the other hand, the RDF becomes homogeneous if the asphaltene molecules are completely dissolved and dispersed in solvents. All the calculated radial distribution functions (RDFs) are based on the distances between the center of mass of asphaltene molecules. Hydrogen bonds (HBs) analysis was also carried out, to investigate how these may affect the size and shape of asphaltene aggregates.

6.5.1.1 Radial distribution functions

Figure 6-2 shows the RDF curves for the A2 asphaltene at different magnetic fields. In the paraffinic medium and magnetic-free environment, the RDF curve shows a clear peak at around 5 Å, and a second smaller and broader peak around 7 Å – 9 Å. Visual inspections of the molecular configurations show that the first peak refers to the face-to-face (F) stacking, where the planes of the aromatic ring systems are aligned in parallel between two asphaltene molecules. The F-stacking distances of about 5 Å were in agreement with the reported

distances from other works (Khalaf and Mansoori, 2018). On the other hand, the second peak was due to the next-nearest neighbor molecules that were loosely stacked to the F-stacked molecules. The much broader peak was because these molecules were either orientated in a parallel-displaced (PD) stacking or a T-shaped stacking. In the latter case, the planes of the aromatic ring systems were approximately orthogonal to each other. In summary, the A2 molecules formed a stable F-stacked two-molecule cluster, with the third molecule loosely stacked to the cluster.

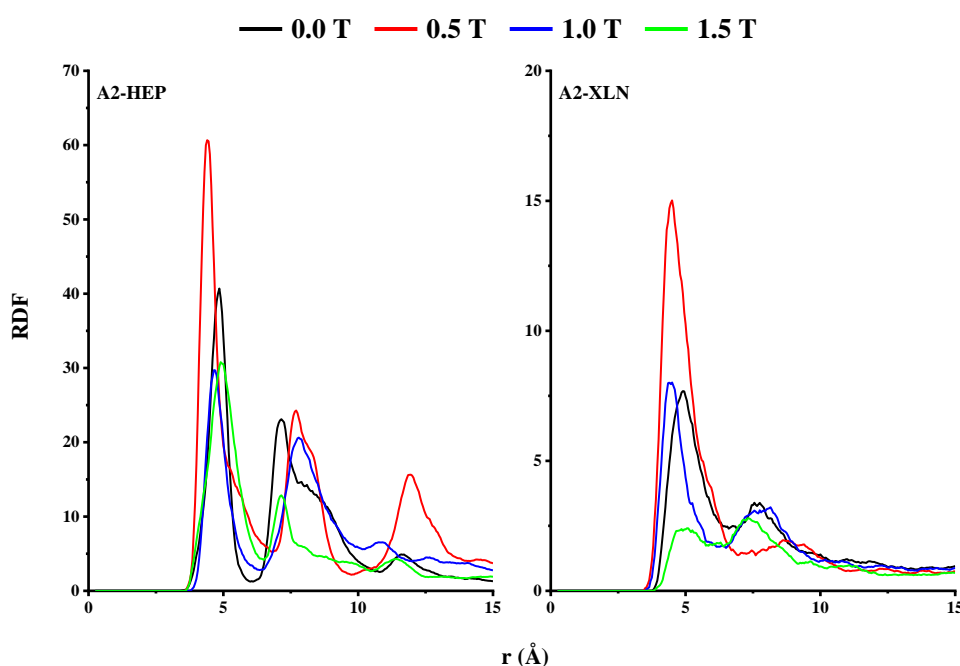


Figure 6-2. RDF curves of A2 asphaltene at different magnetic fields in both mediums.

When the magnetic field was applied, at 0.5 T, three RDF peaks of approximately regular intervals become visible. Also, the second peak was more clearly defined when compared with that of the second peak without the magnetic field application. This indicates the enhancement of the molecular aggregation, with multiple-layer stacking as a result of the magnetic field effect. This was confirmed by visual inspections of the molecular configurations, which show the appearance of much larger clusters, of which, the third peak in the RDF curves were due to the fourth-layer stacking of molecules. Note that the third

peak was centered around 12 Å, which was farther than the reported cutoff of asphaltene stacking (Yaseen and Mansoori, 2018).

Surprisingly, when the magnetic field was increased to 1.0T, there was a clear reduction of peaks, both regarding the number and intensity of peaks. In fact, by comparing the intensities of the first peaks between 0.0 T and 1.0 T, it can be seen that the 1.0T field strength reduced the onset of asphaltene aggregation by about 25%. The disruption of molecular aggregates became even more evident at a higher magnetic field strength of 1.5T. In this case, the second peak was significantly reduced, leaving only one predominant peak at around 5 Å.

In summary, we can conclude that the A2 asphaltene molecules naturally forms aggregates in the magnetic-free environment in paraffinic medium, due to the strong quadrupole interactions between the extensive π -aromatic ring systems of the molecules. A weak magnetic field (0.5 T) can enhance the aggregate size, whereas, stronger magnetic field (> 1.0 T) could disrupt the aggregates.

It is known that asphaltene is soluble in aromatic medium due to the π - π interactions between asphaltene's aromatic core and the aromatic solvent molecules. It is known that the asphaltene molecules tend to form micelles (Pacheco-Sanchez and Mansoori, 1998) in such mediums. Thus, in the absence of a magnetic field, two RDF peaks of much weaker intensities were formed, when compared with those of paraffinic medium in, Figure 6-2. This means that the A2 solute is less likely to form a stable two-molecule core cluster since it can also interact competitively with the aromatic solvent molecules.

In aromatic medium and at 0.5T, the A2 asphaltene showed a clear, higher association affinity with each other in an F- stacking fashion. Visually, this means a noticeable increase in the formation of two-molecule clusters. However, most of these clusters were disrupted when the magnetic strength was increased to 1.0 T. Further increase of the magnetic strength

(1.5 T) results in almost complete disruption of the F-stacking clusters. The resulting clusters were now loosely associated with one another via a mix of T-shape and F- stacking modes.

Figure 6-3 shows RDF curves of the A3 asphaltene in paraffinic medium at different magnetic fields. From previous studies (Khalaf and Mansoori, 2018), the A3 asphaltene has low aggregation affinity when compared to A2. This is because A3 is topologically a more flexible molecule with two separate aromatic systems: a small benzene-base structure and the other a fusion of phenanthrene and naphthalene polyaromatic sheet. Conversely, the A2 molecule contains a single, large aromatic coronene-like core structure. For this reason, in the magnetic-free environment, A3 does not readily form the typical F-stacking cluster as would be the case for A2. The RDF curve does not provide a clear indication of the structure of the molecular cluster. This may be because unlike the A2 molecule, the center of gravity of the A3 molecules was less well-defined and likely to have located off the aromatic ring systems, of which the location is depending on the conformational structure of the molecules.

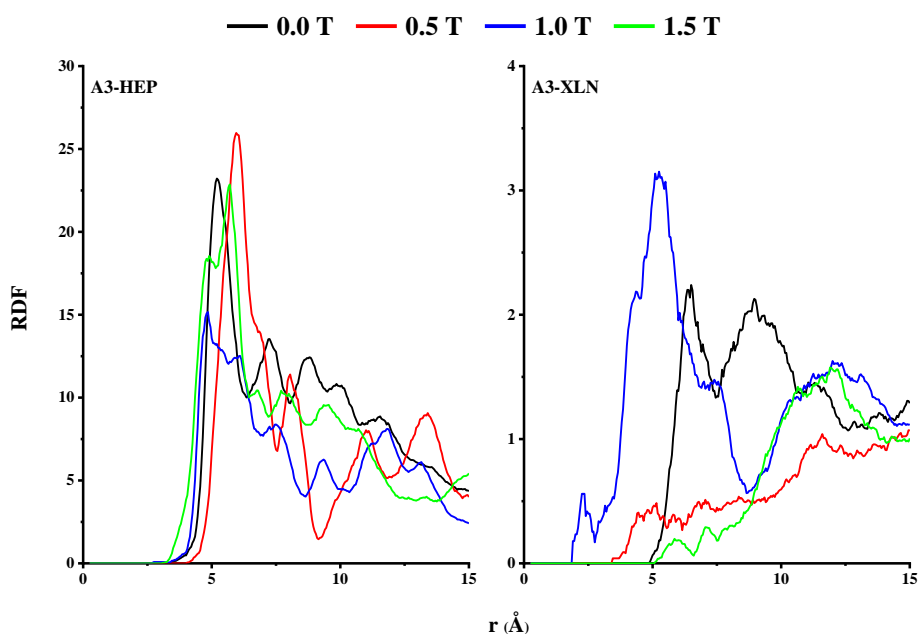


Figure 6-3. RDF curves of A3 asphaltene at different magnetic fields in both mediums.

The A3 structure is archipelago and the distribution of the heteroatoms are all around the aromatic cores. Thus, the magnetic field will be on all sides, rather than the core or a single side. For instance, a magnetic field of 0.5 T could have shifted the F-stacking and created two RDF peaks beyond the reported stacking limits. Even then, some form of cluster associations was still evident with or without a magnetic field, as the first prominent RDF peaks occurred at around a close-packing distance of 5 Å.

The highest effect on the aggregation disruption was at 1.0T magnetic field, where the aggregation onset was reduced by ~35% with compared with the magnetic-free model. In general, the effects of other magnetic field strengths were only on the preferred stacking and the separation distances.

Once again, A3 is shown to be more soluble in the aromatic medium than the paraffinic medium, as shown in Figure 6-3 with much lower peak intensities when compared with those in the paraffinic solvent. In the absence of magnetic field, the molecular association was low and visual inspection of the molecular configurations showed were mainly due to a mix of PD and T-shape stacking, instead of the F stacking. As a result, this gave rise to the appearance of the first peak at a larger distance, of around 6.3 Å.

Applying 0.5T and 1.5T result in the aggregates being completely dispersed, with no discernable RDF peak at close distances. However, when the magnetic field was at the moderate strength of 1.0 T, the association increased and shifted the stacking to be mainly some form of F-stacking, as evident by the appearance of the peak at around 5 Å.

Figure 6-4 shows RDF curves of A4 asphaltene in both mediums at different magnetic fields. The A4 asphaltene molecule contains a smaller center aromatic core when compared with that of A2 molecule but contains longer side chains when compared with that of A3 molecule. This means that the core packing is more well defined when compared with that of A3, although the long and large number of side arms may disrupt such packing from taking

place. This is evident in the RDF curves, where A4 generally produced broader peaks concerning the other asphaltene molecules when comparing Figure 6-2, Figure 6-3, and Figure 6-4 for the paraffinic mediums.

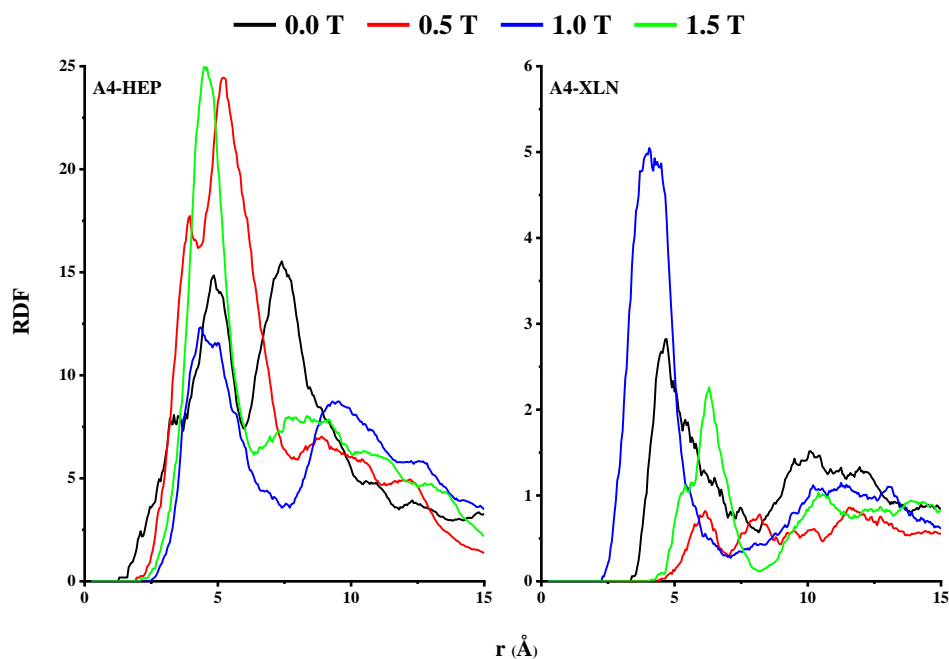


Figure 6-4. RDF curves of A4 asphaltene at different magnetic fields in both mediums.

The effect of side chain flexibilities in A4 was also evident in the molecular configurations. In the absence of a magnetic field, A4 showed moderate aggregation affinity with face-to-face and T-shaped stackings, with some structural hindrances due to the flexible sulfide chains.

Applying 0.5T and 1.5T increased the F-stacking aggregation by ~65% when comparing the intensity of the first prominent peaks in Figure 6-4. However, at the moderate magnetic strength of 1.0 T, the aggregation effect was decreased by ~17% and reduced the peak of T-shape stacking. Such a varying trend may be due to the opposing competitive effect between the aromatic plane and the sulfide side chains. A4 has 4 side chains and some of these chains

have heteroatoms which may reduce the effect of the magnetic field. It is known that side chains play a role in hindering the aggregation process. The magnetic field may have the potential to control the movement and directions of these chains, which finally enhance or reduce the onset of the aggregation.

Once again, similar to the previous cases, the RDF curves show that A4 is more soluble in the aromatic medium when compared with the paraffinic one. In the absence of a magnetic field, the association of A4 asphaltene was low and the F-stacking appears to be the preferred mode of stacking. By applying 0.5 T, the aggregated structure was diminished. When the applied field was increased to 1.0T, the molecular association was restored and doubled in the amount when compared with the magnetic-free case. The clusters were mostly packed in the F-stacking mode. However, at the highest strength of 1.5 T, the association was reduced and changed the preferred stacking to be a T-shape.

Trajectory visualization and RDF calculations showed that the onset of asphaltene aggregation was changing with magnetic field strength and the medium as well as asphaltene molecular structure. Figure 6-5 shows snapshots of asphaltenes in paraffinic and aromatic mediums at different magnetic fields. It shows the effect of magnetic field on stacking and aggregate size.

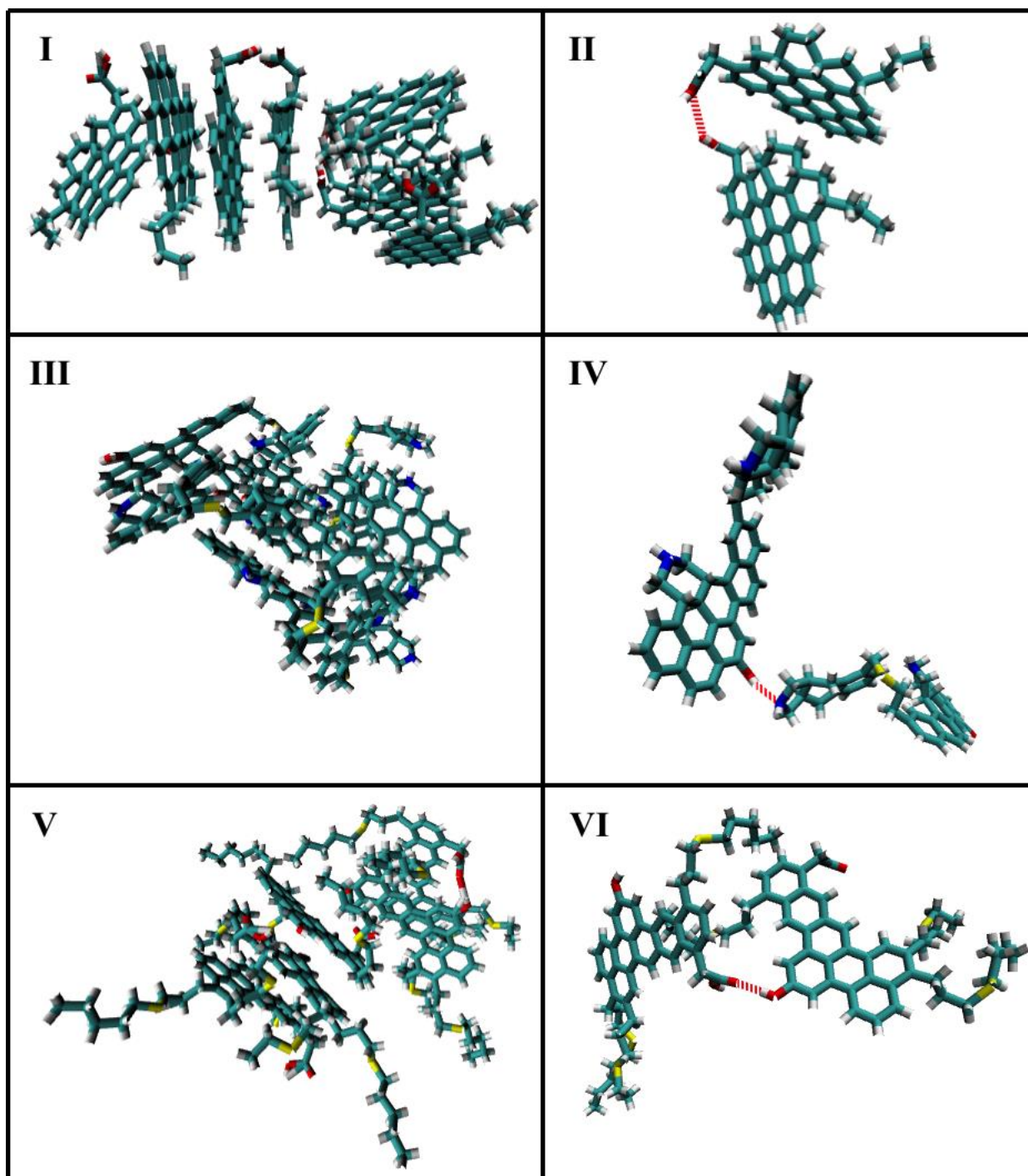


Figure 6-5. Snapshots of A2-A4 asphaltenes in paraffin and aromatic mediums at different magnetic fields. Where: I represents A2 in paraffin at 1.5T, II represents A2 in aromatic at 1.5T, III represents A3 in paraffin at 1.0T, IV represents A3 in aromatic at 1.0T, V represents A4 in paraffin at 0.5T, and VI represents A4 in aromatic at 0.5T.

6.5.1.2 Hydrogen bonds

Hydrogen bonds (HB) are due to a high charge difference between a hydrogen atom that bonded to a highly negative atom with another highly negative atom (oxygen, nitrogen or fluorine). In this study, hydrogen bond interactions predominantly occur among the carboxylic groups (COOH) between asphaltene molecules because o-xylene and n-heptane do not have a polar site for such interactions. However, it is reported that HB interactions play a minor role in asphaltene aggregation, which is mainly due to π - π interactions (Khalaf and Mansoori, 2018). On the contrary, HB may affect the structure of aggregated asphaltene (Yaseen and Mansoori, 2018). The asphaltene models that were used in this study have a different distribution of HB sites that could participate in asphaltene aggregation. As reported above, magnetic fields have effects on a highly charged particle. In asphaltene, the highly charged atoms are polar functional groups such as amino (NH) and carboxylic groups. Thus, magnetic fields may have effects on the orientation and interactions of these atoms which may affect HB interactions. The average number of HB between asphaltene molecules at different magnetic fields in paraffinic and aromatic mediums are reported in Figure 6-6. It can be seen that magnetic fields have effects on HB interactions in both mediums, where it caused an increase and decrease in the average number of HB interactions. For example, at 0.5T, the average number of HBs increased in a similar way of RDF curves. The changes in HBs are due to the changes in the separation distances and/or the orientations of asphaltene molecules. Note that there is no discernable trend in HB counts with respect to magnetic strength and this may strongly indicate the magnetic field strength predominantly affect the main aromatic systems of asphaltene and that the change in HB counts is merely due to weak coupling of geometrical rearrangement of these aromatic systems with respect to the side chains where HB interactions occur.

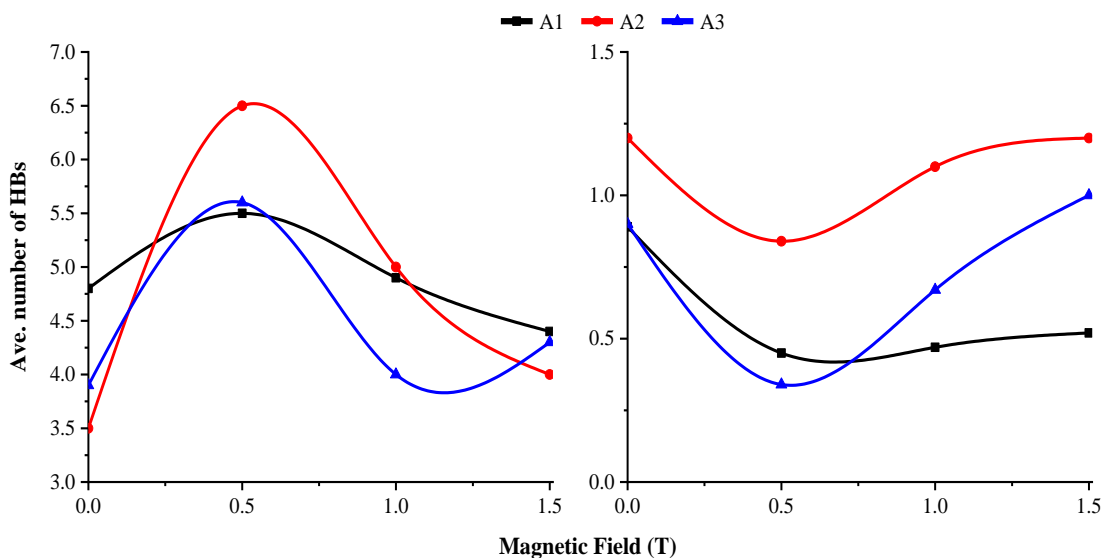


Figure 6-6. The average number of hydrogen bonds of asphaltenes in both mediums.

6.5.2 The effect of magnetic field on asphaltene disaggregation

Twenty-four molecules of each of the four kinds of asphaltenes (A1, A2, A3, and A4) reported in Figure 1 were dissolved in an equimolar of xylene and heptane. Radial distribution functions (RDFs), and hydrogen bond (HB) interactions, transport properties, and trajectories were investigated to understand the effect of magnetic fields on various asphaltene's behavior and asphaltene disaggregation.

6.5.2.1 Radial distribution functions

Figure 6-7 shows the RDF curves for the A1 asphaltenes at different magnetic fields. In the magnetic-free environment, the RDF curve shows multiple peaks at different distances. The first clear peak is at 5.2 Å, and a second larger peak around 6.3 Å. Trajectory inspections of the molecular configurations show that the first peak refers to due to face-to-face stacking. In this stacking mode, the planes of the aromatic ring systems are aligned in parallel between two asphaltene molecules. Moreover, the second peak is due to the parallel-displaced or T-shaped stackings where the aromatic cores are approximately orthogonal to each other. The

stacking distances agreed with the reported distances from our previous works (Khalaf and Mansoori, 2018; Khalaf et al., 2019). In summary, the A1 molecules showed high aggregation affinity and formed a big aggregate where it was beyond clustering point, see Figure 6-8.

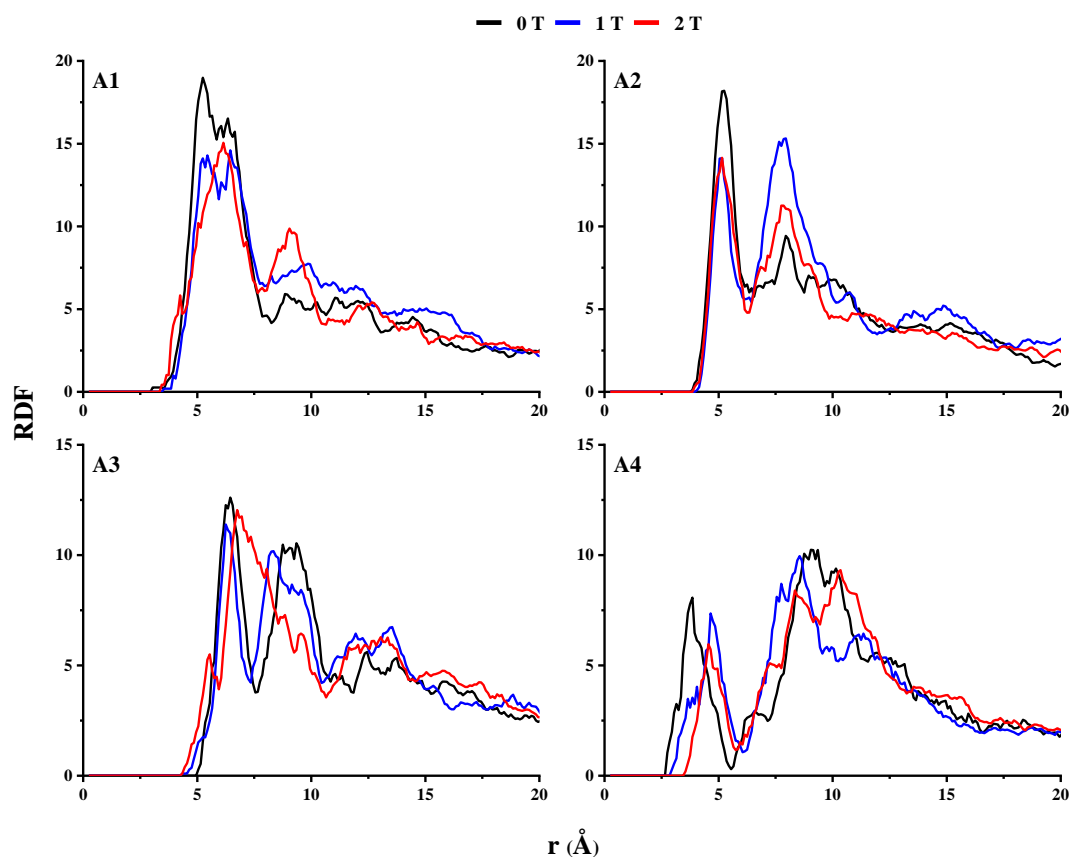


Figure 6-7. RDF curves of A1-A4 asphaltenes at different magnetic fields.

When the magnetic field was applied, at 1 T, a reduction in the RDF peaks at 5.2 and 6.3 Å became visible. The reduction in the first peak was more clear than the second peak. This means that magnetic field changed the dominated stacking to be parallel-displaced or T-shaped stacking. In addition, a wide peak from 8.5 to 10.5 Å was appeared which was due to the loosely stacked layer to the stacked molecules when compared with that of the peak without the magnetic field application. Increasing the magnetic field to 2 T showed

interesting results. It showed a clear reduction in both peaks in comparison with magnetic free case. In fact, by comparing the intensities of the first peaks between 0 T and 2 T, the 2.0 T field strength could reduce asphaltene aggregation by about 22%. The disruption of molecular aggregates become even more evident at this magnetic field strength where the second peak shifted from 6 Å to be at around 9 Å. In this case, the second peak was significantly reduced, leaving only one predominant peak. These results are agreed with our recently published work (Khalaf et al., 2019) where magnetic field has effects on asphaltene aggregation.

In conclusion, we can see that A1 asphaltene molecules have an affinity to form stable and large aggregates in the magnetic-free systems, due to the strong quadrupole interactions between the aromatic ring systems of the molecules. Moderate magnetic fields can disturb could disrupt the aggregates and may help in reduce asphaltene problem.

For A2 asphaltene in the absence of a magnetic field, the RDF curve shows multiple peaks at different distances where they represent multiple stackings. The first clear peak is at 5.2 Å, and a second smaller and border peak is at 8 Å. Tracking the molecular configurations show that the first peak is due to face-to-face stacking which is dominated stacking while the second peak is due to parallel-displaced or T-shaped stackings. In general, A2 asphaltene showed a high aggregation in two modes of stacking and formed big aggregates of different sizes. The stacking distances and aggregation behavior of A2 asphaltene are in agreement with our previous study (Khalaf and Mansoori, 2018).

When the magnetic field of 1 T strength was introduced into the system, an increase and decrease in RDF peaks became clear in comparison with the magnetic-free system. The calculations showed that the first peak reduced by about 22% while the second peak increased by about 35%. This could be explained by the changes in molecular orientations and stackings due to magnetic interactions. The ability of magnetic field to change molecular

orientations of asphaltene was proved in another study (Khalaf et al., 2019). This was also reported by Loskutova et al., (2008) where they concluded that magnetic fields change polar species interactions and producing new structures. Surprisingly, applying a magnetic field of 2 T showed a clear reduction in the second peak in comparison with the magnetic field of 1 T. Comparing RDF peaks of the magnetic-free system and 2 T field strength showed that 2 T could cause asphaltene disaggregation. It could be seen that higher magnetic field reduced the size of aggregation and slightly changed the preferred stacking. It is clear that A2 asphaltene tends to produce large aggregates in the absence of magnetic field due to π - π interactions in the same way of A1 asphaltene. Moderate magnetic fields (1 and 2 T) could increase and reduce asphaltene aggregation trends and the highest effects were on the stacking modes.

For A3 in the absence of magnetic field, the RDF curve shows multiple peaks at different distances where they represent multiple stackings. The first clear and higher peak is at 6.5 Å, a second border peak is about 7.7-10.5 Å. 8.2 Å, with a third peak at round 12.5 Å. Inspection of the molecular configurations show that the first peak is due to face-to-face stackings and the second and third peaks represent two layers of parallel-displaced or T-shaped stacking molecules that are stacked to the first peak. Moreover, the whole aggregate is a complex structure due to the different and the multilayer stackings. A3 asphaltene is archipelago asphaltene and its structure is more flexible than other used asphaltenes. Thus, A3 may have hydrogen bond and aromatic-aromatic interactions in the same molecule which could allow A3 to form multi-layer of stacking asphaltenes.

Applying 1 T to the system slightly reduced the first peak and changed and shifted the distance of the second peak. The other peaks were enhanced and became more visible comparing with magnetic free system. Increasing magnetic field strength to 2 T showed a high change in the second peak where it was almost faded while the first peak did not show

change. Unlike to A1 and A2, applying magnetic field strength of 1 T and 2 T did not show any reduction in A3 aggregation. It changed the molecular configurations and stacking distances. The response of A3 to the magnetic fields showed that not all asphaltene aggregations could be broken by magnetic fields. In general, the aggregation trend of A3 asphaltene did not show changes as was observed in A1 and A2 asphaltenes. We believe the behavior of A3 during magnetic treatments is due to its archipelago structure. The flexibility of the molecules and the bridging chain played a role during molecular orientations providing better core-core interactions.

For A4 in the absence of magnetic field, the RDF curve shows two peaks at different distances where they represent multiple stackings. The first clear peak is at 3.9 Å followed by a wider peak that exceeded 10 Å. Inspection of the molecular configurations show that the first peak is due to face-to-face stacking and the second peak is because of a compensation of parallel-displaced and T-shaped stackings. The wider peak is because the series of stacked molecules in this stacking mode, as shown in Figure 6-8. Even with the long side chains, A3 asphaltene showed moderate aggregation affinity comparison with A3 with some structural hinderance due to flexible sulfide chains.

In a similar observation of previous asphaltenes, introducing the magnetic field of 1 T strength into the system showed a small change in the orientation and stacking. Besides shifting the second peak, a small third peak appeared at 11.5 Å which was due to loosely stacked molecules. Increasing the magnetic field to 2 T showed a 7% reduction in the RDF curve which means a reduction in the aggregation mode and the reduction in the first peak was more clear than the second peak. The structure of A4 is long core connected to three long chains may help in reducing the effect of magnetic forces because of the flexibility of the sulfide bond in comparison with the aromatic core.

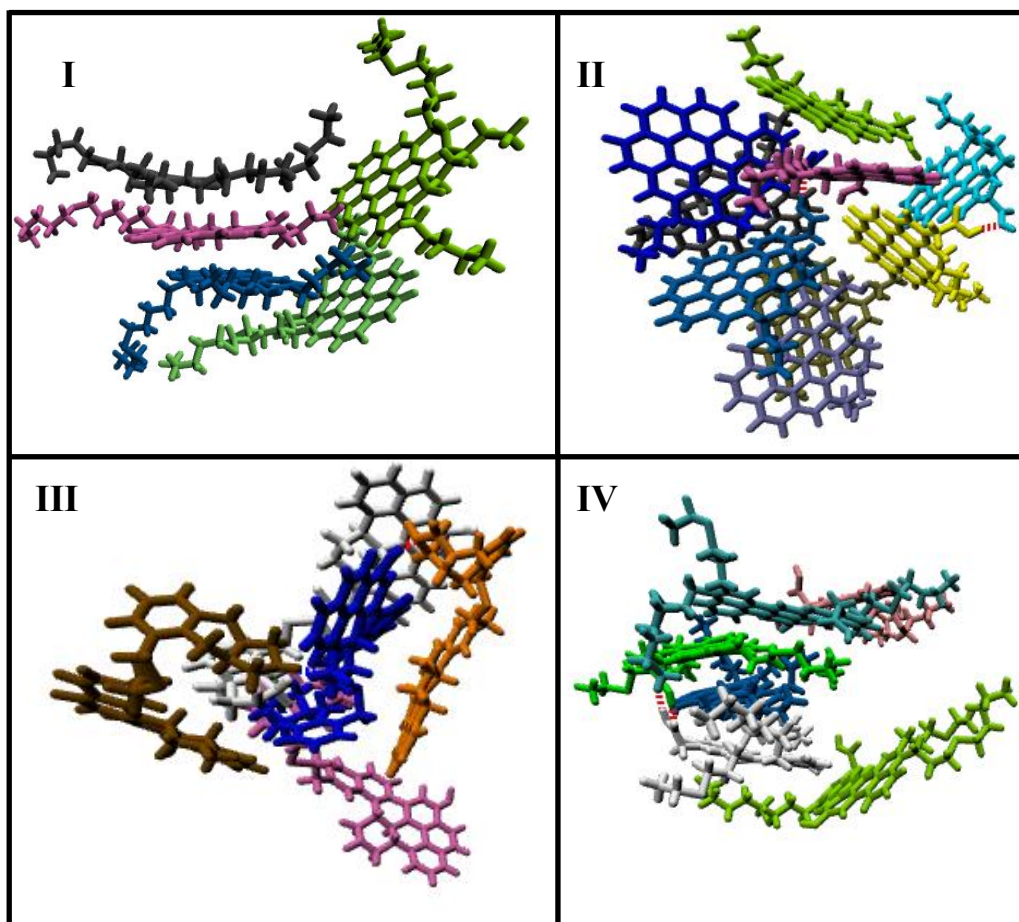


Figure 6-8. Snapshots of different asphaltenes at different magnetic fields. Where: I represents A1 at 0 T, II represents A2 at 1 T, III represents A3 at 2 T, and IV represents A4 at 0 T.

6.5.2.2 Hydrogen bond

In this study, hydrogen bond interactions predominantly occur among the polar groups that have the ability for HB interactions between asphaltene molecules (o-xylene and n-heptane do not have polar sites for such interactions). According to Lorentz force and magnetic field application, highly charged particles will be affected more than other particles in the system. In asphaltene, the highly charged atoms are polar functional groups such as amino (NH) and carboxylic groups. The used asphaltenes have different sites that could participate in HB

interactions, thus magnetic fields may have effects on the orientation and interactions of these atoms which may affect asphaltene aggregation. It is reported that HB interactions may affect the morphology of aggregated asphaltene (Yaseen and Mansoori, 2018).

The average number of HB between asphaltene molecules at different magnetic fields are reported in Figures 7. It shows the magnetic field effects on HB interactions where it caused an increase and decrease in the average number of HB interactions. The changes in HBs are due to the changes in the separation distances and/or the orientations of asphaltene molecules. Note that there is no discernible trend in HB counts with respect to magnetic strength and this may strongly indicate the magnetic field strength predominantly affect the main aromatic systems of asphaltene and that the change in HB counts is merely due to weak coupling of geometrical rearrangement of these aromatic systems with respect to the side chains where HB interactions occur.

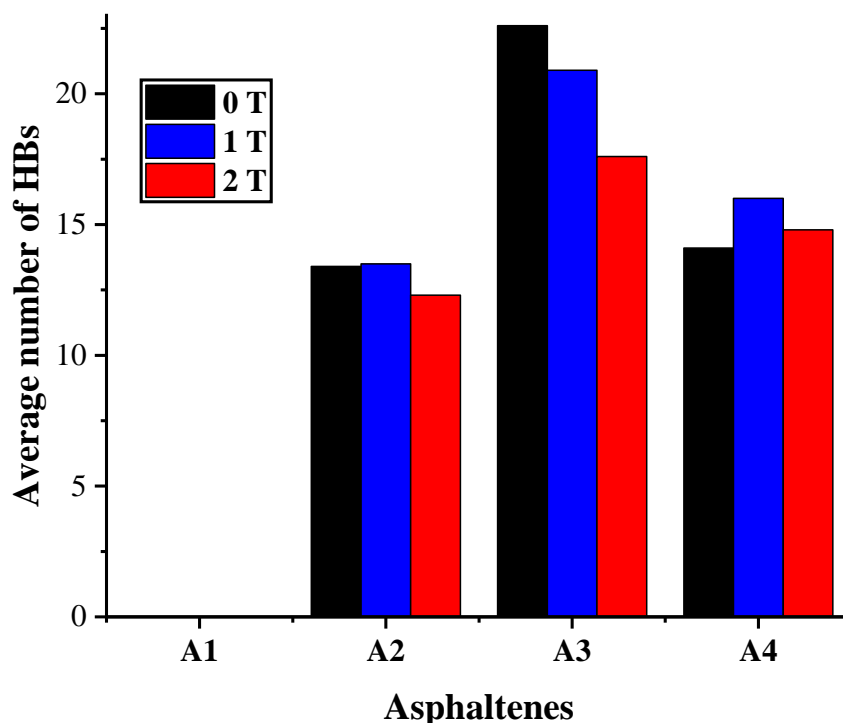


Figure 7. Average number of hydrogen bonds (HBs) of asphaltenes at different magnetic fields. A1 does not have any donor and acceptor thus it has zero HB interactions.

6.6 Conclusions

In this study, we have investigated the effect of different magnetic field strengths concerning the asphaltene aggregation behavior in paraffinic and aromatic mediums. Radial distribution functions and hydrogen bond interactions were investigated through molecular dynamics simulation. Our MD results indicated that magnetic field has effects on the onsets of asphaltene aggregation in different mediums. In paraffinic medium, 0.5T increased the onsets of aggregation and changed the kind and distances of preferred stacking for all the used asphaltenes. Besides that, the effect of 1.0T, as well as the effects of 1.5T, were different depending on the asphaltene molecular structure. In aromatic medium, 0.5T increased the association of A1 and decreased the association of A2 and A3.

The different behaviors of asphaltenes could be explained as magnetic fields have a high effect on polar species and the effects become higher with increasing the polarity of the molecules. Thus, we see different behaviors in different mediums and with increasing the magnetic fields. 0.5T is a moderate magnetic field. Thus its effect on asphaltene is higher than other molecules in the system due to its polarity. This means the effects on asphaltene are more observable than other molecules, which increased the onset of aggregation in paraffinic mediums. The interactions between asphaltene molecules and magnetic field of 0.5T strength were not high enough to control the movement and rotation of asphaltene molecules. We believe that magnetic forces due to 0.5T helped in the rotation of asphaltene molecules which helps in better π - π interactions.

This study clearly shows the complex relationship of the topological structures of asphaltene concerning magnetic field strength. In our future studies, we intend to look into details the role of solvents and their interactions with asphaltene molecules to investigate their influences on the asphaltene aggregation with and without the presence of magnetic field. Also, this study also highlights that center of gravity base RDF analysis may not be

able to reveal the packing structure, especially for those molecules with flexible topological structures. A more localized structural analysis would be needed to quantify the molecular packing of such structures.

Hydrogen bond results indicated that magnetic field did change the average number of the interactions depending on the medium and asphaltene architecture. These changes are due to the changes in the orientation and the distances between asphaltene molecules (as reported in RDFs). Also, trajectory visualization showed different changes due to the magnetic field. Generally, the effects of magnetic field on the onset of asphaltene aggregation are due to Lorentz force. Asphaltene is the most polar species in the system. Thus the effects of magnetic field on its onset of aggregation are high. The effects of magnetic field are dependent on the strength of the applied magnetic field, the medium, and the architecture of asphaltene, where the number and position of heteroatoms are very important.

The results showed 1 T could break up A1 aggregation by 22% while 2 T showed a reduction in A2 RDF curve. Because of the flexibility of the bridge chain in A3 and the distribution of heteroatoms, A3 showed small changed due to magnetic treatments in comparison with the previous two cases. The aggregation trend of A4 asphaltene was affected by 2 T field intensity. The reduction in A4 was less than A1 and A2 due to the flexibility of the long three sulfur-containing chains. Hydrogen bond results indicated that magnetic field did change the average number of the interactions depending on asphaltene architecture. These changes are due to the changes in the orientation and the distances between asphaltene molecules (as reported in RDFs). Moreover, the diffusivities of used asphaltenes were influenced by magnetic field. Magnetic field changed the diffusivities of all the used asphaltene even when they had low aggregation status. Also, trajectory visualization showed different changes due to the magnetic field. Generally, the effects of magnetic field on asphaltene aggregation are due to Lorentz force which is high for polar species. Since

asphaltene is the most polar species in the system, the effects of magnetic field on aggregation are high. The effects of magnetic field are totally dependent on the strength of the applied magnetic field and the architecture of asphaltene, where the number and position of heteroatoms are very important. It was observed that asphaltene with large single aromatic core changed more than others during magnetic treatments and the archipelago structure was less affected. This study clearly shows the complex relationship of the topological structures of asphaltene concerning magnetic field strength. Also, it highlights that magnetic field could be used for asphaltene aggregation alteration. More studies of different structures and in the presence of resins at different temperatures are required to predict the general trends of asphaltene disaggregation process.

7 Asphaltenes Adsorption on Solid Calcite Surfaces

7.1 Abstract

In enhanced oil recovery, asphaltene instability is due to the changes in pressure, temperature, and composition of the reservoir fluids. Molecular dynamics simulations were conducted to investigate the onset of asphaltene adsorption on calcite surfaces. The results showed that a fixed layer of ortho-xylene rapidly adsorbed on calcite. The onset of asphaltene adsorption was a function of its structure and the distribution of the heteroatoms. The morphology of the solid surface had a key role in the asphaltene adsorption, whereas the adsorption of asphaltene was higher on the rough surface than that on the smooth surface. In the absence of air, asphaltenes showed a high adsorption affinity on calcite than in the presence of air. The presence of different heteroatoms enhances the adsorption of asphaltene to the surface. Sulfur works as an adsorption site where the sulfur atoms pull the asphaltene molecules toward the surface. The trajectory showed that the first stacked Asphaltene and hypothetical structures' atoms to the surface were sulfur. In general, the results demonstrated a reduction in asphaltene adsorption on calcite in the presence of air. Also, more investigations about different surfaces and large-scales are required for robust predictions and observations.

7.2 Introduction

During petroleum production, asphaltenes may aggregate and deposit in the porous media and production facilities. The adverse effect of asphaltene deposition in reservoir pores is pore clogging and alteration of pore surface wettability. Deposition of asphaltenes may lead to significant reservoir damage, reduced oil flow in the reservoir pores, and deterioration of oil recovery efficiency. To understand and correct this problem, much research has been

performed on conditions under which asphaltenes may start to aggregate due to miscible gas flooding, and the factors which may contribute to its deposition and adsorption on reservoir surfaces (Khalaf and Mansoori, 2018, 2019; Kim et al., 1990; Mansoori, 1997). For example, experimental results of a Middle Eastern core flooding indicated high asphaltene precipitation in carbonate cores (Dehghani et al., 2007; Leontaritis and Mansoori, 1988; Takahashi et al., 2003). It has been shown that calcite (CaCO_3) is a highly active mineral for asphaltene adsorption (Jada and Debih, 2009; Tu et al., 2006). Studies of the stacked asphaltenes on the calcite surfaces showed irreversible adsorption which is more significant compared to the silica surfaces (Gonzalez and Travalloni-Louvisse, 1993). Other studies showed a rapid adsorption on silica. However, the solvent plays a key role in determining the strength of asphaltene adsorption due to the difference in asphaltene solubility in these solvents (Adams, 2014; Mohammed and Gadikota, 2019).

Our interest in this research is to understand the molecular nature of asphaltene adsorption on reservoir rocks forming the petroleum reservoirs porous media. To our knowledge, there are little or no fundamental studies on the molecular basis of asphaltene adsorption on solid surfaces. Because calcite is the main fraction of limestone rocks in many oil reservoirs around the world, the present study focuses on asphaltenes adsorption on calcite (Taheri-Shakib et al., 2018). Understanding asphaltene adsorption on calcite may give an indication about the process at the molecular level and help in identifying the main factors that lead to the adsorption.

Accordingly, MD simulations were carried out to investigate the molecular nature of asphaltene adsorption on the calcite surface. The intention was to examine the impact of different heteroatoms on asphaltene adsorption on calcite. Thus, various structures containing different heteroatoms were used. The aromatic cores and length of aliphatic chains are the

same in all the used structures. This helps in focusing on the effects of location and type of heteroatoms on the onset of asphaltene adsorption on different solid surfaces.

7.3 Asphaltene Structures

The asphaltene molecular structure used in this study, Asphaltene (A) in Figure 1, is proposed by Takanohashi et al., (2004) for Khafji crude oil in Saudi Arabia. This asphaltene is extensively used in various studies and has all the reported heteroatoms in asphaltenes. In order to understand the effect of asphaltene molecular structures and the presence of different heteroatoms on the onset of asphaltene adsorption on calcite surface, four additional hypothetical structures similar to A were proposed and used. These additional structures are named M1-M4, respectively. The main shape (aromatic core and length of aliphatic chains) is the same in all structures shown in Figure 1. This helped in focusing on the effects of location and type of heteroatoms on the onset of asphaltene adsorption on calcite surface.

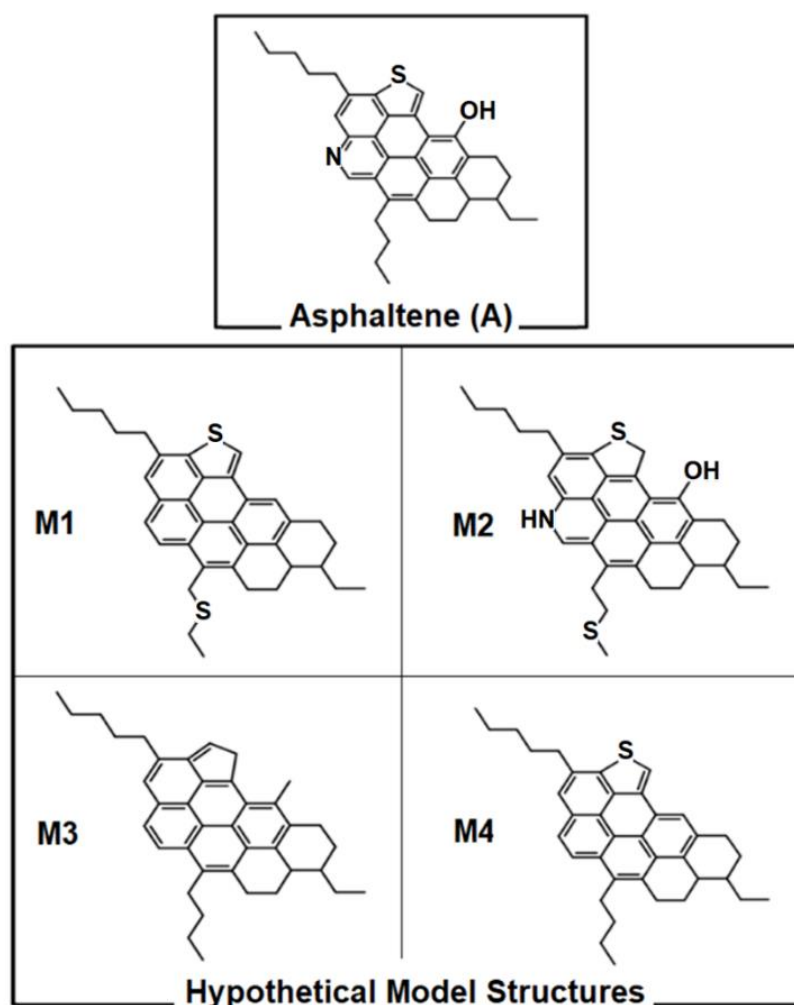


Figure 7-1. Structure of asphaltene (A) and the four hypothetically modified structures M1-M4 used in this study.

7.4 Simulation Method

7.4.1 Initial configurations

Every simulation system was composed of a mixture of Asphaltene A (or one of the 4 hypothetical structures in Figure 1) originally dissolved in the crude oil and located next to a calcite surface. The crude oil was represented by a mixture of ortho-xylene and normal-heptane. Then a miscible injectant was introduced that would cause the separation of asphaltene from the oil phase and its possible adsorption on calcite. For the miscible

injectant, we used air at high pressure. Then, through MD simulation, we studied the onset of stacking of the separated asphaltene on solid calcite surface was studied.

The calcite surface was constructed by cutting along the (104) crystallographic surface. The obtained surface initially had dimensions of 9.28 nm x 7.63 nm x 2.40 nm which was composed of 6 calcite layers. The simulation box was expanded in the z-direction to get the desired size. An equimolar mixture of n-heptane and o-xylene in which 7 wt% of asphaltene (or the four hypothetical molecules) was used in all simulations. Twenty-four molecules of asphaltene (and the four hypothetical molecules) were randomly distributed in the simulation box. Then, all the remaining molecules of n-heptane and o-xylene were sequentially placed in the box. To study the effects of the miscible injectant, 20 wt% of air was added to the system. The ingredients of added air were based on 79% nitrogen and 21% oxygen only (neglecting the effects of small concentrations of other gases).

7.4.2 Force fields

The calcite surface was modeled using a force field developed by Xiao et al. (2011). For air (nitrogen and oxygen), the force field developed by Vujić and Lyubartsev (2016) was used. For other molecules (asphaltene, the four hypothetical molecules, n-heptane, and o-xylene), OPLS-AA force field was employed.

The total energy was calculated based on the summation of bonded (bending, stretching, and torsion) and non-bonded (van der Waals represented by Lennard-Jones and electrostatic represented by coulomb) energies. The OPLS-AA is shown to work well for organic liquids in reproducing the experimental data. In addition, it is shown that the OPLS-AA works well in calculating and producing hydrogen bond interactions between all possible donors and acceptors (Khalaf and Mansoori, 2019; Mohammed and Mansoori, 2018; Yaseen and Mansoori, 2017, 2018).

7.4.3 Simulation details and algorithms

A series of classical MD simulations were carried out using GROMACS 5.1.2 simulation package (Van Der Spoel et al., 2005). After preparing the simulation box in the desired dimensions, energy minimizations were conducted to eliminate the effect of the assumed energy of the initial configurations. To relax the system at reservoir conditions (389 K and 472 bars), energy minimization was followed by 100 ps canonical (NVT) ensemble using V-rescale thermostat. This NVT was followed by 500 ps isothermal-isobaric (NPT) ensemble using Berendsen pressure coupling. To study asphaltene deposition on one solid-fluid interface, the periodic boundary conditions were applied in x-y directions. In all the simulations, leapfrog algorithm with a timestep of 2 fs was used to integrate the equation of motion. The Particle Mesh Ewald (PME) method was applied to calculate the long-range Coulomb interaction forces. In all non-bonded interactions, the cutoff was set to 1.2 nm. After reaching the desired temperature and pressure, the simulations were performed in NVT ensemble for 40 ns. The bond lengths were constrained using LINCS algorithm. Over the course of simulations, the atomic positions were recorded every 100 ps which allowed the tracking of the position of the molecules.

7.5 Results and Discussions

To understand the adsorption of asphaltene and the four hypothetical structures shown in Figure 1 on calcite surface in the absence and presence of air, two kinds of solid surfaces were considered. In reality, rocks are not smooth and straight. There are a lot of protrudes and pore constriction inside the porous media. To understand the adsorption of asphaltene molecules on pore entrances and the edge of the rock surfaces, rough calcite was used.

7.5.1 Asphaltene adsorption on solid surfaces

To understand the stacking of the different structures reported in Figure 1 on rough and smooth calcite surfaces in the absence and presence of air, density profiles of system species were calculated along the z-direction (perpendicular to the solid surface). It provides the distribution of asphaltene molecules on the surface. Also, trajectory inspections were considered in this section to find out which kind of stacking and which segments were close to the surface.

Figure 7-2 shows the density profile of Asphaltene (A) in the presence (black line) and absence (red line) of injected air on smooth and rough surfaces. It shows that asphaltene molecules tend to be adsorbed on the calcite surface. Visual inspection showed that Asphaltene was stacked in two modes, adsorption of single molecules and adsorption of asphaltene aggregates. On a smooth surface, the dominated stacking were single molecules adsorption and the molecules were distributed all over the surface. However, on the rough surface asphaltene molecules were all stacked and accumulated on protrudes of the calcite, see Figure 7-3, where asphaltene molecules appeared to adsorb more. These results showed that the geometry of the surface is an important factor during asphaltene adsorption into solid surfaces.

Adding air to the system enhanced the onset of asphaltene aggregation of A and reduced its adsorption on both kinds of surfaces. It can be seen that air reduced the stacking and displaced asphaltene molecules from the surface. In the case of smooth surface, the distance between Asphaltene (A) and the surface before adding air was less than in the presence of air. The displacement was due to the air layer between the highly adsorbed xylene layer and asphaltene. In the case of rough calcite, the distance between asphaltene and the surface did not show much change as compared with the smooth surface. This is due to the fact that air could not cause detachment of all the asphaltene molecules, but it disturbed the stacked

layers. Inspection of the simulation trajectory confirmed the difference in the close distances as shown in Figure 7-3.

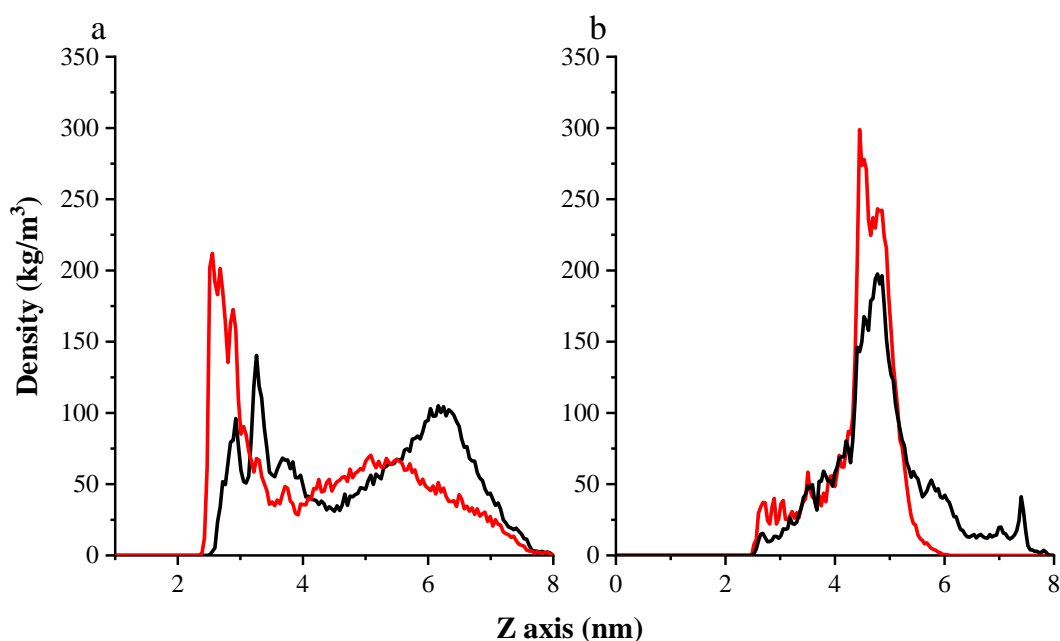


Figure 7-2. Density profile of A asphaltene in the presence (black line) and absence (red line) of injected air, on smooth (a) and rough (b) surfaces.

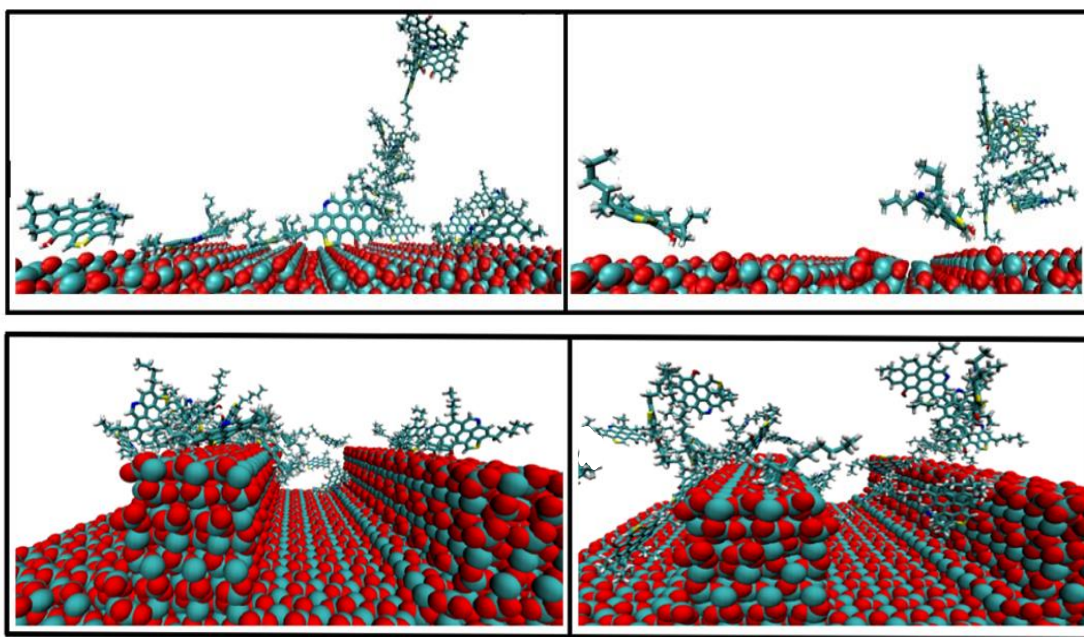


Figure 7-3. Snapshots of the final configurations of onset of adsorption of Asphaltene (A) in the absence (left-side figures) and presence (right-side figures) of injected air, on smooth (top figures) and rough (bottom figures) surfaces.

Investigation of other systems (M1-M4) showed similar behavior. The adsorption of asphaltene molecules on rough calcite was higher than the adsorption on smooth calcite. In addition, air could reduce asphaltene adsorption on calcite surface, Figure 7-4, Figure 7-5, Figure 7-6, and Figure 7-7. It was reported that aggregated asphaltenes adsorbed less than individuals on rock surfaces. In the results, it is shown that asphaltene stacking and desorption are independent of the aggregation, especially in the cases of the rough surface. For example, visualization showed that M1 aggregation behaviors in the presence and absence of air were almost the same. While in the case of M1 stacking, the results showed a high reduction in asphaltene adsorption on rough and smooth calcite surfaces. Moreover, air reduced M2 aggregation and a high change in the adsorption on the rough surface. However, M3 asphaltene showed different behavior than previous asphaltenes. It was shown that air did not enhance M3 aggregation, but did show a high improvement in its desorption on smooth surface. It is reported that polarity is the driving force for asphaltene adsorption on solid surfaces (Piro et al., 1996). It is known that heteroatoms increase the polarity of asphaltene. Surprisingly, M3 showed similar adsorption affinity to other asphaltenes. In all other asphaltenes (A, M1, M2, and M4), air could reduce asphaltene adsorption onto calcite. In the M3 case, the reduction was higher than others in the case of smooth calcite. This behavior is because M3 has less interaction affinity with air and calcite surface that comes from heteroatoms.

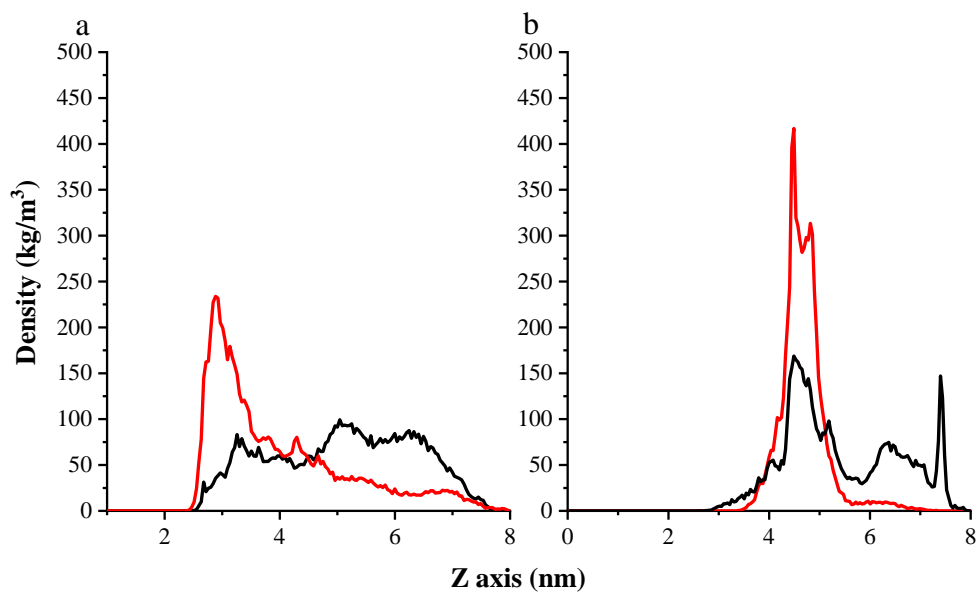


Figure 7-4. Density profile of M1 asphaltene in the presence (black line) and absence (red line) of injected air, on smooth (a) and rough (b) surfaces.

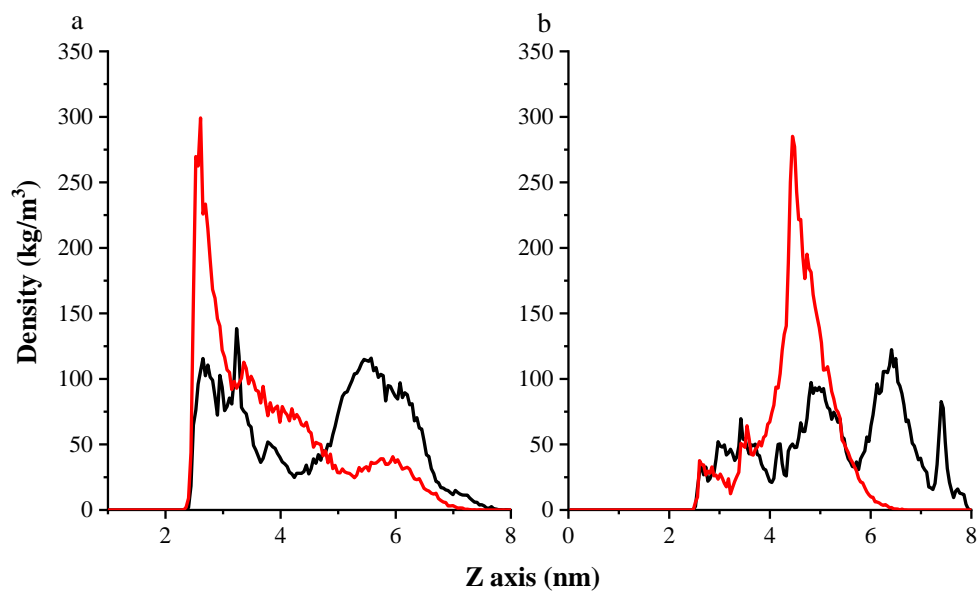


Figure 7-5. Density profile of M2 asphaltene in the presence (black line) and absence (red line) of injected air, on smooth (a) and rough (b) surfaces.

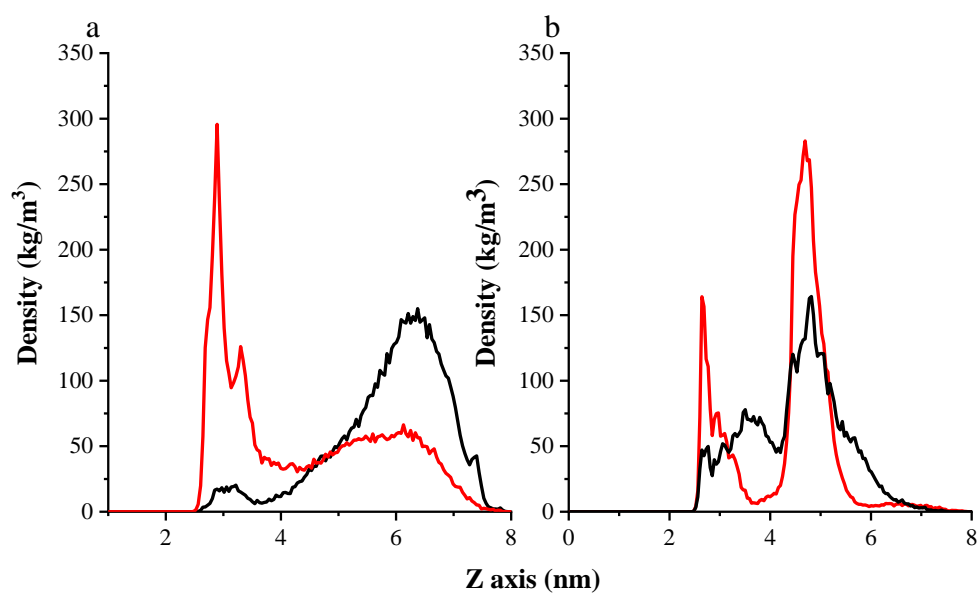


Figure 7-6. Density profile of M3 asphaltene in the presence (black line) and absence (red line) of injected air, on smooth (a) and rough (b) surfaces.

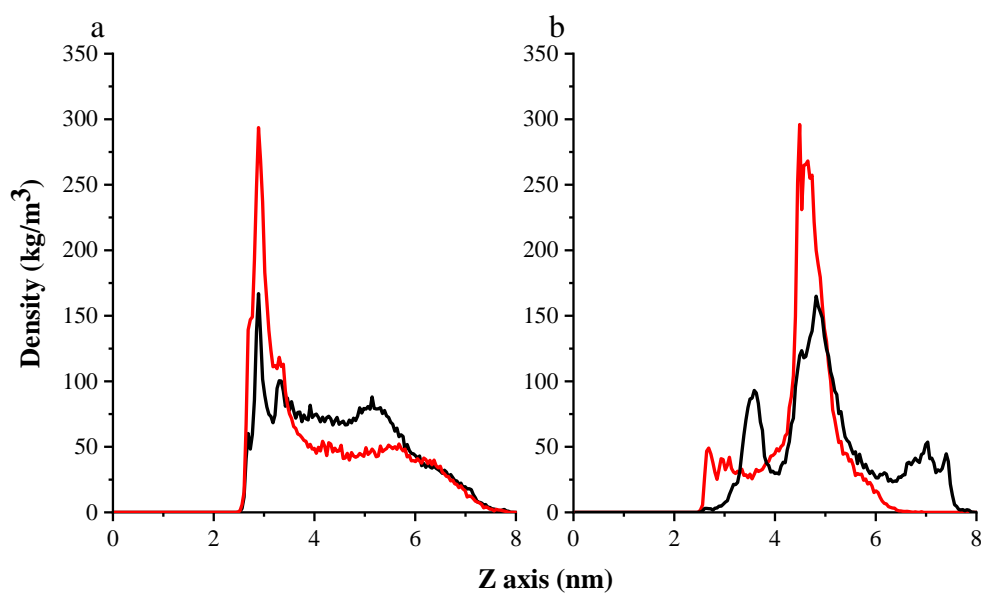


Figure 7-7. Density profile of M4 asphaltene in the presence (black line) and absence (red line) of injected air, on smooth (a) and rough (b) surfaces.

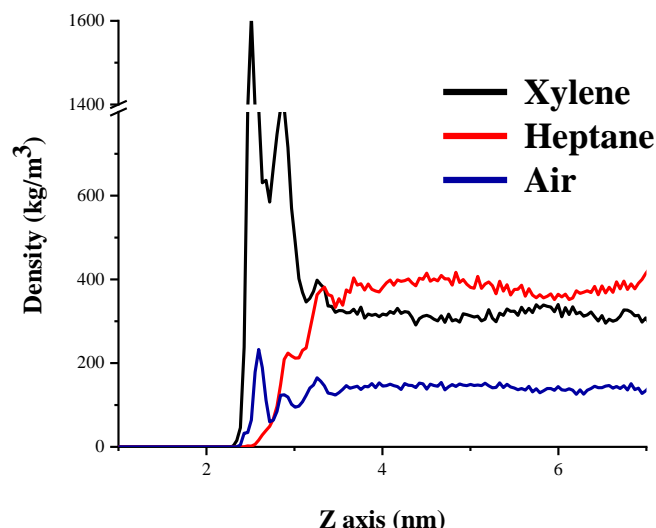


Figure 7-8. Density profiles of xylene, heptane, and air in z-direction away from the surfaces.

7.5.2 Interaction energies

To evaluate the driving forces for the onset of asphaltene aggregation and adsorption on calcite surface, interaction energies between asphaltene structures and smooth and rough surfaces in the presence of air were analyzed and reported in Figure 7-9. The results showed that both vdW and ES interactions were attractions to the calcite which suggested that the chemistry of the surface had a role in these interactions. In addition, the interactions between the surfaces and the structures were different even with the similar architecture of the used asphaltenes. This means that the distribution and the kind of heteroatoms have roles in the adsorption of asphaltene to the surfaces. The Figure also showed that the attraction energies between asphaltene-rough calcite were much higher than between asphaltene-smooth calcite. Both vdW and ES interactions of A, M1, and M3 and rough calcite were much higher than the interactions with smooth calcite. M2 showed different behavior from other structures which may have been due to the distribution of the heteroatoms, where they might equally interact with the calcite surfaces.

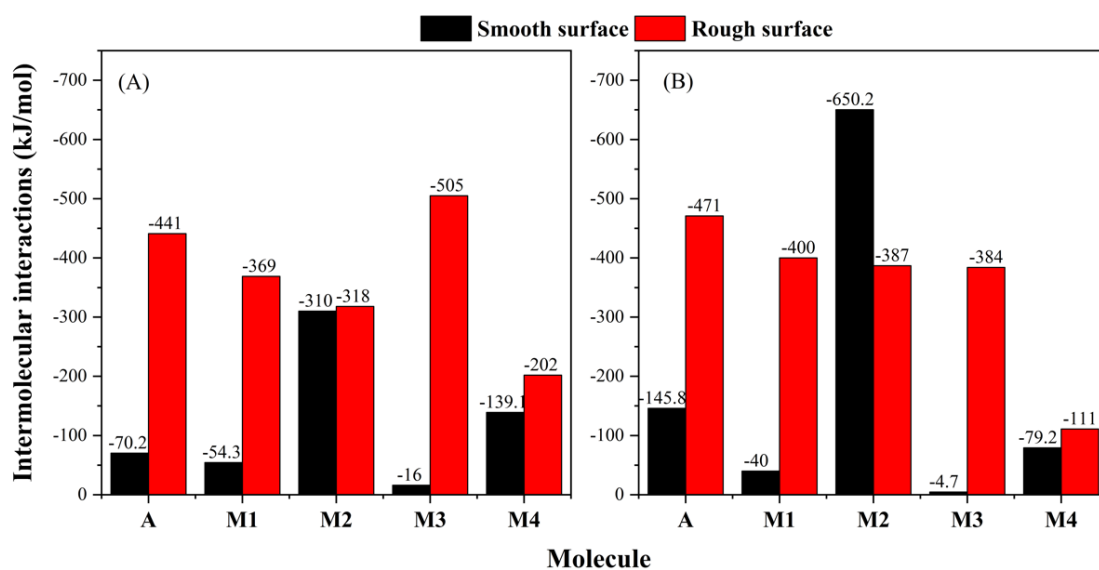


Figure 7-9. Intermolecular interactions between asphaltene molecules and smooth and rough surfaces. (A) vdW interactions (B) Electrostatic interactions.

In addition to the molecular interactions shown in Figure 7-9, the total interactions of selected atoms of asphaltenes with calcite were calculated and analyzed. The selected atoms were chosen all around the used structures (A, M1, M2 and M3) to closely look into the contribution of heteroatoms during asphaltene adsorption. It is reported that asphaltene adsorption on calcite is due to the polarity of the asphaltene and the chemistry of the surface. The results here showed that heteroatoms have high contributions during asphaltene adsorption in the absence and presence of injected air, see Table 7-1, Table 7-2, Table 7-3, Table 7-4, and Table 7-5. In each structure, comparing the contribution of the selected atoms showed that heteroatoms had very high attraction energies to the calcite. Also, comparing the structure with no heteroatoms with other structures shows that hydrocarbons have low interaction affinity to the surface. It supports the fact that asphaltene behavior is highly affected by the presence of heteroatoms. Generally, sulfur helps in the stacking, and the results here showed the sulfur has a high attraction to the calcite in smooth and rough surfaces. Trajectory visualization showed that the first atoms that stuck to the surfaces were sulfur atoms, see Figure 7-3. This suggests that sulfur works as a site of adsorption on calcite

and other surfaces. The attraction energy of sulfur to the surface was much higher than other atoms. This confirms the role of sulfur in the adsorption on solid surfaces.

Table 7-1. Total interactions (kJ/mol) between selected atoms of asphaltene A and smooth and rough calcite. The chosen atoms are shown on the structure.

	C1	C2	C3	C4	N	O	S
Smooth	-0.76	-0.5	-0.15	1.2	-1.3	98.3	-9.2
Rough	9.6	-1.7	65.6	29.5	-2.4	-12.4	-27.6

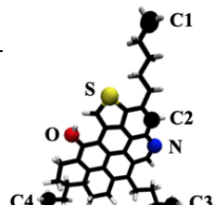


Table 7-2. Total interactions (kJ/mol) between M1 hypothetically selected segments and smooth and rough calcite. The chosen atoms are shown on the structure.

	C1	C2	C3	C4	C5	S1	S2
Smooth	-0.7	-0.37	-13.7	-0.7	1.5	-1	-6.9
Rough	10.3	15.2	28.5	6.4	-2.5	-97.4	-12.5

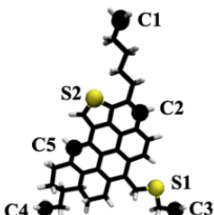


Table 7-3. Total interactions (kJ/mol) between M2 hypothetically selected segments and smooth and rough calcite. The chosen atoms are shown on the structure.

	C1	C2	C3	N	O	S1	S2
Smooth	-1.36	14.9	-6.2	72	-6.34	-37	-60.4
Rough	-0.8	58.7	22.1	97	32.4	-10.6	-82.8




Table 7-4. Total interactions (kJ/mol) between M3 hypothetically selected segments and smooth and rough calcite. The chosen atoms are shown on the structure.

	C1	C2	C3	C4	C5	C6
Smooth	0.41	-0.5	-1.89	-0.58	-0.1	0.1
Rough	-6.8	-2.4	-6.7	42	52.6	-2.6

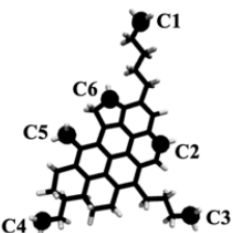
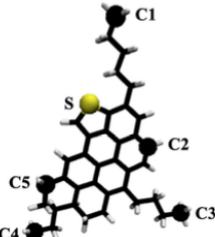


Table 7-5. Total interactions (kJ/mol) between M4 hypothetically selected segments and smooth and rough calcite. The chosen atoms are shown on the structure.

	C1	C2	C3	C4	C5	S
Smooth	2.5	-0.98	12.4	7.1	4.3	-27.9
Rough	12.7	33	8.2	49.7	20.6	-39.7



7.6 Conclusions

Molecular dynamics simulation provides the advantage of predicting the behavior of asphaltene molecules at reservoir conditions which is very challenging to be experimentally determined. Different simulations were conducted to predict the adsorption of asphaltene on rough and smooth calcite surfaces. The effect of injected air on different asphaltenes dissolved in an equimolar mixture of n-heptane and o-xylene was studied. An immobile and high dense layer of o-xylene adsorbed on calcite first. Asphaltenes showed different adsorption affinities to the calcite. On the smooth surface, the high adsorption affinity was observed in the air-free system and the dominated stacking was a molecular mode. A

reduction of asphaltene adsorption was achieved by injection 20 wt% of high-pressure air. A layer of air adsorbed to the immobile o-xylene layer next to calcite surface. Air layer displaced asphaltene molecules away from the surface. On rough calcite, the adsorption was much more than smooth surface. The adsorbed molecules were accumulated on the edge of the rough surface. Adding air disturbed some of this accumulation and displaced some of the molecules to the bulk of the system. Intermolecular energies showed higher interaction energies between asphaltene-rough calcite than asphaltene-smooth calcite. The interactions of asphaltene atoms with calcite showed that heteroatoms have a high contribution to the adsorption process. Sulfur may work as a stacking site that may be enhanced by other heteroatoms. Visualization showed that sulfur atoms were stacked to the surface before other atoms. Overall, this study found that air reduced asphaltene adsorption on calcite regarding the asphaltene structure. The results here showed the need to consider the roughness of the solid surfaces during asphaltene calculations where it had a high impact on the asphaltene accumulation. These findings support the use of air in enhanced oil recovery. More investigations about the effect of injected air concentrations, different asphaltene architecture, and different surfaces will be addressed in the future.

8 Conclusions and Recommendations

8.1 Conclusions

The main goal of this dissertation was to demonstrate and highlight the asphaltene problems and asphaltene behavior in the petroleum industry. The investigations were on asphaltene aggregation due to composition changes, the effect of external magnetic fields on the onset of asphaltene aggregation and disaggregation, and the effect and role of different heteroatoms on asphaltene adsorption on calcite surfaces. The thesis has shown the following results:

In chapter 4, the onsets of asphaltene aggregation of three different model asphaltenes in different mixtures of n-heptane and o-xylene were propped. The roles of van der Waals, hydrogen bond, and electrostatic interaction energies on the interaction between asphaltenes were investigated. The preferred stacking of asphaltene molecules was face-to-face at high paraffin content due to the high aromatic interactions between the aromatic cores. The electrostatic interactions were either attraction due to the presence of the heteroatoms in the aromatic core, or repulsion due to aliphatic chains that do not contribute in hydrogen bond interactions. The results of this study showed that the number and length of the chains, the number and position of the heteroatoms, and the number and size of the aromatic cores were all contributors in the asphaltene behavior.

In chapter 5, the effect of injected misciblized gas concentrations and the role of interaction energies were investigated. The asphaltene aggregation process was a function of the concentration of injected gases. Asphaltenes with long aliphatic chains and archipelago architecture showed low association affinity than other flat asphaltenes. Generally, there were no appreciable differences between the use of misciblized nitrogen and air on asphaltene aggregation. Additionally, the architecture of asphaltene played an important role in the aggregation process.

Chapter 6 includes investigations about the effect of different magnetic field strengths on the onset of asphaltene aggregation and its behavior in paraffinic and aromatic mediums. In paraffinic mediums, low magnetic fields increased the onsets of aggregation and changed the types and distances of preferred stacking. In aromatic mediums, low magnetic fields increased the association of A2 and decreased the association of A3 and A4. The different behaviors of asphaltenes could be explained as magnetic fields having effects on polar species. These effects could become higher with increasing the polarity of the molecules. This study clearly reveals the complex relationship of the topological structures of asphaltene concerning magnetic field strength. This study also highlights that center of gravity base RDF analysis may not be able to reveal the packing structure, especially for those molecules with flexible topological structures. Hydrogen bond results indicated that the magnetic field did change the average number of the interactions depending on the medium and asphaltene architecture. These changes are due to the changes in the orientation and the distances between asphaltene molecules. The effects of the magnetic field are completely dependent on the strength of the applied magnetic field, the medium, and the architecture of asphaltene, where the number and position of heteroatoms are very important.

In chapter 7, different simulations were conducted to predict the adsorption of asphaltene on rough and smooth calcite surfaces. The effect of injected air and the morphology of the surface on the adsorption of different asphaltenes were studied. Asphaltenes showed different adsorption affinities to the calcite. On a smooth surface, the high adsorption affinity was observed in the air-free system, and the dominated stacking mode was molecular mode. On the rough calcite, the adsorption of asphaltene was much higher than on the smooth surface. The adsorbed molecules were accumulated on the edge of the rough surface. Adding air could disturb some of this accumulation and displace some of the molecules to the bulk of the system. Intermolecular energies showed higher interaction energies between asphaltene-

rough calcite than the asphaltene-smooth calcite. The interactions of asphaltene atoms with calcite showed that heteroatoms have a high contribution in the adsorption process. Overall, this study found that air enhanced asphaltene aggregation and reduced asphaltene adsorption on calcite regardless of asphaltene structure. The results here revealed the need to consider the roughness of the solid surfaces during asphaltene calculations where it had a high impact on the asphaltene accumulation.

It is important to mention that the author is aware that molecular dynamics (MD) simulations in general, and what is done in this research, are incapable of predicting the behavior of complex petroleum fluids and no such calculations are reported here. What was done and reported here are the onsets of interaction/aggregation of two individual dissolved-in-oil asphaltene molecules as a result of the presence or absence of miscible injectants (i.e. high pressure nitrogen or air in a model oil). There is confidence that the results reported in this dissertation are applicable to onsets of asphaltenes' behavior in real crude oils.

8.2 Recommendations for Future Research

The investigations about asphaltene aggregation and deposition at molecular level opened up several research opportunities. These ideas may help in better understanding and fill up an important gap in asphaltene behavior. Here is a list of the suggested future researches:

- A- The results in chapters 4 and 5 showed that asphaltene aggregation was affected by asphaltene architecture, the aromaticity of the medium, and the concentration of injected fluids. These results have suggested that there is a need to do more simulations of different asphaltenes in different mediums. As reported in the literature, asphaltene could be found in different architectures in the same crude oil. Thus, simulations of mixtures of different asphaltenes (polydisperse) from the same crude oil are required to give a better understanding of the effects of asphaltene

molecular structure on its aggregation path. Also, simulations of asphaltenes in aromatic, paraffinic and/or their mixtures do not include the effects of other important species in the real crude oil mixtures. Thus, studies of asphaltene aggregation in the presence of a wide range of species that are reported in the same crude oil of used asphaltene are encouraged. These studies will include the interactions of asphaltene with different species and may show different aggregation paths, especially if these species provide acid-base interactions with asphaltene.

- B- The effects of external magnetic field on asphaltene aggregation showed interesting results where magnetic fields could disturb asphaltene aggregation. However, more and deep investigations are required to investigate the effect of magnetic field on heavy organics aggregation and deposition. Simulations of mixtures of different species, including asphaltene (and a mixture of asphaltenes), are suggested to include the effect of magnetic field on the aggregation/disaggregation. It is suggested to do annealing simulations in the presence of magnetic field to investigate the effects of an increase or decrease of system temperature on the aggregation/disaggregation process.

In addition, it was reported that resins and asphaltenes fractions possess paramagnetic properties (Retcofsky et al., 1979; Unger, 1997; Yen et al., 1962; Yen, Tynan et al., 1970). When metals like iron, nickel, cobalt, and vanadium are present in petroleum fluids, the metals increase oil's paramagnetic properties (El-Mohamed et al., 1986; Ivakhnenko, 2012; Khristoforov, 1971; Lesin et al., 2010; Miller, 2002; Veciana, 1996; Yen et al., 1962). The metals that are present in the crudes are usually associated with asphaltenes. Different studies reported that metals and free radicals were concentrated in asphaltene fraction aggregates (Chen et al., 2016; Ganeeva et al., 2011; Ivakhnenko, 2012; Loskutova and Yudina, 2003). For example, the asphaltene

fractions of Boscan and Bachaquero crudes have 9700 and 2700 ppm vanadium respectively (Yen et al., 1970). Dickie and Yen (1967) showed that vanadium complexes were not a part of asphaltene, but they worked as a site for aggregation. This means most of asphaltene aggregates have metals if there are metals in the system. However, there is no clear conclusion about the magnetic properties of asphaltene or asphaltene aggregates that include metals and how these aggregates behave in the presence of magnetic fields. Thus, experimental and theoretical calculations of wide ranges of heavy organic species (including organometallic species) are required to find out the exact magnetic properties of these compounds and connect them with asphaltene aggregation and deposition in the presence and absence of magnetic fields. These investigations have to investigate each fraction separately before mixing them to build up a model oil and compare their behaviors.

- C- It is very important to focus on asphaltene deposition and the consequences with it. The simulations of asphaltene adsorptions on calcite surfaces have shown that heteroatoms play roles in the adsorption. These results have suggested that there is a need for more simulations of different asphaltenes that have a different distribution of heteroatoms. Also, the simulations should consider different rock surfaces to investigate all the possibilities of asphaltene deposition on these rocks (calcite, silica, and clay). Also, the studies have to consider different species that are found in reservoir fluids. The interactions with water, ions, injection fluids (such as air or CO₂) should also be investigated during these simulations to probe the role of these species on asphaltene deposition that may cause wettability reversal of the rocks. Moreover, one of the oil industry problems is the deposition of asphaltene and/or heavy organics in production and transportation lines. Almost all of the pipelines are made of carbon steel which may help asphaltene deposition. However, with the development of

nanotechnology and coating of solid surfaces, these pipes could be coated by a thin layer of a material that may reduce or eliminate asphaltene deposition. Thus, simulations of different asphaltenes on metals or polymer surfaces are encouraged to find out a good coating material and understand asphaltene deposition on different surfaces.

Appendix



RightsLink®

Home

Account
Info

Help



Title: A new insight into asphaltenes aggregation onset at molecular level in crude oil (an MD simulation study)
Author: Mohammed H. Khalaf, G. Ali Mansoori
Publication: Journal of Petroleum Science and Engineering
Publisher: Elsevier
Date: March 2018

© 2017 Elsevier B.V. All rights reserved.

Logged in as:
Mohammed Khalaf
UIC
Account #:
3001480066

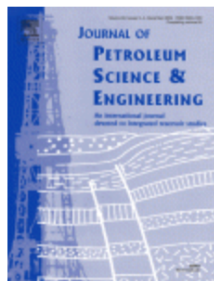
LOGOUT

Please note that, as the author of this Elsevier article, you retain the right to include it in a thesis or dissertation, provided it is not published commercially. Permission is not required, but please ensure that you reference the journal as the original source. For more information on this and on your other retained rights, please visit: <https://www.elsevier.com/about/our-business/policies/copyright#Author-rights>

BACK

CLOSE WINDOW

Copyright © 2019 Copyright Clearance Center, Inc. All Rights Reserved. [Privacy statement](#). [Terms and Conditions](#).
Comments? We would like to hear from you. E-mail us at customercare@copyright.com



Title: Asphaltenes aggregation during petroleum reservoir air and nitrogen flooding

Author: Mohammed H. Khalaf, G. Ali Mansoori

Publication: Journal of Petroleum Science and Engineering

Publisher: Elsevier

Date: February 2019

© 2018 Elsevier B.V. All rights reserved.

Logged in as:
Mohammed Khalaf
UIC
Account #:
3001480066

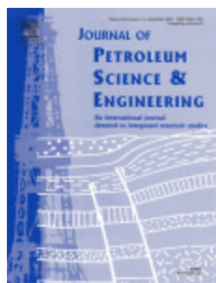
LOGOUT

Please note that, as the author of this Elsevier article, you retain the right to include it in a thesis or dissertation, provided it is not published commercially. Permission is not required, but please ensure that you reference the journal as the original source. For more information on this and on your other retained rights, please visit: <https://www.elsevier.com/about/our-business/policies/copyright#Author-rights>

BACK

CLOSE WINDOW

Copyright © 2019 [Copyright Clearance Center, Inc.](#) All Rights Reserved. [Privacy statement](#). [Terms and Conditions](#).
Comments? We would like to hear from you. E-mail us at customercare@copyright.com



Title: Magnetic treatment of petroleum and its relation with asphaltene aggregation onset (an atomistic investigation)

Author: Mohammed H. Khalaf, G. Ali Mansoori, Chin W. Yong

Publication: Journal of Petroleum Science and Engineering

Publisher: Elsevier

Date: May 2019

© 2019 Elsevier B.V. All rights reserved.

Logged in as:
Mohammed Khalaf
UIC
Account #:
3001480066

LOGOUT

Please note that, as the author of this Elsevier article, you retain the right to include it in a thesis or dissertation, provided it is not published commercially. Permission is not required, but please ensure that you reference the journal as the original source. For more information on this and on your other retained rights, please visit: <https://www.elsevier.com/about/our-business/policies/copyright#Author-rights>

BACK

CLOSE WINDOW

Copyright © 2019 Copyright Clearance Center, Inc. All Rights Reserved. [Privacy statement](#). [Terms and Conditions](#).
Comments? We would like to hear from you. E-mail us at customer@copyright.com

References

- Abouie, A., Shirdel, M., Darabi, H., Sepehrnoori, K.: Modeling asphaltene deposition in the wellbore during gas lift process. Western Regional Meeting, Old Horizons, New Horizons Through Enabling Technology, SPE 174067, 2015.
- Abraham, M.J., van der Spoel, D., Lindahl, E., Hess, B., and the GROMACS development team. (2014). GROMACS User Manual version 5.1.2, 2014.
- Adams, D.J., Adams, E.M., Hills, G.J.: The computer simulation of polar liquids. *Molecular Physics*, 38(2), 387–400, 1979.
- Adams, J.J.: Asphaltene Adsorption, a Literature Review. *Energy Fuels*, 28(5), 2831–2856, 2014.
- Adialalis, S.: Investigation of physical and chemical criteria as related to the prevention of asphalt deposition in oil well tubings. MSc Thesis Petroleum Engineering Department, Imperial College of the University of London, London, 1982.
- Akhmetov, B.R., Evdokimov, I.N., Eliseev, N.Y.: Some features of the supramolecular structures in petroleum media. *Chemistry and Technology of Fuels and Oils*, 38(4), 266–270, 2002.
- Alvarez-Ramirez, F., Ramirez-Jaramillo, E., Ruiz-Morales, Y.: Calculation of the interaction potential curve between asphaltene-asphaltene, asphaltene-resin, and resin-resin systems using density functional theory. *Energy Fuels*, 20(1), 195–204, 2006.
- Anisimov, M.A., Yudin, I.K., Nikitin, V., Nikolaenko, G., Chernoutsan, A., Toulhoat, H., Briolant, Y.: Asphaltene aggregation in hydrocarbon solutions studied by photon correlation spectroscopy. *Journal of Physical Chemistry*, 99(23), 9576–9580, 1995.
- Bagdat, M., Masoud, R.: Control of Paraffin Deposition in Production Operation by Using Ethylene–TetraFluoroEthylene (ETFE). *Proceedings of the International Conference on Integrated Petroleum Engineering and Geosciences*, pp. 13–22, 2005.
- Barré, L., Simon, S., Palermo, T.: Solution properties of asphaltenes. *Langmuir*, 24(8), 3709–3717, 2008.
- Benmekki, E.H., Mansoori, G.A.: Accurate vaporizing gas-drive minimum miscibility pressure prediction. *SPE Reservoir Engineering*, 3(2), 559–564, 1988.
- Boek, E.S., Yakovlev, D.S., Headen, T.F.: Quantitative molecular representation of asphaltenes and molecular dynamics simulation of their aggregation. *Energy Fuels*, 23(3), 1209–1219, 2009.
- Boussingault, M.: Memoire sur la Composition des Bitumes. *Annales de Chimie et de Physique*, 64(1), 141, 1837.
- Branco, V.A.M, Mansoori, G.A., De Almeida Xavier, L.C., Park, S.J., Manafi, H.: Asphaltene flocculation and collapse from petroleum fluids. *Journal of Petroleum Science and Engineering*, 32(2–4), 217–230, 2001.
- Carauta, A.N.M., Correia, J.C.G., Seidl, P.R., Silva, D.M.: Conformational search and dimerization study of average structures of asphaltenes. *Journal of Molecular Structure: THEOCHEM*, 755(1–3), 1–8, 2005.
- Chang, K.T., Weng, C.I.: The effect of an external magnetic field on the structure of liquid water using molecular dynamics simulation. *Journal of Applied Physics*, 100(4), 043917, 2006.

- Chen, X., Hou, L., Li, W., Li, S., Chen, Y.: Molecular dynamics simulation of magnetic field influence on waxy crude oil. *Journal of Molecular Liquids*, 249, 1052–1059, 2018.
- Chen, Z., Zhang, L., Zhao, S., Shi, Q., Xu, C.: Molecular structure and association behavior of petroleum asphaltene. *Structure and Bonding*, 168, 1–38, 2016.
- Daaou, M., Modarressi, A., Bendedouch, D., Bouhadda, Y., Krier, G., Rogalski, M.: Characterization of the nonstable fraction of Hassi-Messaoud asphaltenes. *Energy Fuels*, 22(5), 3134–3142, 2008.
- De León, J., Hoyos, B., Cañas-Marín, W.: Insights of asphaltene aggregation mechanism from molecular dynamics simulation. *DYNA*, 82(189), 39–44, 2015.
- Dehghani, S.A.M., Sefti, M.V., Mansoori, G.A.: Simulation of natural depletion and miscible gas injection effects on asphaltene stability in petroleum reservoir fluids. *Petroleum Science and Technology*, 25(11), 1435–1446, 2007.
- Della Valle, E., Marracino, P., Setti, S., Cadossi, R., Liberti, M., Apollonio, F.: Magnetic molecular dynamics simulations with Velocity Verlet algorithm. In 2017 32nd General Assembly and Scientific Symposium of the International Union of Radio Science, URSI GASS, pp. 1–4, 2017.
- Dickie, J.P., Yen, T.F.: Macrostructures of the Asphaltic Fractions by Various Instrumental Methods. *Analytical Chemistry*, 39(14), 1847–1852, 1967.
- Dodda, L.S., De Vaca, I.C., Tirado-Rives, J., Jorgensen, W.L.: LigParGen web server: An automatic OPLS-AA parameter generator for organic ligands. *Nucleic Acids Research*, 45(1), 331–336, 2017.
- Durand, E., Clemancey, M., Lancelin, J.M., Verstraete, J., Espinat, D., Quoineaud, A.A.: Aggregation states of asphaltenes: Evidence of two chemical behaviors by ¹H diffusion-ordered spectroscopy nuclear magnetic resonance. *Journal of Physical Chemistry C*, 113(36), 16266–16276, 2009.
- El-Mohamed, S., Achard, M.F., Hardouin, F., Gasparoux, H.: Correlations between diamagnetic properties and structural characters of asphaltenes and other heavy petroleum products. *Fuel*, 65(11), 1501–1504, 1986.
- Energy Information Administration. U.S. Energy Information Administration (EIA)-Data. Retrieved May 6, 2019.
- Escobedo, J., Mansoori, G.A.: Heavy Organic Deposition and Plugging of Wells (Analysis of Mexico's Experience). Second Latin Petroleum Engineering Conference, SPE 23696, 1992.
- Escobedo, J., Mansoori, G.A.: Solid Particle Deposition During Turbulent Flow Production Operations. *Proceedings of SPE Production Operations Symposium*, 439–446, 1995.
- Escobedo, J., Mansoori, G.A.: Heavy-organic particle deposition from petroleum fluid flow in oil wells and pipelines. *Petroleum Science*, 7(4), 502–508, 2010.
- Ganeeva, Y.M., Yusupova, T.N., Romanov, G.V.: Asphaltene nano-aggregates: structure, phase transitions and effect on petroleum systems. *Russian Chemical Reviews*, 80(10), 993–1008, 2011.
- Ghanavati, M., Shojaei, M.J., Ahmad Ramazani, S.A.: Effects of asphaltene content and temperature on viscosity of Iranian heavy crude oil: Experimental and modeling study. *Energy Fuels*, 27(12), 7217–7232, 2013.
- Gonçalves, J.L., Bombard, A.J.F., Soares, D.A.W., Carvalho, R.D.M., Nascimento, A., Silva,

- M.R., Rocha, N.O.: Study of the factors responsible for the rheology change of a Brazilian crude oil under magnetic fields. *Energy Fuels*, 25(8), 3537–3543, 2011.
- Gonzalez, G., Travalloni-Louvisse, A.M.: Adsorption of Asphaltenes and Its Effect on Oil Production. *SPE Production and Facilities*, 8(02), 91–96, 1993.
- Griffiths, D.J., Reeves, A.: *Electrodynamics. Introduction to Electrodynamics*, 3rd ed., Prentice Hall, Upper Saddle River, New Jersey, 1999.
- Grijalva-Monteverde, H., Arellano-Tánori, O.V., Valdez, M. A.: Zeta potential and langmuir films of asphaltene polar fractions. *Energy Fuels*, 19(6), 2416–2422, 2005.
- Hammami, A., Ratulowski, J.: Precipitation and Deposition of Asphaltenes in Production Systems: A Flow Assurance Overview. *Asphaltenes, Heavy Oils, and Petroleomics*, pp. 617–660, 2007.
- Headen, T.F., Boek, E.S.: Molecular Dynamics Simulations of Asphaltene Aggregation in Supercritical Carbon Dioxide with and without Limonene. *Energy Fuels*, 25(2), 503–508, 2011.
- Headen, T. F., Boek, E. S., Skipper, N. T.: Evidence for asphaltene nanoaggregation in toluene and heptane from molecular dynamics simulations. *Energy Fuels*, 23(3), 1220–1229, 2009.
- Hillman, E.S. Barnett, B.: The constitution of cracked and uncracked asphalts. *Proc of 40th Meeting of ASTM*, pp. 558–568, 1937.
- Hirschberg, A., DeJong, L.N.J., Schipper, B.A., Meijer, J.G.: Influence of Temperature and Pressure on Asphaltene Flocculation. *Society of Petroleum Engineers Journal*, 24(03), 283–293, 1984.
- Humphrey, W., Dalke, A., Schulten, K.: VMD: Visual molecular dynamics. *Journal of Molecular Graphics*, 14(1), 33–38, 1996.
- Ivakhnenko, O.P.: Magnetic Susceptibility of Petroleum Reservoir Crude Oils in Petroleum Engineering. *Crude Oil Exploration in the World*, 3, 71-88, 2012.
- Jada, A., Debih, H.: Hydrophobation of clay particles by asphaltenes adsorption. *Composite Interfaces*, 16(2–3), 219–235, 2009.
- Jamaluddin, A.K. M., Joshi, N., Iwere, F., Gурpinar, O.: An Investigation of Asphaltene Instability Under Nitrogen Injection. *SPE International Petroleum Conference and Exhibition in Mexico*, SPE 74393, 2002.
- Johnsen, S.G., Hanetho, S.M., Tetlie, P., Johansen, S.T., Einarsrud, M.A., Kaus, I., Simon, C.R.: Studies of Paraffin Wax Deposition on Coated and Non-Coated Steel Surfaces. *Proceedings of International Conference on Heat Exchange Fouling and Cleaning*, pp. 251–258, 2011.
- Kawanaka, S., Park, S.J., Mansoori, G.A.: The Role of Asphaltene Deposition in EOR Gas Flooding: a Predictive Technique. *Proceedings of SPE/DOE Enhanced Oil Recovery Symposium*. Tulsa, Oklahoma. SPE 17376, 1988.
- Kawanaka, S., Park, S.J., Mansoori, G.A.: Organic Deposition From Reservoir Fluids: A Thermodynamic Predictive Technique. *SPE Reservoir Engineering*, 6(02), 185–192, 1991.
- Khalaf, M.H., Mansoori, G.A.: A new insight into asphaltenes aggregation onset at molecular level in crude oil (an MD simulation study). *Journal of Petroleum Science and*

- Engineering, 162, 244–250, 2018.
- Khalaf, M.H., Mansoori, G.A.: Asphaltenes aggregation during petroleum reservoir air and nitrogen flooding. *Journal of Petroleum Science and Engineering*, 173, 1121–1129, 2019.
- Khalaf, M.H., Mansoori, G.A., Yong, C.W.: Magnetic treatment of petroleum and its relation with asphaltene aggregation (an atomistic investigation). *Journal of Petroleum Science and Engineering*, 176, 926–933, 2019.
- Khrstoforov, V.S.: Study of crude oil and some of its high molecular compounds using electron paramagnetic resonance (Review). *Chemistry and Technology of Fuels and Oils*, 7(8), 629–631, 1971.
- Kim, S.T., Boudh-Hir, M.E., Mansoori, G.A.: The Role of Asphaltene in Wettability Reversal. *Proceedings of SPE Annual Technical Conference and Exhibition*. New Orleans, Louisiana, SPE 20700, 1990.
- Kulkarni, A.D., Wani, K.S.: Magnetic Field Conditioning: An Energy Efficient Method for Crude Oil Transportation. *International Journal of Science, Spirituality, Business and Technology*, 2(1), 2277–7261, 2013.
- Lei, Y., Han, S., Zhang, J.: Effect of the dispersion degree of asphaltene on wax deposition in crude oil under static conditions. *Fuel Processing Technology*, 146, 20–28, 2006.
- Leontaritis, K.J. Mansoori, G.A.: Asphaltene deposition: a survey of field experiences and research approaches. *Journal of Petroleum Science and Engineering*, 1(3), 229–239, 1988.
- Leontaritis, K.J. Mansoori, G.A.: A colloidal model for asphaltene flocculation from petroleum fluids. *Iranian Journal of Science and Technology*, 16(2) 249-267, 1992.
- Leontaritis, K.J., Mansoori, G.A.: Asphaltene deposition: a survey of field experiences and research approaches. *Journal of Petroleum Science and Engineering*, 1(3), 229–239, 1988.
- Lesin, V.I., Koksharov, Y.A., Khomutov, G.B.: Magnetic nanoparticles in petroleum. *Petroleum Chemistry*, 50(2), 102–105, 2010.
- Liao, Z., Geng, A., Graciaa, A., Creux, P., Chrostowska, A., Zhang, Y.: Different Adsorption/Occlusion Properties of Asphaltenes Associated with Their Secondary Evolution Processes in Oil Reservoirs. *Energy Fuels*, 20(3), 1131–1136, 2006.
- Lichaa, P.M.: Asphaltene deposition problem in Venezuela crudes-usage of asphaltenes in emulsion stability. *Oil Sands*, 609(1), 1977.
- Lisitz, N.V, Freed, D.E., Sen, P. N., Song, Y.Q.: Study of asphaltene nanoaggregation by nuclear magnetic resonance (NMR). *Energy Fuels*, 23(3), 1189–1193, 2009.
- Loskutova, Y.V., Yudina, N.V.: Effect of Constant Magnetic Field on the Rheological Properties of High-Paraffinicity Oils. *Colloid Journal*, 65(4), 469–474, 2003.
- Loskutova, Y.V., Yudina, N.V., Pisareva, S.I.: Effect of magnetic field on the paramagnetic, antioxidant, and viscosity characteristics of some crude oils. *Petroleum Chemistry*, 48(1), 51–55, 2008.
- Luo, P., Gu, Y.: Effects of asphaltene content on the heavy oil viscosity at different temperatures. *Fuel*, 86(7–8), 1069–1078, 2007.
- Mansoori, G.A. Jiang, T.S.: Asphaltene deposition and its role in EOR gas flooding processes. *The 3rd European Conference on Enhanced Oil Recovery*. Rome, pp. 75-86,

- 1985.
- Mansoori, G.A. Jiang, T.S. and S. Kawanaka: Asphaltene Deposition and its Role in Petroleum Production and Processing. *Arabian J. Science & Engineering*, Vol. 13, pp.17-34,, 1988.
- Mansoori, G.A.: Modeling of asphaltene and other heavy organic depositions.pdf. *Journal of Petroleum Science and Engineering*, 17(1–2), 101–111, 1997.
- Mansoori, G.A.: Deposition and Fouling of Heavy Organic Oils and Other Compounds. In 9th International Conference on Properties and Phase Equilibria for Product and Process Design, Japan, pp. 1-9, 2001.
- Mansoori, G.A.: A unified perspective on the phase behaviour of petroleum fluids. *International Journal of Oil, Gas and Coal Technology*, 2(2), 141-167, 2009.
- Mansoori, G.A.: Remediation of asphaltene and other heavy organic deposits in oil wells and in pipelines. *SOCAR Proceeding*, Institute of State Oil Company of Azerbaijan Republic, pp. 12–23, 2010.
- Marcusson, J.: *Die Naturlichten und Kunstlichen Asphalte*. Leipzig, 1931.
- Marques, L.C.C., Rocha, N.O., Machado, A.L.C., Neves, G.B.M., Vieira, L.C., Dittz, C.H.: Study of Paraffin Crystallization Process Under The Influence of Magnetic Fields and Chemicals. *Latin American and Caribbean Petroleum Engineering Conference*, SPE 38990, 1997.
- Miller, J.S.: Organic magnets - A history. *Advanced Materials*, 14(16), 1105–1110, 2002.
- Mirzayi, B., Vafaie-Sefti, M., Mousavi-Dehghani, S. A., Fasih, M., Mansoori, G.A.: The effects of asphaltene deposition on unconsolidated porous media properties during miscible natural gas flooding. *Petroleum Science and Technology*, 26(2), 231–243, 2008.
- Mohammed, S., Gadikota, G.: The influence of CO₂ on the structure of confined asphaltenes in calcite nanopores. *Fuel*, 236, 769–777, 2019a.
- Mohammed, S., Gadikota, G.: The role of calcite and silica interfaces on the aggregation and transport of asphaltenes in confinement. *Journal of Molecular Liquids*, 274, 792–800, 2019b.
- Mohammed, S., Mansoori, G.A.: Effect of CO₂ on the Interfacial and Transport Properties of Water/Binary and Asphaltenic Oils: Insights from Molecular Dynamics. *Energy Fuels*, 32(4), 5409–5417, 2018a.
- Mohammed, S., Mansoori, G.A.: Molecular insights on the interfacial and transport properties of supercritical CO₂/brine/crude oil ternary system. *Journal of Molecular Liquids*, 263, 268–273, 2018b.
- Mohammed, S., Mansoori, G.A.: The Role of Supercritical/Dense CO₂ Gas in Altering Aqueous/Oil Interfacial Properties: A Molecular Dynamics Study. *Energy Fuels*, 32(2), 2095–2103, 2018c.
- Moosavi, F., Gholizadeh, M.: Magnetic effects on the solvent properties investigated by molecular dynamics simulation. *Journal of Magnetism and Magnetic Materials*, 354, 239–247, 2014.
- Morozov, V.I., Usatenko, S.T., Savchuk, O.V. (1978). Influence of a magnetic field on the physical properties of hydrocarbon fluids. *Chemistry and Technology of Fuels and Oils*, 13(10), 743–746, 1978.

- Mousavi-Dehghani, S.A., Riazi, M.R., Vafaie-Sefti, M., Mansoori, G.A.: An analysis of methods for determination of onsets of asphaltene phase separations. *Journal of Petroleum Science and Engineering*, 42(2–4), 145–156, 2004.
- Mungan, N.: High Pressure Nitrogen Injection for Miscible/Immiscible Enhanced Oil Recovery. *Latin American and Caribbean Petroleum Engineering Conference*, SPE 81008, 2003.
- Murgich, J. (2003). Molecular Simulation and the Aggregation of the Heavy Fractions in Crude Oils. *Molecular Simulation*, 29(6–7), 451–461.
- Murgich, J., Jesús Rodríguez, M., Aray, Y.: Molecular recognition and molecular mechanics of micelles of some model asphaltenes and resins. *Energy Fuels*, 10(1), 68–76, 1996.
- Nellensteyn, F. J.: The constitution of asphalt. *J. Inst. Pet*, 10(1), 311–325, 1924.
- Pacheco-Sánchez, J.H., Álvarez-Ramírez, F., Martínez-Magadán, J.M.: Morphology of aggregated asphaltene structural models. *Energy Fuels*, 18(6), 1676–1686, 2004.
- Pacheco-Sanchez, J.H., Mansoori, G.A.: Prediction of the phase behavior of asphaltene micelle/aromatic hydrocarbon systems. *Petroleum Science and Technology*, 16(3–4), 377–394, 1998.
- Pacheco-Sánchez, J.H., Zaragoza, I.P., Martínez-Magadán, J.M.: Asphaltene aggregation under vacuum at different temperatures by molecular dynamics. *Energy Fuels*, 17(5), 1346–1355, 2003.
- Pacheco-Sánchez, J.H., Zaragoza, I.P., Martínez-Magadán, J.M.: Preliminary Study of the Effect of Pressure on Asphaltene Disassociation by Molecular Dynamics. *Petroleum Science and Technology*, 22(7–8), 927–942, 2004.
- Pacheco, J., Mansoori, G.A.: In situ remediation of heavy organic deposits using aromatic solvents. *5th Latin American and Caribbean Petroleum Engineering Conference and Exhibition*, SPE 38966, 1997.
- Park, S.J., Kwak, T.Y., Mansoori, G.A.: Statistical mechanical description of supercritical fluid extraction and retrograde condensation. *International Journal of Thermophysics*, 8(4), 449–471, 1987.
- Piro, G., Canonico, L., Galbariggi, G., Bertero, L., Carniani, C.: Asphaltene adsorption onto formation rock: an approach to asphaltene formation damage prevention. *SPE Production and Facilities*, 11(3), 156–160, 1996.
- Priyanto, S., Mansoori, G.A., Suwono, A.: Measurement of property relationships of nano-structure micelles and coacervates of asphaltene in a pure solvent. *Chemical Engineering Science*, 56(24), 6933–6939, 2001.
- Retcofsky, H.L., Hough, M.R., Clarkson, R.B.: Nature of the Free Radicals in Coals, Pyrolyzed Coals, Solvent-Refined Coal, and Coal Liquefaction Products. *ACS Division of Fuel Chemistry*, 37-58, 1979.
- Rogel, E.: Studies on asphaltene aggregation via computational chemistry. *Colloids and Surfaces A: Physicochemical and Engineering Aspects*, 104(1), 85–93, 1995a.
- Rogel, E.: Studies on asphaltene aggregation via computational chemistry. *Colloids and Surfaces A: Physicochemical and Engineering Aspects*, 104(1), 85–93, 1995b.
- Rogel, E., Carbognani, L.: Density estimation of asphaltenes using molecular dynamics simulations. *Energy Fuels*, 17(2), 378–386, 2003.
- Rogel, E.: Simulation of Interactions in Asphaltene Aggregates. *Energy Fuels*, 14(3), 566–

- 574, 2000.
- Ru, T. W., Alta'ee, A. F.: Investigation of Asphaltene Onset Pressure (AOP) in Low Asphaltenic Light Oil Samples, 23–45, 2015.
- Sheu, E.Y.: Physics of asphaltene micelles and microemulsions - theory and experiment. *Journal of Physics: Condensed Matter*, 8(25), 125–141, 1996.
- Storm, D. A., Barresi, R. J., Sheu, E. Y.: Flocculation of asphaltenes in heavy oil at elevated temperatures. *Fuel Science and Technology International*, 14(1–2), 243–260, 1996.
- Taheri-Shakib, J., Rajabi-Kochi, M., Kazemzadeh, E., Naderi, H., Salimidelshad, Y., Esfahani, M.R.: A comprehensive study of asphaltene fractionation based on adsorption onto calcite, dolomite and sandstone. *Journal of Petroleum Science and Engineering*, 171, 863–878, 2018.
- Takahashi, S., Hayashi, Y., Takahashi, S., Yazawa, N., Sarma, H.: Characteristics and Impact of Asphaltene Precipitation During CO₂ Injection in Sandstone and Carbonate Cores: An Investigative Analysis Through Laboratory Tests and Compositional Simulation. *International Improved Oil Recovery Conference, SPE 84895*, 2003.
- Takanohashi, T., Iino, M., Nakamura, K.: Evaluation of Association of Solvent-Soluble Molecules of Bituminous Coal by Computer Simulation. *Energy Fuels*, 8(2), 395–398, 1994.
- Takanohashi, T., Iino, M., Nakamura, K.: Simulation of Interaction of Coal Associates with Solvents Using the Molecular Dynamics Calculation. *Energy Fuels*, 12(15), 1168–1173, 1998.
- Takanohashi, T., Sato, S., Saito, I., Tanaka, R.: Molecular dynamics simulation of the heat-induced relaxation of asphaltene aggregates. *Energy Fuels*, 17(1), 135–139, 2003.
- Takanohashi, T., Sato, S., Tanaka, R.: Structural relaxation behaviors of three different asphaltenes using MD calculations. In *Petroleum Science and Technology*, 22, 901–914, 2004.
- Tao, R., Xu, X.: Reducing the viscosity of crude oil by pulsed electric or magnetic field. *Energy Fuels*, 20(5), 2046–2051, 2006.
- Todorov, I., Smith, W.: The DL POLY 4 user manual. Science and Technology Facilities Council (STFC). Cheshire, UK, 2016.
- Tojima, M., Suhara, S., Imamura, M., Furuta, A.: Effect of heavy asphaltene on stability of residual oil. *Catalysis Today*, 43(3–4), 347–351, 1998.
- Tu, Y., Kingston, D., Kung, J., Kotlyar, L.S., Sparks, B.D., Chung, K.H.: Adsorption of pentane insoluble organic matter from oilsands bitumen onto clay surfaces. In *Petroleum Science and Technology*, 24, 327–338, 2006.
- Tung, N.P., Van Vuong, N., Long, B.Q.K., Vinh, N.Q., Hung, P.V., Hue, V.T., Hoe, L.D.: Studying the mechanism of magnetic field influence on paraffin crude oil viscosity and wax deposition reductions. *Asia Pacific Oil and Gas Conference and Exhibition, SPE 68749*, 2001.
- Unger, F. (1997). The nature of resins and asphaltenes. *ACS Division of Fuel Chemistry, Preprints*, 42(2), 445–448.
- Van Der Spoel, D., Lindahl, E., Hess, B., Groenhof, G., Mark, A.E., Berendsen, H.J.C.: GROMACS: Fast, flexible, and free. *Journal of Computational Chemistry*, 26(16), 1701–1718, 2005.

- Vazquez, D., Mansoori, G.A.: Identification and measurement of petroleum precipitates. *Journal of Petroleum Science and Engineering*, 26, 49–55, 2000.
- Veciana, J.: Organic Magnetic Materials. *Molecular Magnetism: From Molecular Assemblies to the Devices*, pp. 425–448, 1996.
- Vicente, L., Soto, C., Pacheco-Sánchez, H., Hernández-Trujillo, J., Martínez-Magadán, J. M.: Application of molecular simulation to calculate miscibility of a model asphaltene molecule. *Fluid Phase Equilibria*, 239(1), 100–106, 2006.
- Vujić, B., Lyubartsev, A.P.: Transferable force-field for modelling of CO₂, N₂, O₂ and Ar in all silica and Na⁺ exchanged zeolites. *Modelling and Simulation in Materials Science and Engineering*, 24(4), 045002, 2016.
- Xiao, S., Edwards, S.A., Gräter, F.: A new transferable forcefield for simulating the mechanics of CaCO₃ crystals. *Journal of Physical Chemistry C*, 115(41), 20067–20075, 2011.
- Yaseen, S., Mansoori, G.A.: Molecular dynamics studies of interaction between asphaltenes and solvents. *Journal of Petroleum Science and Engineering*, 156, 118–124, 2017.
- Yaseen, S., Mansoori, G.A.: Asphaltene aggregation due to waterflooding (A molecular dynamics study). *Journal of Petroleum Science and Engineering*, 170, 177–183, 2018.
- Yen, T.F., Erdman, J.G. Pollack, S. S.: Investigation of the structure of petroleum asphaltenes by X-ray diffraction. *Analytical Chemistry*, 33(11), 1587–1594, 1961.
- Yen, T.F., Erdman, J.G., Saraceno, A.J.: Investigation of the Nature of Free Radicals in Petroleum Asphaltenes and Related Substances by Electron Spin Resonance. *Analytical Chemistry*, 34(6), 694–700, 1962.
- Yen, T.F., Tynan, E.C., Vaughan, G.B., Boucher, L.J.: Electron Spin Resonance Studies of Petroleum Asphaltics. *Spectrometry of Fuels*, pp. 187–201, 1970.
- Yong, C.W.: Descriptions and Implementations of DL-F Notation: A Natural Chemical Expression System of Atom Types for Molecular Simulations. *Journal of Chemical Information and Modeling*, 56(8), 1405–1409, 2016.
- Yong, C.W., Todorov, I.T.: DL_ANALYSER Notation for Atomic Interactions (DANAI): A Natural Annotation System for Molecular Interactions, Using Ethanoic Acid Liquid as a Test Case. *Molecules*, 23(1), 36, 2018.
- Zhang, L., Greendfield, M.L.: Molecular orientation in model asphalts using molecular simulation. *Energy Fuels*, 21(2), 1102–1111, 2007.